

Thesis

Dynamics of Solitons
in
Nonlinear Systems

(非線形系におけるソリトンのダイナミクス)



0065134652

8552

Thesis

Dynamics of Solitons
in
Nonlinear Systems

by

Masao OGATA

Institute for Solid State Physics
University of Tokyo

(December 1986)

ACKNOWLEDGEMENTS

The author would like to express his sincere gratitude to Professor Yasushi Wada, who introduced him to this field of research, for continual encouragement, instructive discussions and a critical reading of the manuscript. He is also grateful to Professor Hiroyuki Shiba for variable discussions and a critical reading of the manuscript. He is pleased to acknowledge stimulating discussions with Professor Ryogo Kubo, Professor Masuo Suzuki, Professor Hajime Takayama, Dr. Yoshiyuki Ono, and Dr. Seiji Miyashita. He also thanks Professor Kiyoshi Kume and Dr. Kenji Mizoguchi for kindly showing him their experimental results prior to publication and for valuable discussions. Many interesting conversations with colleagues of the research groups under Professor Yasushi Wada and Professor Masuo Suzuki are also acknowledged. Especial thanks are due to Miss K. Terai for typing of the manuscript. Finally the author's gratitude is dedicated to his parents for many years of upbringing and encouragements.

CONTENTS

List of papers submitted for the requirement of the Degree

List of papers added for references

Chapter I. Introduction	1
§1.1 Solitons and Kinks in Nonlinear Systems	1
§1.2 Kink-Phonon Interactions in the ϕ^4 System	10
§1.3 Solitons in trans-Polyacetylene	16
§1.4 Soliton-Phonon Interactions in trans-Polyacetylene	31
§1.5 Outline of the Thesis	38
References	42
Chapter II. Brownian-like Motion of Kinks in One-Dimensional ϕ^4 System	49
§2.1 Introduction	49
§2.2 The ϕ^4 Model and the Collective Coordinate Method	53
§2.3 Friction of the Lowest Order	62
§2.4 Friction of the Next Order	68
§2.5 Diffusion Constant and Fluctuation-Dissipation Theorem of the Kink Motion	75
§2.6 Summary and Discussion	80
Appendix 2.A The Sine-Gordon Case	88
Appendix 2.B Velocity Autocorrelation Function	89
Appendix 2.C Diffusion Constant D_ω	92
Appendix 2.D Interaction Hamiltonians and Vertex Function $C_{n,m}$	97
Appendix 2.E Details of Calculations	101
References	117

Chapter III. Brownian Motion of a Soliton in	
trans-Polyacetylene	118
§3.1 Introduction	118
§3.2 Collective Coordinate Method for trans-(CH) _x	120
§3.3 Friction Function	129
§3.4 Diffusion Constant	136
§3.5 Quantum Corrections	139
§3.6 Summary and Discussion	144
Appendix 3.A Dynamical Component of $\Gamma_t^{(0)}(\omega)$	146
References	149
Chapter IV. Peierls Potential for a Soliton in	
Su-Schrieffer-Heeger's Model	150
§4.1 Introduction	150
§4.2 Soliton Solutions	152
§4.3 Peierls Potential Barrier of Solitons	158
§4.4 Discussion	167
References	169
Chapter V. Summary, Future Problems, and Discussion	170
References	176

FIGURE CONTENTS

Chapter I.		Fig. 3.3	--- 143
Fig. 1.1	--- 6	Chapter IV.	
Fig. 1.2	--- 6	Fig. 4.1	--- 155
Fig. 1.3	--- 8	Fig. 4.2	--- 157
Fig. 1.4	--- 14	Fig. 4.3	--- 159
Fig. 1.5	--- 18	Fig. 4.4	--- 161
Fig. 1.6	--- 18	Fig. 4.5	--- 162
Fig. 1.7	--- 20	Fig. 4.6	--- 163
Fig. 1.8	--- 22	Fig. 4.7	--- 165
Fig. 1.9	--- 25	Fig. 4.8	--- 166
Fig. 1.10	--- 27		
Fig. 1.11	--- 29		
Fig. 1.12	--- 29		
Fig. 1.13	--- 35		
Chapter II.			
Fig. 2.1	--- 60		
Fig. 2.2	--- 60		
Fig. 2.3	--- 65		
Fig. 2.4	--- 71		
Fig. 2.5	--- 71		
Fig. 2.6	--- 78		
Fig. 2.7	--- 79		
Fig. 2.8	--- 111		
Chapter III.			
Fig. 3.1	--- 128		
Fig. 3.2	--- 138		

List of papers submitted for the requirement of the Degree

- 1) Viscosity of a Kink in the One-Dimensional ϕ^4 System.
M. Ogata and Y. Wada: J. Phys. Soc. Jpn. 54 (1985) 3425.
- 2) Brownian-like Motion of a One-Dimensional ϕ^4 Kink and
Fluctuation-Dissipation Theorem.
M. Ogata and Y. Wada: J. Phys. Soc. Jpn. 55 (1986) 1252.
- 3) Brownian Motion of a Soliton in trans-Polyacetylene. I.
Random Walk Mechanism.
M. Ogata, A. Terai and Y. Wada: J. Phys. Soc. Jpn. 55 (1986)
2305.
- 4) Brownian Motion of a Soliton in trans-Polyacetylene. II.
Mechanism of Ordinary Brownian Motion.
M. Ogata, A. Terai and Y. Wada: to be submitted to J. Phys.
Soc. Jpn.
- 5) Peierls Potential of Solitons in trans-Polyacetylene.
M. Ogata: to be submitted to J. Phys. Soc. Jpn.

List of papers added for references

- 1) Momentum Transfer between a Kink and a Phonon in the One-Dimensional ϕ^4 System.

M. Ogata and Y. Wada: J. Phys. Soc. Jpn. **53** (1984) 3855.

- 2) Soliton-Phonon Interactions in trans-Polyacetylene.

A. Terai, M. Ogata and Y. Wada: J. Phys. Soc. Jpn. **55** (1986) 2296.

Chapter I. Introduction

§1.1. Solitons and Kinks in Nonlinear Systems

In the last twenty years, a new concept of "soliton" has been constructed and developed in nonlinear physics. Notion of the soliton was first introduced by Zabusky and Kruskal¹⁾, who carried out a computer simulation of Korteweg- de Vries (KdV) equation²⁾ in 1965. They observed that localized solitary waves do not change their shapes or velocities after collisions and behave as if they were noninteracting particles. It was a great impact that such nonlinear excitations, which are particular solutions of the equation, should not decay into other modes immediately. Similar phenomenon had been observed in a computer simulation of sine-Gordon equation performed by Perring and Skyrme in 1962.³⁾

Since then, it has become apparent that the systems bearing the solitons have very beautiful mathematical structure.⁴⁾ At first, a powerful method was developed by Gardner, Greene, Kruskal and Miura⁵⁾ in 1967 and by Lax⁶⁾ in 1968, in order to solve the initial value problem of the KdV equation. This method is called the inverse scattering method (ISM), which transforms the nonlinear equation into a series of three linear equations. Up to now there are many nonlinear equations which can be solved by the inverse scattering method;⁷⁾ for example, nonlinear Schrödinger equation,⁸⁾ Toda Lattice,⁹⁾ KdV equation¹⁰⁾ and the sine-Gordon equation.¹¹⁾ They are called as completely integrable systems. Other methods for obtaining N-soliton

solutions have been devised. One is Hirota's direct method¹²⁾ and another is Bäcklund transformation.¹³⁾

The solitons have two important features:

(1) They are localized objects which can not be obtained by conventional perturbative expansion from one of the ground states; in other words, they are essentially nonlinear excitations. It is thus interesting to regard the system bearing the soliton as an unperturbed ground state.¹⁴⁾

(2) They are stable against collisions with other excitations; other solitons, small or large oscillations (breathers), and so on. The result of the collisions is perfectly known. The solitons only suffer shifts of their locations. This unique character of the solitons is mainly due to the fact that the system has an infinite number of conserved quantities.⁴⁾

For instance, the Hamiltonian of the sine-Gordon system has the form,

$$H = A \int \frac{dx}{\ell} \left\{ \frac{1}{2} \left(\frac{\partial \phi}{\partial t} \right)^2 + \frac{C_0^2}{2} \left(\frac{\partial \phi}{\partial x} \right)^2 + \omega_0^2 (1 - \cos \phi) \right\}, \quad (1.1.1)$$

with $\phi(x,t)$ being displacement field, ℓ lattice constant, C_0 coupling strength between neighboring ions, and ω_0 characteristic frequency of small vibrations at one of the potential minima. One soliton solution is given by

$$\begin{aligned} \phi_s(x) &= 4 \tan^{-1} \left\{ \exp(x/d) \right\}, \\ d &= C_0 / \omega_0, \end{aligned} \quad (1.1.2)$$

which is easily derived from integration of the equation of motion. It has been shown that the sine-Gordon system has an infinite number of conserved quantities.¹¹⁾

The completely integrable systems are, so to speak, ideal systems. They hold unique positions among the nonlinear systems. From the physical point of view, it is necessary to extend the concept of the soliton to excitations in non-integrable systems. As an example, we take up the ϕ^4 system whose Hamiltonian has the form,

$$H = A \int \frac{dx}{\ell} \left\{ \frac{1}{2} \left(\frac{\partial \phi}{\partial t} \right)^2 + \frac{c_0^2}{2} \left(\frac{\partial \phi}{\partial x} \right)^2 + \frac{\omega_0^2}{8\phi_0^2} (\phi^2 - \phi_0^2)^2 \right\}. \quad (1.1.3)$$

As in the sine-Gordon system, we can obtain a kink-type solution which connects the two different ground states, $\pm\phi_0$. It is expressed in an explicit form,

$$\phi_k(x) = \phi_0 \tanh(x/2d), \quad (1.1.4)$$

with $d=c_0/\omega_0$. We will call this solution as a kink, hereafter. Computer simulations show that the kink and the antikink do not pass through (or reflect) each other.¹⁵⁾ This implies that kink-antikink solution does not exist in the ϕ^4 system. Furthermore, this system is considered to have only two conserved quantities; one is the total momentum and the other is the total energy.

Nonlinear and localized solutions in the non-integrable systems will decay into other modes after a long time. However, if their life time is long enough compared with the time scale we are interested in, it is useful to regard them as elementary

excitations. From this point of view, many works have been carried out in various fields of physics:¹⁶⁾ A fluxon in a Josephson junction,¹⁷⁾ domain walls in magnetic systems,¹⁸⁾ excitations in one-dimensional polymer chains,¹⁹⁾ charge-density-wave systems,²⁰⁾ biological systems,²¹⁾ field theory and elementary particle physics,²²⁾ and so on.

In statistical mechanics, the concept of the soliton has been widely introduced. Krumhansl and Schrieffer²³⁾ studied the thermodynamic properties of the ϕ^4 model, assuming that the system was composed of non-interacting kinks and usual phonon-like modes. In this ideal gas phenomenology, static properties such as the free energy and the equal time correlation functions were calculated. Furthermore, Currie et al. pointed out that the kink-phonon interaction must be taken into account through a self-energy correction of the kink.²⁴⁾ It has been established that the ideal gas phenomenology reproduces the exact results obtained by transfer integral method.^{25,26)}

There are some other approaches to the statistical mechanics of the soliton (kink) bearing systems.^{27,28)} Recently the path integral approach using collective coordinate method was performed.²⁹⁾ In this method, the location of the soliton (kink) was introduced as a collective coordinate. This approach also reproduces the exact results.

On the contrary, dynamical aspects of the soliton (kink) bearing systems have not been discussed by the transfer integral method. They have been studied in the ideal soliton (kink) gas phenomenology. Krumhansl and Schrieffer²³⁾ showed that the kink

motion contributes to the appearance of a central peak in the structure factor $S(k, \omega)$. The dynamical properties in the sine-Gordon system was also studied in the ideal gas phenomenology.³⁰⁾ Effect of the kink-phonon interaction on $S(k, \omega)$ was also investigated, by taking account of the phonon phase shift.³¹⁾

Indeed in the completely integrable systems, collisions between the solitons and the other excitations lead only to the shifts of their locations and the phases. Therefore the ideal soliton gas phenomenology will be justified in this case. On the contrary, in the non-integrable systems, interesting and highly nontrivial interactions can occur in the collision. It is thus quite important to study the dynamics of the kinks.

Various kinds of phenomena were observed in computer simulations. Koehler, Bishop, Krumhansl and Schrieffer carried out a molecular dynamics study of the ϕ^4 chain, using the deterministic equation of motion.³²⁾ In Fig. 1.1, typical displacements are plotted as a series of snapshots in time. Koehler et al. observed that the kinks did not carry out free translational motion between collisions with other kinks. Rather, isolated kinks appeared to undergo Brownian-like motion. Schneider and Stoll³³⁾ also observed similar Brownian-like motion. The time evolution of the displacement pattern is shown in Fig. 1.2. Lattice sites with positive displacement are marked by a black dot, while lattice sites with negative displacement are not shown. Propagating kinks will then be represented by a line separating black and white regions. In Fig. 1.2, we can see that there are various kinds of events as well as the Brownian-like motion of the kinks: ①~⑤.

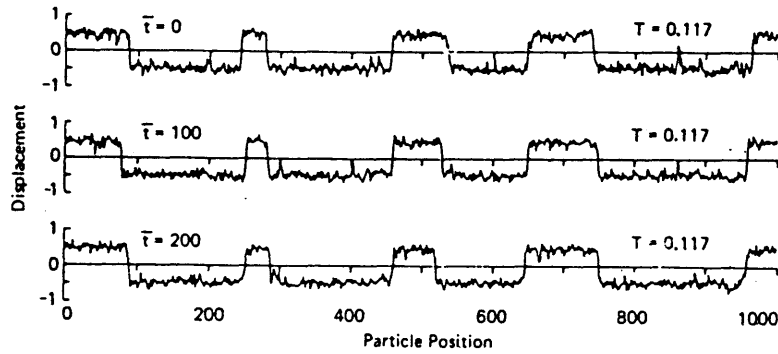


Fig. 1.1 Displacements at 1000 lattice sites as a series of snapshots in time for $T=0.117$; $t=0, 100$ and 200 . Here the temperature is estimated from the time average of the kinetic energy. It is normalized by four times of the potential barrier between the two minima. The excitation energy of the kink is $2\sqrt{2/3}$ in this normalization. (Cited from Ref. 32, T.R. Koehler et al.: Solid State Commun. 17 (1975) 1515.)

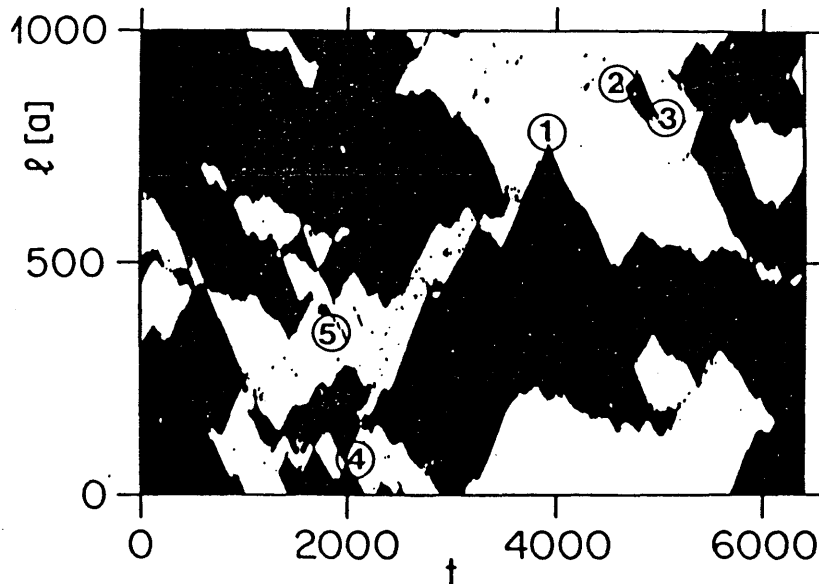


Fig. 1.2 Time evolution of the displacement patterns in the ϕ^4 system for $T=0.00448$. The potential barrier is 0.001875 and $E_k=0.0224$ in this simulation. Lattice sites with positive displacement are marked by a black dot, and lattice sites with negative displacement are not shown. The marked events denote: ① kink reverses its velocity, ② creation of a kink-antikink pair, ③ kink-antikink collision and decay into "phonons," ④ kink-antikink collision, ⑤ breather-like features. (Cited from Ref. 33, T. Schneider and E. Stoll: Phys. Rev. B23 (1981) 4631.)

The propagation properties are distinctly different from those of the sine-Gordon solitons. In Fig. 1.3, the time evolution in the sine-Gordon system is shown. Dots represent lattice sites passing the maximum of the single-site potential. The soliton motion is then characterized by the line patterns. The occurrence of bubbles is attributed to large amplitude breathers. As expected, almost free propagations of the solitons are observed. We can also see that the soliton-soliton ① and soliton-antisoliton ② collisions are associated only with a phase shift without changing the velocity.

In the present thesis, the Brownian-like motion is taken up and discussed. It is, however, worth while referring to several other works on the kink dynamics.

For example, kink-antikink collision was extensively studied by means of computer simulation.^{15,34)} On energetic grounds, the kink and the antikink can not pass through each other in the ϕ^4 system. There are two possible final states of the kink-antikink collision; the kink and antikink reflect each other, or they are trapped by their mutual attraction. Computer simulation showed that, over a small range of initial velocities, intervals of initial relative velocity for which the trapping occurs alternate with region for which the reflection takes place. This structure was accounted for in terms of a resonant energy exchange between the translational motion of the two kinks and a small oscillation mode ("amplitude oscillation mode" or "shape mode") localized at each kink location.¹⁵⁾

Another example is numerical studies of the kink dynamics in highly discrete models.^{35,36)} As shown by Peyrard and Kruskal,

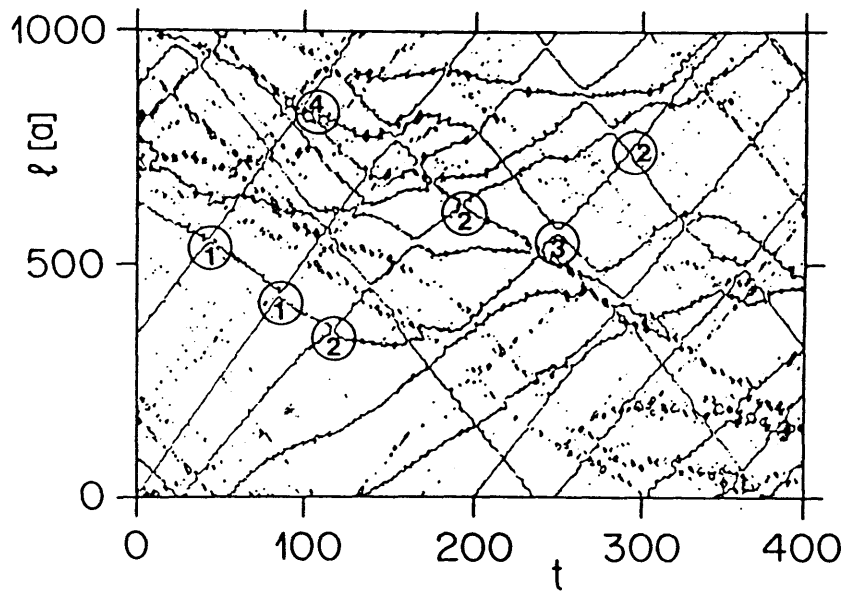


Fig. 1.3 Time evolution of the lattice patterns in the sine-Gordon system for $T=12.5$. (Potential barrier is 2.0 and $E_s=43.244$ in this case.) Dots represent lattice sites s passing the maximum of the single-site potential ($\pi, 3\pi, \dots$). The marked collisions denote: ① soliton-soliton collision ($0-2\pi \rightarrow 2\pi-4\pi$), ② soliton-antisoliton collision, ③ breather creation, ④ breather decay.
(Cited from Ref. 33, T. Schneider and E. Stoll: Phys. Rev. B23 (1981) 4631.)

there are some particular velocities at which the kink can propagate with a little energy dissipation. This phenomenon was explained by a simple model that the kink moving at a velocity v can excite the phonon mode whose wave number k satisfies the following resonance condition,

$$\omega_k = vk, \quad (1.1.5)$$

where ω_k is the dispersion of the phonon in the discrete system. Whether the kink tends to dissipate energy or not depends on the number of k 's satisfying the above condition.

§1.2. Kink-Phonon Interactions in the ϕ^4 System

From the configurations in Fig. 1.1, it is supposed that the Brownian-like motion of the ϕ^4 kink is induced by nonlinear interactions between the kink and thermally excited phonons. From this point of view, the motion of the kink was discussed by Wada and Schrieffer.³⁷⁾ In this section, we briefly summarize the kink-phonon interactions in the ϕ^4 system.

If the temperature is low enough, the interactions between kinks are negligible and the amplitudes of thermally excited phonons are small. Then, the interaction between the kink and the phonons can be investigated using a perturbation method, the phonon amplitude being the small parameter.³⁸⁾ It is worth while noting that this method differs from the conventional perturbation in the sense that the kink solution is regarded as the ground state.

The complete set of the linear modes around one kink solution, $\phi_K(x)$, can be obtained in the ϕ^4 system.^{14,39)} If there is a small deviation around the kink, we can introduce the deviation field $\psi(x,t)$ by

$$\phi(x,t) = \phi_K(x) + \psi(x,t). \quad (1.2.1)$$

Substituting eq. (1.2.1) into the equation of motion and linearizing with respect to $\psi(x,t)$, we obtain the following equation,

$$\frac{\partial^2 \psi}{\partial t^2} - c_0^2 \frac{\partial^2 \psi}{\partial x^2} + \left(\omega_0^2 - \frac{3\omega_0^2}{2\omega \sinh^2(x/2d)} \right) \psi = 0. \quad (1.2.2)$$

Eigenfunctions and eigenfrequencies of eq. (1.2.2) can be calculated analytically. Their explicit forms are^{14,39)}

$$\begin{aligned} 1) \quad \omega^2 &= 0, & \varphi_0(x) &= \sqrt{\frac{3}{8d}} \cosh^{-2}(x/2d), \\ 2) \quad \omega^2 &= \frac{3}{4} \omega_0^2 \equiv \omega_1^2, & \varphi_1(x) &= \sqrt{\frac{3}{4d}} \sinh(x/2d) \cosh^{-2}(x/2d), \\ 3) \quad \omega^2 &= \omega_0^2 + c_0^2 k^2 = \omega_k^2, \end{aligned}$$

$$\begin{aligned} \varphi_k(x) &= \frac{1}{\sqrt{4L(1+k^2d^2)(1+4k^2d^2)}} e^{ikx} \\ &\times \left\{ 3 \tanh^2(x/2d) - 6ikd \tanh(x/2d) - 1 - 4k^2d^2 \right\}, \end{aligned}$$

(1.2.3)

with L being the length of the system. These eigenfunctions (linear modes) satisfy the orthonormality conditions and the completeness relation.

These three kinds of the eigenfunctions have simple physical interpretations. The function $\varphi_0(x)$ corresponds to the "Goldstone mode" which arises owing to the translational symmetry breaking by the presence of the kink. If the shift of the location of the kink $\delta(t)$ is small enough in comparison with d , we can expand the kink solution as follows:

$$\phi_k(x - \delta(t)) = \phi_k(x) - \delta(t) \frac{d\phi_k(x)}{dx} + O((\delta/d)^2).$$

(1.2.4)

Since the Goldstone mode is proportional to $d\phi_k(x)/dx$, the coefficient of the mode gives the first approximation of the kink

shift $\delta(t)$.

When the function $\varphi_1(x)$ is added to the kink solution, the center of the kink does not move, but its form undergoes a vibration with frequency ω_1 . We may call $\varphi_1(x)$ as an "amplitude oscillation mode".

The third function $\varphi_k(x)$ corresponds to the "phonon mode". Except in the vicinity of the kink, it is in the form of a propagating plane wave,

$$\begin{aligned}\varphi_k(x) &\longrightarrow \frac{1}{\sqrt{L}} e^{ikx + \frac{i}{2}\Delta(k)}, & (x \longrightarrow \infty) \\ &\longrightarrow \frac{1}{\sqrt{L}} e^{ikx - \frac{i}{2}\Delta(k)}, & (x \longrightarrow -\infty)\end{aligned}\quad (1.2.5)$$

where $\Delta(k)$ is a phase shift,

$$\Delta(k) = 2 \tan^{-1} \left(\frac{3kd}{2k^2d^2 - 1} \right). \quad (1.2.6)$$

The presence of the kink yields an effective potential in the Schrödinger-type equation, (1.2.2). In the ϕ^4 model, this effective potential is reflectionless; in other words, the phonon is not reflected by the presence of the kink but suffers only the phase shift. The phonon dispersion is identical to that of small oscillations around one of the potential minima in the case of the absence of the kink.

Nonlinear interactions between the kink and the phonon was studied by Wada and Schrieffer.³⁷⁾ They investigated the kink-phonon collision by integrating the equation of motion in a

perturbation with respect to the phonon amplitude. A schematic view of the collision is shown in Fig. 1.4. In the lowest order, the phonon suffers only a phase shift and the kink seems to be transparent to the phonon. In the second order approximation, the nonlinear interaction generates higher harmonics with typical frequencies zero and $\pm 2\omega_q$, where ω_q is the frequency of the incident wave packet phonon. The former gives rise to a shift of the kink in the opposite direction to the propagation of the incident phonon (see Fig. 1.4(b)). The latter corresponds to a transmitted higher harmonics as well as a reflected phonon.

When the phonons are thermally excited and collide with the kink at random, the above shifts lead to a random walk of the kink. Wada and Schrieffer calculated the diffusion constant of this diffusive motion by

$$D = \lim_{t \rightarrow \infty} \langle \delta(t)^2 \rangle / 2t, \quad (1.2.7)$$

where $\delta(t)$ was the shift of the kink position and the brackets indicated thermal average in a sector where the kink is at rest initially. Since the shift $\delta(t)$ was proportional to square of the amplitude of the incident phonon, the diffusion constant calculated by eq. (1.2.7) was proportional to $(k_B T)^2$.³⁷⁾

Theodorakopoulos discussed the diffusive motion of the ϕ^4 -kink phenomenologically.⁴⁰⁾ The diffusion constant he obtained was also proportional to $(k_B T)^2$, but it was four times as large as the result of Wada and Schrieffer. This difference will be discussed in Chapter II.

Higher order processes yield other phenomena. A computer

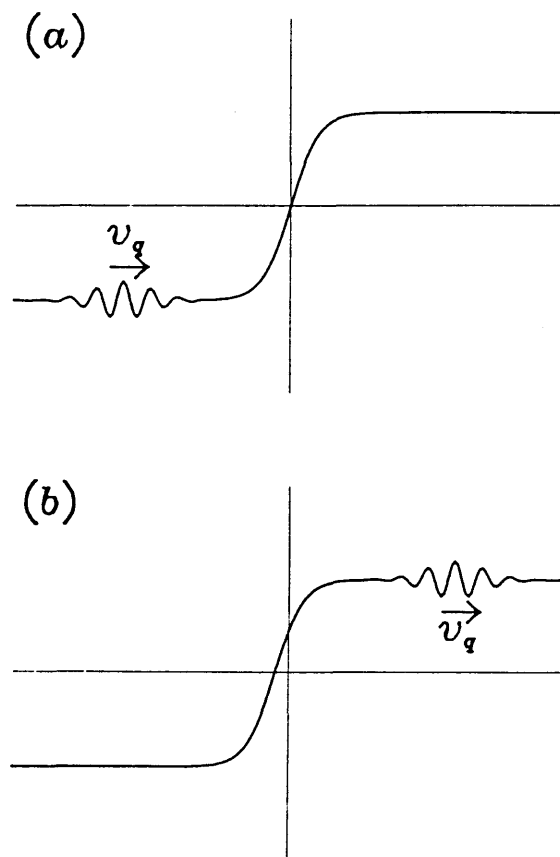


Fig. 1.4 The initial condition (a). A kink is located at the origin. A wave packet, moving with a group velocity v_g approaches the kink from the left. The final state (b). The kink is shifted in the direction of the initial phonon location.

simulation of the ϕ^4 -kink has shown that the wave packet phonon also transfers momentum to the kink in the collision.⁴¹⁾ The velocity, which the kink gains after the collision, is proportional to fourth power of the incident phonon amplitude. Simple application of energy and momentum conservation laws gives an expression of the velocity, which agrees with the result of the simulation.⁴¹⁾ The same expression can be obtained by extending the Wada and Schrieffer's perturbative calculation to the fourth order.⁴²⁾ This momentum transfer is mainly due to the fact that the second order phonons with frequencies $\pm 2\omega_{\vec{q}}$ carry away the momentum. The effective interaction between the kink and the phonon is attractive.

In an ordinary Brownian system, the momentum exchange between fluid molecules and a Brownian particle leads to the viscosity of the particle. If this applies to the kink in the ϕ^4 system, it is predicted that the momentum transfer would give rise to a friction (viscosity) in the ϕ^4 kink motion. In this case the friction would be proportional to $(k_B T)^2$, because the momentum transfer is in the fourth order with respect to the phonon amplitude.

If we substitute this friction Γ into the Einstein relation, $D = k_B T / M \Gamma$, we obtain the diffusion constant proportional to $(k_B T)^{-1}$, where M is "mass" of the kink. This temperature dependence is apparently different from that of the diffusion constant calculated by Wada and Schrieffer.³⁷⁾ One of the main purposes of the present thesis is to calculate the friction and to clarify the relation between the obtained friction and the Wada and Schrieffer's diffusion constant.

§1.3 Solitons in trans-Polyacetylene

Over the past several years, static and dynamical properties of trans-polyacetylene, [trans-(CH)_x], have been extensively studied.⁴³⁾ It has become apparent that there are mobile unpaired spins, presumably solitons, which are more mobile at higher temperatures. However, the soliton motion in real samples is considered to be very complicated owing to various kinds of disorder; network of fibres, impurities, and defects. In this thesis, we study the diffusion constant of the soliton in simple models proposed for polyacetylene, to find out possible mechanisms of the diffusive motion and to discuss what is needed for interpretation of the experiments.

For polyacetylene, the concept of the soliton was first introduced by Su, Schrieffer and Heeger.^{19,44)} They proposed the following Hamiltonian, (SSH model),

$$H = \frac{M}{2} \sum_n \dot{u}_n^2 + \frac{K}{2} \sum_n (u_{n+1} - u_n)^2 - \sum_{n,s} [t_0 - \alpha(u_{n+1} - u_n)] (C_{n+1,s}^\dagger C_{n,s} + C_{n,s}^\dagger C_{n+1,s}), \quad (1.3.1)$$

where u_n is the displacement of the n -th (CH) unit from its undimerized equilibrium position, $C_{n,s}^\dagger$ and $C_{n,s}$ the creation and annihilation operators of a π -electron with spin s at the n -th site, respectively, M the mass of the (CH) unit, K the spring constant mainly due to σ -bonds, t_0 the nearest-neighbor transfer integral of the π -electrons in the undimerized state, and α the coupling constant which comes from the modulation of the transfer integral due to the change of the nearest-neighbor distance.

Figure 1.5 shows two degenerate ground states where lattice dimerization is realized owing to the Peierls instability.⁴⁵⁾ In this case, the lattice displacement is

$$U_n = (-1)^n U_0 , \quad (1.3.2)$$

and the electronic eigenvalues are

$$\begin{aligned} \varepsilon_{k,s} &= \pm E_k , \\ E_k &= 2 \sqrt{t_0^2 \cos^2 ka + 4 \alpha^2 U_0^2 \sin^2 ka} , \end{aligned} \quad (1.3.3)$$

with a being the lattice constant. The magnitude of u_0 is determined so as to minimize the total energy,

$$\frac{K}{2} \sum_n (U_{n+1} - U_n)^2 + \sum_{k,s}' \varepsilon_{k,s} , \quad (1.3.4)$$

where the prime on the summation means the sum over the occupied states (half-filled).

A kink-type excitation connecting the two ground states is called as a "soliton" in $\text{trans}-(\text{CH})_x$. In this case, there appears one electronic state at $\varepsilon=0$, the gap center, for each spin orientation. As discussed by Su, Schrieffer and Heeger,¹⁹⁾ a neutral soliton is supposed to have an unpaired spin, while a charged soliton carries no spins. This unique relation is called as the reversed spin-charge relation.

In the following, we summarize the experimental results especially on the dynamics of the solitons in $\text{trans}-(\text{CH})_x$.

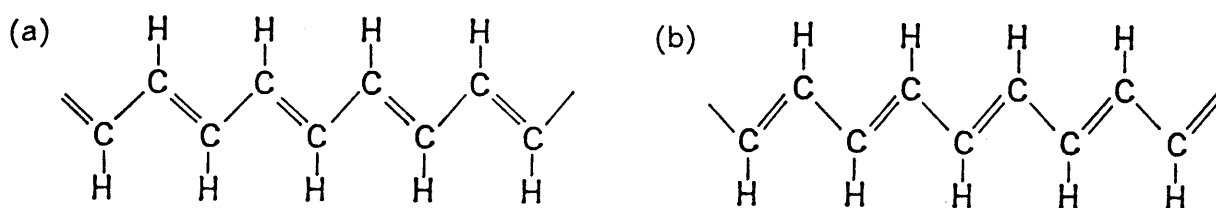


Fig. 1.5 Two degenerate ground state of trans-polyacetylene. Lattice dimerization is realized owing to the Peierls instability.

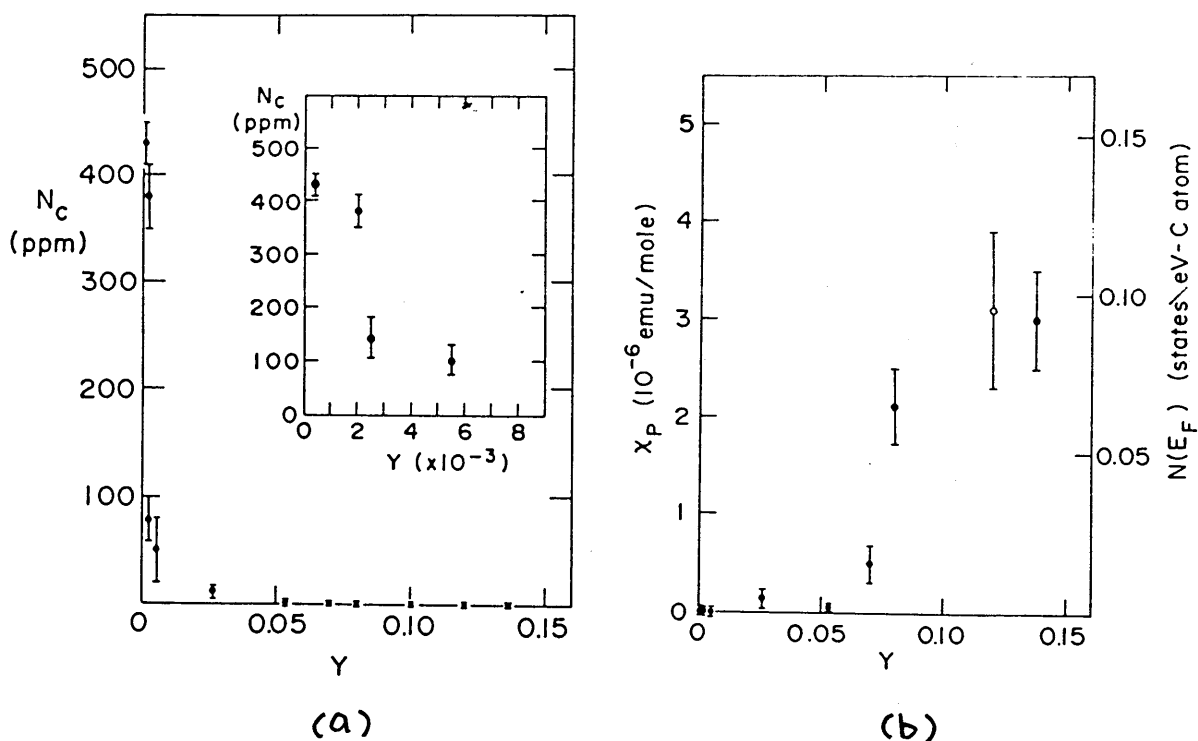


Fig. 1.6 (a) Number of unpaired spins satisfying Curie-law (N_c) as a function of (A_{F5}) dopant concentration γ . The low doping range is shown on an expanded scale in the inset. (b) Pauli susceptibility χ_p as a function of γ . The right-hand scale gives the implied density of states of the Fermi energy. The open-circle datum point is from Ref. 46. (Cited from Ref. 47, S. Ikehata et al.: Phys. Rev. Lett. **45** (1980) 1123.)

The existence of the solitons was verified by observing the reversed spin-charge relation. From the spin susceptibility, the number of unpaired spins N_C and Pauli susceptibility χ_P were estimated as a function of the A_5F_5 -dopant concentration y .^{46,47)} (see Fig. 1.6) In the range $0.005 < y < 0.05$, χ_P does not turn on, whereas the transport data indicate that the polymer is an excellent conductor. This implies that the charge carriers generated by dilute doping are spinless.⁴⁷⁾ It is consistent with the soliton doping mechanism. The rapid decrease of N_C is probably due to ionization of neutral solitons which have existed in the undoped polyacetylene intrinsically.

The reversed spin-charge relation was also shown in the ESR studies of $\text{trans}-(\text{CH})_x$ carried out during photoexcitation.⁴⁸⁾ Flood et al. estimated the number of photoinduced unpaired spins. It was 10^{-2} times as large as that of photogenerated charge carriers.⁴⁹⁾ From these results, Flood et al. concluded that (1) the photogenerated charge carriers were spinless and (2) the branching ratio (photogeneration of charged solitons compared to neutral solitons) was at least 10^2 . The latter conclusion is consistent with a theoretical calculation⁵⁰⁾ in the SSH model.

NMR and ESR experiments on undoped polyacetylene were carried out extensively to study the motion of unpaired spins in it. At first, the features of the spin motion was verified by the motional narrowing of the ESR line⁵¹⁻⁵³⁾ and by the observation of the Overhauser effect.⁵⁴⁻⁵⁷⁾

The temperature dependence of the ESR line widths is displayed in Fig. 1.7, where ΔH becomes smaller as the

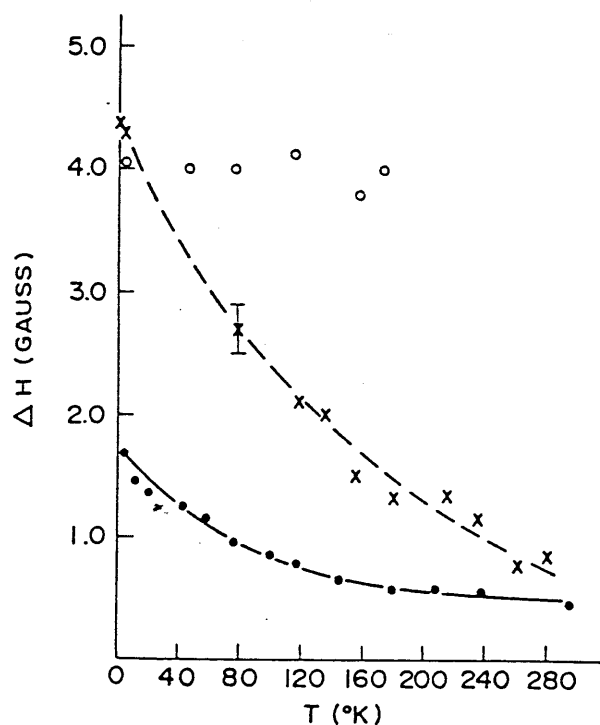
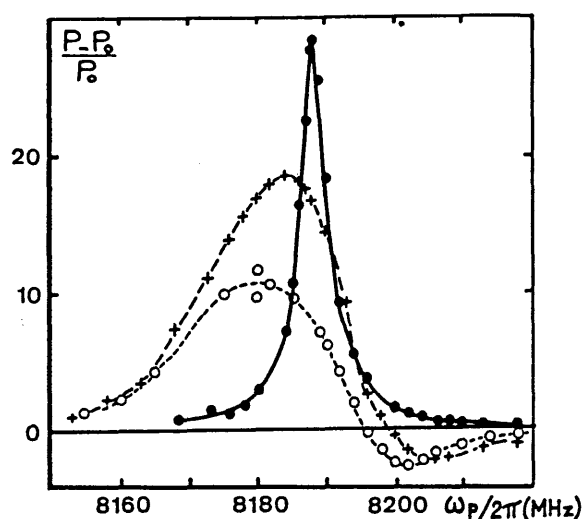


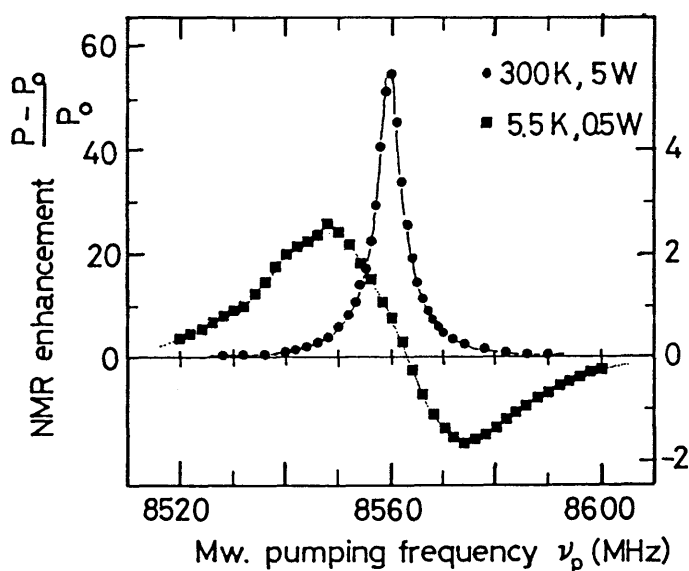
Fig. 1.7 Temperature dependence of the ESR line width of undoped (xxx) trans-(CH)_x; (ooo) trans-(CD)_x; (ooo) 80% cis-rich (CD)_x. The difference between (CH)_x and (CD)_x indicates that the hyperfine interaction_x is the major source of the line width. (Cited from Ref. 52, B.R. Weinberger et al.: J. Chem. Phys. 72 (1980) 4749.)

temperature increases.^{51,52)} Similar motional narrowing was observed in the ESR study by spin echo method.⁵³⁾ It was pointed out that the ESR line width showed inhomogeneous broadening below 170 K. These results indicate that the unpaired spin becomes less mobile as the temperature decreases. As seen in Fig. 1.7, the cis-rich sample exhibits resonances with weakly temperature dependent line width, apparently not motionally narrowed. This is consistent with the soliton picture, because the unpaired spin observed in the cis-rich sample are associated with small length of trans isomer locked in by regions of cis.

Another evidence of the mobile unpaired spin was shown in the dynamical nuclear polarization (DNP) experiments.⁵⁴⁻⁵⁷⁾ This experiment consists of observing the NMR while pumping the electronic system near $\hbar\omega_e$, the electronic Zeeman energy. Two limiting results may occur according to whether the electron-nuclear coupling is static or dynamic.⁵⁸⁾ If the electronic spin is moving, it is possible to enhance the NMR signal by pumping the electronic system at $\hbar\omega_e$. This is the Overhauser effect (OE). On the other hand, in the static case, the NMR signal can be enhanced by pumping at $\hbar\omega_e \pm \hbar\omega_I$. This is the so-called "solid-state effect" (SSE). In Fig. 1.8(a), the enhancement of the NMR signal is shown for undoped $(CH)_x$ samples with different degrees of cis-trans content.⁵⁴⁾ In the all-trans- $(CH)_x$, a pure OE is seen which means that the electronic spins are moving at least a frequency $\omega_e \sim 5 \times 10^{10}$ rad/sec. On the contrary, in mixed samples, both OE and SSE are observed. This implies that the unpaired spins are mobile in trans- $(CH)_x$ and fixed in cis-rich samples. Temperature dependence of the enhancement of NMR signal



(a)



(b)

Fig. 1.8 Results of dynamical nuclear polarization experiments. (a) Enhancement of proton NMR amplitude (P) as a function of the pumping frequency ω_p near $\omega_p/2\pi=8190$ MHz for (○) 50%, (+) 65%, and (●) 100% trans-content undoped $(CH)_x$. P_0 is the NMR signal amplitude without pumping. (Cited from Ref. 54, M. Nechtschein et al.: Phys. Rev. Lett. 44 (1980) 356.)

(b) Enhancement of proton NMR amplitude P as a function of ω_p for undoped trans- $(CH)_x$ at (●) 300K and (■) 5.5K. Microwave pumping power is reduced to avoid heating. (Cited from Ref. 56, K. Holczer et al.: Solid State Commun. 39 (1981) 881.)

for $\text{trans}-(\text{CH})_x$ is shown in Fig. 1.8(b), where a mixture of SSE and small OE is observed at 5.5 K.⁵⁶⁾

Both the ESR line width and DNP results indicate that there are mobile unpaired spins in $\text{trans}-(\text{CH})_x$, which become less mobile or fixed as the temperature decreases. In order to identify the unpaired spins with the neutral solitons, however, dimensionality of the spin dynamics must be clarified. It has been discussed in the analyses of (1) ESR line shape,^{52,55)} (2) phase memory time in spin echo experiments,⁵³⁾ (3) frequency dependence of proton NMR T_1 ,^{54,59)} and (4) frequency dependence of ESR T_1 .⁶²⁾

(1) The line shape of $\text{trans}-(\text{CH})_x$ was compared with those expected in the one- and three-dimensional cases.⁵²⁾ The experimental absorption line lay between the one- and three-dimensional line shapes. Weinberger et al. analyzed their results to estimate the intra- and inter-chain diffusion rates (or correlation times).⁵²⁾ They found, at room temperature, $D_{\parallel} \sim 10^{11} \text{sec}^{-1}$ for intra-chain and $D_{\perp} \sim 6 \times 10^7 \text{sec}^{-1}$ for inter-chain diffusion rate.

(2) From the spin echo experiment, Shiren et al. also estimated the diffusion rate.⁵³⁾ They analyzed the phase memory time, T_M , in order to avoid the ambiguity due to the inhomogeneous broadening below 170 K. The obtained diffusion rate showed a strong temperature dependence for $T > 40$ K. They concluded that the largest possible diffusion rate was 10^{11}sec^{-1} at room temperature, which was consistent with the results of Weinberger et al..⁵²⁾

(3) Dimensionality of the spin motion affects the frequency dependence of the nuclear spin lattice relaxation time, T_1^{-1} , which is proportional to the spectral density function $f(\omega_N)$ with ω_N being the nuclear Larmor frequency. In one dimension, $f(\omega) = (2D_{\parallel}\omega)^{-1/2}$, whereas in two dimension $f(\omega) \propto \ln(1/\omega)$ and in three it is frequency independent. Nechtschein et al.^{54,59} showed that T_1^{-1} was proportional to $\omega_N^{-1/2}$. The diffusion rates they estimated were $D_{\parallel} \sim 6 \times 10^{13} \text{ sec}^{-1}$ and $D_{\perp} \lesssim 6 \times 10^7 \text{ sec}^{-1}$ at room temperature.⁵⁴⁾

It is apparent that there is inconsistency between the magnitude of the diffusion rate obtained by NMR T_1 ($D_{\parallel} \sim 6 \times 10^{13} \text{ sec}^{-1}$) and that obtained from the ESR line shape ($D_{\parallel} \sim 10^{11} \text{ sec}^{-1}$). In order to explain this inconsistency, Holczer et al. suggested the existence of two spin species (diffusive spin and localized spin).⁵⁵⁾ They considered that a small amount of the localized spins, about 10%, completely masked the ESR line features of a large majority of the diffusive spins, while they had only negligible effect on the nuclear relaxation. The diffusive spins were supposed to be trapped by residual oxygen and turn into the localized spins. In their model, however, the concentration of each spin species must be determined from some phenomenological models or from other experimental data. For example, it was determined so that the frequency dependence of ESR line width might be reproduced consistently.⁵⁹⁾ By this prescription, Nechtschein et al. estimated the diffusion rate in the temperature range 4-300 K.⁵⁹⁾ Their result is shown in Fig. 1.9. The proton relaxation rate, T_1^{-1} , was supposed to be proportional to $C/\sqrt{D_{\parallel}}\omega$, where C was the number of the diffusive spins

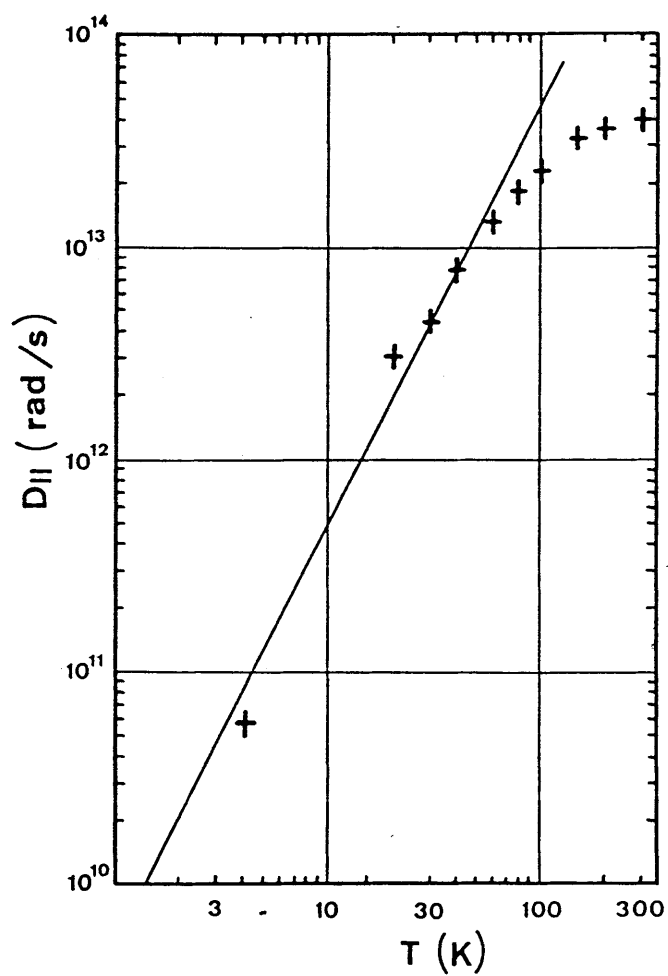


Fig. 1.9 Temperature dependence of the spin diffusion rate in $\text{trans}-(\text{CH})_x$, determined from combined analysis of proton relaxation time T_1 and ESR line width ΔH data. The solid straight line is the theoretical curve proportional to T^2 obtained in the ϕ^4 model by Wada and Schrieffer. (Cited from Ref. 59, M. Nechtschein et al.: Phys. Rev. B27 (1983) 61.)

determined by the above prescription. Owing to the trapping effect, C became fewer and fewer as the temperature decreased. On the other hand, the original data of T_1^{-1} also decreased with decreasing temperature. Consequently, the temperature dependence of $D_{||}$ was determined from delicate balance between T_1^{-1} and C .

There are two problems in the analysis of the NMR results. First, it was pointed out^{53,60)} that the same frequency dependence of T_1^{-1} can be observed in the nuclear relaxation due to spin diffusion to paramagnetic impurities.⁵⁸⁾ Second, T_1^{-1} of ^{13}C is frequency independent, as observed by Scott and Clarke.⁶¹⁾ This is not consistent either with the soliton picture or the spin diffusion to paramagnetic impurities. Because of these problems, the analysis of Nechtschein et al. is now open to question.

(4) Recently a new evidence of one-dimensional spin motion was provided by Mizoguchi, Kume and Shirakawa.⁶²⁾ They found $\omega^{-1/2}$ frequency dependence of ESR T_1 (see Fig. 1.10). In this case, the possibility of the spin diffusion to paramagnetic impurities is excluded, because there is a relaxation mechanism due to the hyperfine interaction (Fig. 1.10). The dependence of ESR T_1^{-1} on the spin concentration also contradicts the spin diffusion mechanism which predicts $T_1^{-1} \propto C^{1/4}$.

In order to determine the diffusion rate $D_{||}$, Mizoguchi et al. calculated T_1^{-1} by assuming the crystalline structure of polyacetylene chains. Comparing the expression of T_1^{-1} with the data in Fig. 1.10, they obtained $D_{||} = (3.7 \pm 1.6) \times 10^{13} \text{sec}^{-1}$ and $D_{||} = (1.1 \pm 0.5) \times 10^{13} \text{sec}^{-1}$ from the dipolar and hyperfine parts, respectively. These values are consistent with the NMR result of

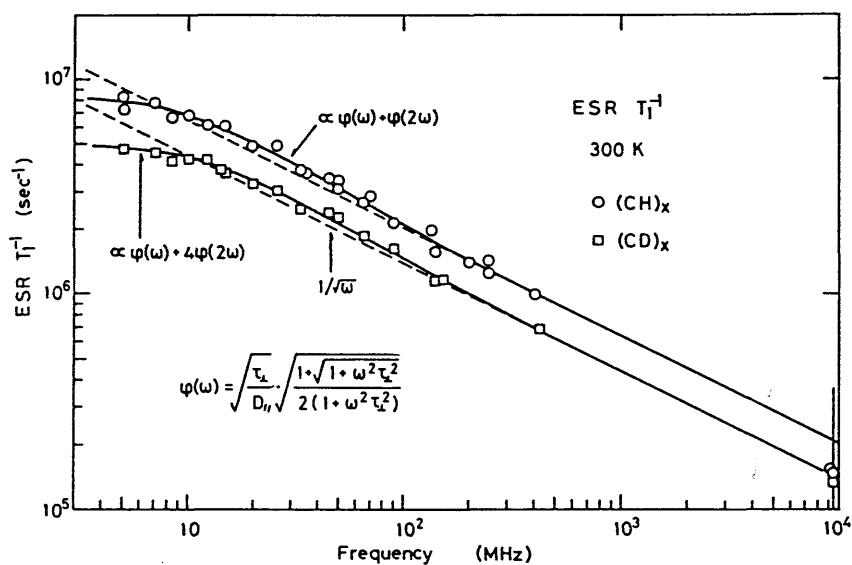


Fig. 1.10 Frequency dependence of ESR T_1^{-1} for trans- $(\text{CH})_x$ and $(\text{CD})_x$ at 300K. The solid curves are fittings using the spectral density function $\varphi(\omega)$ which represents the fluctuation of the local field due to the one-dimensional diffusive motion (D_{\parallel}) of the electron spins with a low frequency cut of (τ_L^{-1}) . For $(\text{CD})_x$, the dipolar interaction ($\varphi(\omega) + 4\varphi(2\omega)$) is considered, while for $(\text{CH})_x$ the hyperfine interaction ($\sim 3\varphi(\omega)$) is also taken into account. The data at X band are taken from other experiments. (Cited from Ref. 62, K. Mizoguchi et al.: Solid State Commun. 50 (1984) 213.)

Nechtschein et al..^{55,59)}

Mizoguchi and Kume⁶³⁾ also studied the frequency dependence of the ESR line width, in order to study the diffusion rate at low temperatures, where the analysis of ESR T_1^{-1} became difficult owing to the inhomogeneous broadening. As shown in Fig. 1.11, they divided the line width into three parts; $T_1'^{-1}$, $T_2'^{-1}$, and ΔH_{trap} . Then they estimated the concentration of trapped spins (solitons) from ΔH_{trap} . The diffusion rate was calculated from $T_1'^{-1}$ and $T_2'^{-1}$ with a correction of the trapping and a similar process to T_1 of ESR. The obtained diffusion rate is shown in Fig. 1.12, together with that obtained from NMR T_1 . Since both data agreed with each other very well, Mizoguchi and Kume suggested that the NMR T_1 might reflect the relaxation due to the one-dimensional spin motion.

There is, however, inconsistency with some other experiments. First, the secular part $T_2'^{-1}$, which represents a motionally narrowed line width due to the soliton diffusion, must correspond to the phase memory time T_M measured in the spin echo experiment.⁵³⁾ However the two experiments show that T_M is shorter than T_2' . Second, Mehring et al.⁶⁴⁾ carried out time resolved ESR experiment to distinguish between the contributions from three types of defects in polyacetylene; the mobile soliton, the trapped soliton and local defects. The diffusion rate was estimated from the line width corresponding to the mobile soliton. Their result was $D_{\parallel} = 4 \times 10^9 \text{ sec}^{-1}$, which was smaller than that of Mizoguchi et al.. Consistent explanation of these results remains a future problem.

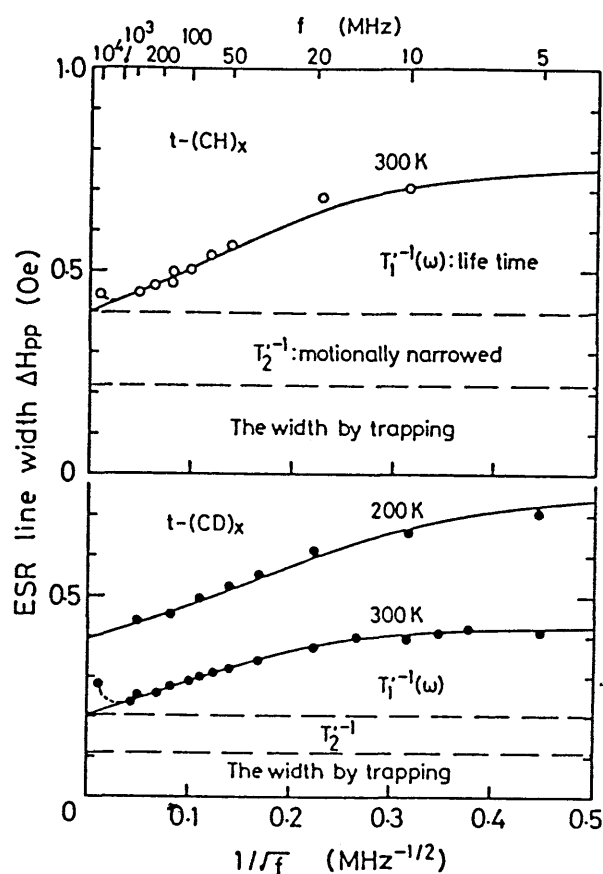


Fig. 1.11 Frequency dependence of the ESR line width for trans-(CH)_x at 300 K and for trans-(CD)_x at 200 K and 300 K. The line width was divided into three parts. (Cited from Ref. 63, K. Mizoguchi et al.: Mol. Cryst. Liq. Cryst. 117 (1985) 459.)

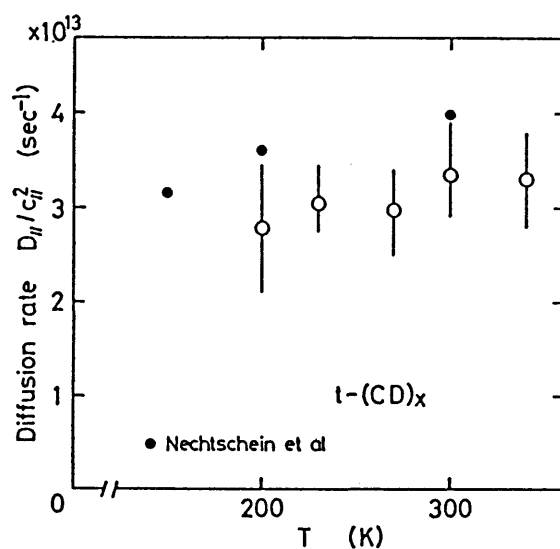


Fig. 1.12 Temperature dependence of one-dimensional diffusion rate, together with that obtained from NMR T_1 in Ref. 59. (Cited from K. Mizoguchi et al. Ref. 63.)

It is worth while noting that there are other kinds of experiments studying the soliton dynamics in polyacetylene. The first is μ^+ SR experiment,⁶⁵⁾ where the one-dimensional diffusive motion of the solitons was verified. The second example is dynamics of photoinduced excitations. From the time evolution of the polarization memory, Vardeny et al.⁶⁶⁾ estimated the diffusion rate $D_{||}(300K)=2.2\times 10^{14}\text{sec}^{-1}$ and $D_{||}(80K)=1.7\times 10^{14}\text{sec}^{-1}$, which were comparable to those obtained from NMR and ESR experiments. Shank et al.⁶⁷⁾ investigated the dynamics of the photoinduced absorption by a model of geminate recombination of the photoinduced excitations. They obtained $D_{||}(300K)=1\times 10^{13}\text{sec}^{-1}$ and $D_{||}(20K)=1\times 10^{12}\text{sec}^{-1}$

In summary, various experiments indicate that the solitons become more mobile at higher temperatures. However, it has not been possible to determine the diffusion rate unambiguously, especially at low temperatures.

§1.4. Soliton-Phonon Interactions in trans-Polyacetylene

In order to consider the soliton motion in polyacetylene, we summarize the soliton-phonon interaction in Takayama, Lin-Liu and Maki's (TLM) model,⁶⁸⁾ which is a continuum limit of the SSH model. In the continuum limit, the Hamiltonian (1.3.1) is transformed to

$$H = \frac{1}{2g^2} \int dx \left(\dot{\Delta}^2(x,t) + \omega_0^2 \Delta^2(x,t) \right) + \sum_s \int dx \psi_s^\dagger(x,t) \left[-i v_F \sigma_3 \frac{\partial}{\partial x} + \sigma_1 \Delta(x,t) \right] \psi_s(x,t), \quad (1.4.1)$$

where the coupling constant g , the bare optical phonon frequency ω_0 and the Fermi velocity v_F are defined by

$$g = 4\alpha \sqrt{\frac{a}{M}},$$

$$\omega_0^2 = \frac{4K}{M},$$

$$v_F = 2a t_0, \quad (1.4.2a)$$

respectively, σ_1 and σ_3 the Pauli matrices, and the order parameter $\Delta(x,t)$ is proportional to the continuum limit of the staggered lattice displacement,

$$\Delta(x,t) = \frac{1}{4\alpha} (-1)^n u_n, \quad (x = na). \quad (1.4.2b)$$

The electron fields $\psi_s^\dagger(x,t)$ and $\psi_s(x,t)$ with spin index s have two components representing the right- and left going waves. In deriving eq. (1.4.1), the electronic dispersion near the Fermi

level has been approximated as a linear dispersion.

From the above Hamiltonian, the following coupled self-consistent equations for $\psi(x,t)$ and $\Delta(x,t)$ are derived,

$$\varepsilon_i \psi_{i,s}(x,t) = [-i v_F \sigma_3 \frac{\partial}{\partial x} + \sigma_1 \Delta(x,t)] \psi_{i,s}(x,t), \quad (1.4.3)$$

$$\ddot{\Delta}(x,t) + \omega_0^2 \Delta(x,t) = -g^2 \sum'_{i,s} \psi_{i,s}^\dagger(x,t) \sigma_1 \psi_{i,s}(x,t), \quad (1.4.4)$$

where the suffix i of ψ implies the electronic state index and the prime attached to the summation indicates the sum over the occupied states. In deriving eq. (1.4.4), the adiabatic approximation has been used, i.e., we have assumed that the occupancy of the electronic states does not change even if $\Delta(x,t)$ varies with time. This assumption is justified, when we consider the linear modes and nonlinear interactions between them in the lowest orders.

As one of exact static solutions of eqs. (1.4.3) and (1.4.4), there is a soliton solution in the form,⁶⁸⁾

$$\Delta_s(x) = \Delta_0 \tanh(x/\xi), \quad \xi = v_F/\Delta_0, \quad (1.4.5)$$

where Δ_0 is the magnitude of the order parameter in the perfect dimerized state,

$$\Delta_0 = W e^{-\frac{1}{2\lambda}}, \quad (1.4.6)$$

with W being the full electronic band width ($4t_0$) and λ the

dimensionless coupling constant

$$\lambda = g^2 / \pi v_F \omega_0^2 . \quad (1.4.7)$$

The corresponding electronic wave functions and eigenvalues are expressed by $\{\psi_{n,s}^{(0)}(x)\}$ and $\{\varepsilon_n\}$, respectively. The electronic band structure is

$$\varepsilon_k = \pm \sqrt{\Delta_0^2 + v_F^2 k^2} , \quad \begin{array}{l} \text{for valence and} \\ \text{conduction band,} \end{array}$$

$$\varepsilon_M = 0 . \quad \text{for mid-gap level.}$$

(1.4.8)

Linear modes around a single soliton were studied by several groups.⁶⁹⁻⁷³ Substituting

$$\Delta(x,t) = \Delta_S(x) + \delta\Delta(x,t) ,$$

$$\psi_{i,s}(x,t) = \psi_{i,s}^{(0)}(x) + \delta\psi_{i,s}(x,t) , \quad (1.4.9)$$

into eq. (1.4.3), we obtain

$$\delta\psi_{i,s}(x,t) = \sum_j \frac{\psi_{j,s}^{(0)}(x)}{(\varepsilon_i - \varepsilon_j)} \int dx \psi_j^{(0)\dagger}(x) \sigma_1 \delta\Delta(x,t) \psi_i^{(0)}(x) , \quad (1.4.10)$$

in the lowest order with respect to $\delta\Delta(x,t)$. Next substitution of eqs. (1.4.9) into eq. (1.4.4) leads to the integral eigenvalue equation for the linear modes in the following form,

$$\left(1 - \frac{\Omega^2}{\omega_0^2}\right) g_\Omega(x) = - \frac{g^2}{\omega_0^2} \int dy K(x, y) g_\Omega(y) ,$$

$$K(x, y) = \sum'_{i,s} \sum''_j \frac{1}{\varepsilon_i - \varepsilon_j} \left\{ [\psi_i^{(0)\dagger}(x) \sigma_1 \psi_j^{(0)}(x)] [\psi_j^{(0)}(y) \sigma_1 \psi_i^{(0)}(y)] \right. \\ \left. + (i \leftrightarrow j) \right\} , \quad (1.4.11)$$

where $g_\Omega(x)$ is the Fourier transform of $\delta\Delta(x, t)$ and the double prime on the summation means the sum over the unoccupied states.

Eigenvalue problem eq. (1.4.11) was numerically solved by replacing the integral by a discrete sum with a uniform mesh dx .^{70,71,73)} It was shown that there are three localized modes; one of them is the Goldstone mode related to the shift of the soliton center.

The phase shifts of the extended phonon modes are of particular interest.⁷³⁾ The phonon modes can be classified into even and odd parity function. They have the form,

$$g_{eq}(x) = \cos[qx + \delta_e(q)/2] + f_{eq}(x) , \\ g_{oq}(x) = \sin[qx + \delta_o(q)/2] + f_{oq}(x) , \quad (1.4.12)$$

where $\delta_e(q)$ and $\delta_o(q)$ are the phase shifts of the even and odd parity functions, respectively, and $f_{eq}(x)$ and $f_{oq}(x)$ are functions localized near the soliton center. Note that, in the absence of the soliton, $g_{eq}(x)$ and $g_{oq}(x)$ have the form $\cos[qx]$ and $\sin[qx]$, respectively. From the explicit forms of the phonon

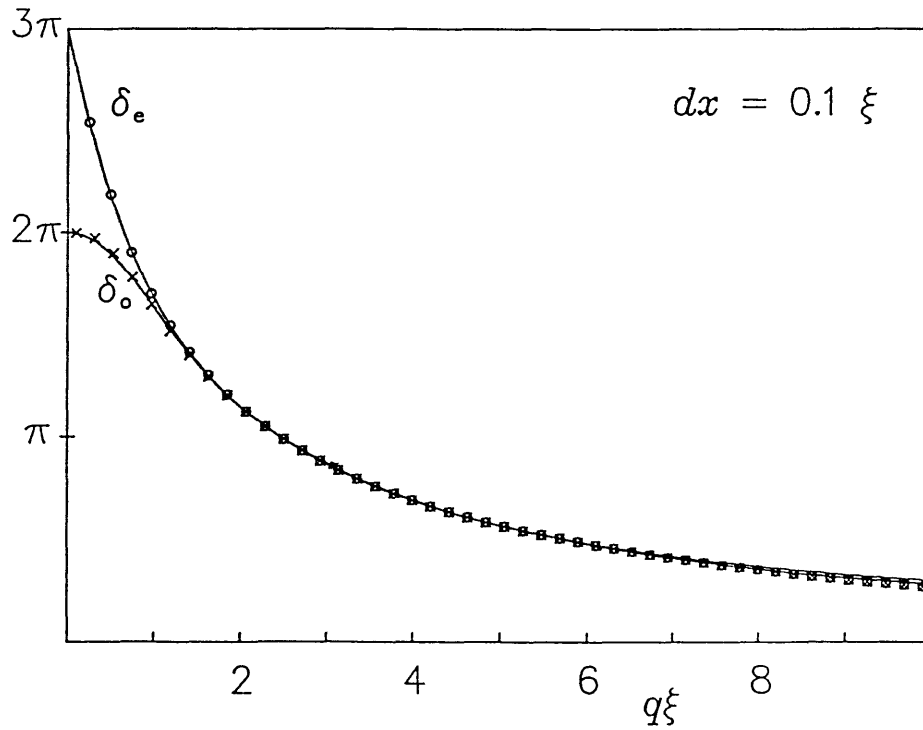


Fig. 1.13 Phase shifts of extended phonon modes with even parity (δ_e) and odd parity (δ_o) for the case $dx=0.1\xi$, as functions of q . The solid lines are functional fitting for first 30 data. (Cited from Ref. 73, Ono et al.: J. Phys. Soc. Jpn. 55 (1986) 1656.)

modes obtained numerically, the phase shifts were calculated through the least square method.⁷³⁾ In Fig. 1.13, the result is shown, where the solid lines indicate functional fitting of the two phase shifts. (Explicit forms of the fitting functions will be shown in §3.3.) The two phase shifts differ each other in the long wave length limit, $k \lesssim \xi^{-1}$, ξ being the soliton width. This means that the effective potential for the phonons in the presence of the soliton is not reflectionless;⁷⁴⁾ in other words, the phonons with small wave numbers suffer reflection. It is apparent if we consider the following scattering state,

$$\varphi_q(x) = e^{i\delta_e(q)/2} g_{eq}(x) + i e^{i\delta_o(q)/2} g_{oq}(x), \quad (1.4.13)$$

which approaches in the region far from the soliton,

$$\begin{aligned} \varphi_q(x) &\xrightarrow{x \rightarrow \infty} \frac{1}{2} (e^{i\delta_e(q)} + e^{i\delta_o(q)}) e^{iqx}, \\ &\xrightarrow{x \rightarrow -\infty} e^{iqx} + \frac{1}{2} (e^{i\delta_e(q)} - e^{i\delta_o(q)}) e^{-iqx}. \end{aligned} \quad (1.4.14)$$

The reflection coefficient,

$$R(q) = (e^{i\delta_e(q)} - e^{i\delta_o(q)}) / 2, \quad (1.4.15)$$

vanishes only when the two phase shifts coincide with mod 2π .

In deriving eq. (1.4.14), we have used the relation

$$\begin{aligned} g_{eq}(x) &= g_{eq}(-x) \xrightarrow{x \rightarrow -\infty} \cos[qx - \delta_e(q)/2], \\ g_{oq}(x) &= -g_{oq}(-x) \xrightarrow{x \rightarrow -\infty} \sin[qx - \delta_o(q)/2]. \end{aligned} \quad (1.4.16)$$

Note that, in the ϕ^4 system, the two phase shifts are identical to $\Delta(k)$ in eq. (1.2.6) and thus the effective potential for phonons is reflectionless.

With the help of these linear modes, a collision between the soliton and a wave packet phonon was studied.⁷⁵⁾ It was shown that the collision gives rise to a shift of the location of the soliton in the second order perturbation approximation. Here the phonon amplitude is the smallness parameter. The shifts of the soliton due to the collisions with thermally excited phonons would lead to the random walk of the soliton, as discussed by Wada and Schrieffer in the ϕ^4 system³⁷⁾ (see also §1.2). This mechanism would yield a diffusion constant proportional to $(k_B T)^2$.

On the other hand, owing to the reflection of the phonon, it is expected that the momentum transfer also takes place in the collision process. On the analogy of the ordinary Brownian motion, the momentum exchange would give rise to the friction in the soliton dynamics. In this case, we can predict that the friction is proportional to $k_B T$, because the velocity change of the soliton after the collision would be proportional to second power of the incident phonon amplitude owing to the momentum conservation law. If we substitute this friction into the Einstein relation, we obtain a temperature independent diffusion constant, which is apparently different from that of the random walk mechanism. We are confronted with similar problem as in the kink dynamics of the ϕ^4 model.

§1.5 Outline of the Thesis

As discussed in the preceding sections, it is very important to study the kink (soliton) dynamics in the thermoequilibrium system. We investigate diffusive motion of the kink in three typical systems; the ϕ^4 system, the sine-Gordon system, and trans-polyacetylene.

In chapter II, the kink dynamics in the ϕ^4 system is considered as a simple example of the non-integrable systems. As discussed in §1.2, the kink-phonon interaction yields the shift of the kink location as well as the momentum transfer. We thus propose that there are two mechanisms in the Brownian-like motion of the ϕ^4 -kink. One is a random walk discussed by Wada and Schrieffer,³⁷⁾ whose basic steps are the shifts of the kink due to collisions with thermally excited phonons. The other is an ordinary Brownian motion, where the friction is caused by the momentum transfers in the collisions. Although the origin of these two mechanisms is the same kink-phonon interaction, we distinguish the two and discuss the relation between them.

At first, we obtain the friction at low temperatures. In order to study the kink motion, we introduce the collective coordinate method in §2.2. In this method, the position of the kink is treated as a new dynamical variable.¹⁴⁾ The friction is investigated with the help of Mori's formula,⁷⁶⁾ which gives a generalized Langevin equation for the kink motion. The Fourier-Laplace transform of the retarded friction function is calculated up to the order of $(k_B T)^2$ in §2.3 and §2.4. The obtained friction Γ is proportional to $(k_B T)^2$ in the zero frequency

limit. It is consistent with the fact that the momentum transfer is in the fourth order with respect to the phonon amplitude. The relation between the two mechanisms is clarified in §2.5 with the help of the fluctuation-dissipation theorem for the kink motion.

As a second typical system, we consider the sine-Gordon system. It is well known that the velocity of the soliton never changes and the soliton-phonon collision only leads to the shift of their locations and phases. We can thus predict that there is no friction of the soliton in the sine-Gordon system. This prediction is verified up to the order of $(k_B T)^2$ in §2.6 and Appendix 2.A. The method to obtain the friction of the ϕ^4 kink can be immediately applied to the sine-Gordon soliton if only the vertex functions are replaced. We believe that any higher order calculations give zero friction. This is one of the most distinguished characteristics of the perfectly integrable systems. The main part of Chapter II has been published in J. Phys. Soc. Jpn. 54 (1985) 3425 and 55 (1986) 1252.

In Chapter III, we take up trans-polyacetylene as the third example of the soliton dynamics. We use the model of Takayama, Lin-Liu, and Maki (TLM).⁶⁸⁾ In §3.2, we apply the collective coordinate method to the TLM model within the adiabatic approximation. It is shown that there are only a few differences between the Hamiltonian in the ϕ^4 model and that in the TLM model when they are written in terms of the collective coordinates. Therefore the method of calculating the friction of the ϕ^4 kink can be also applied to the polyacetylene. It is performed in §3.3. The friction of the polyacetylene soliton

becomes proportional to $k_B T$, reflecting the fact that the momentum transfer occurs in the second order processes. We conclude that the diffusive motion of the soliton is induced by the same two mechanisms as in the ϕ^4 system. The first half of Chapter III has already been published in J. Phys. Soc. Jpn. 55 (1986) 2305.

Here it is useful to summarize the kink dynamics in the above three typical systems. With respect to the kink (soliton)-phonon interaction, they have different characters. (a) In the ϕ^4 system the momentum transfer occurs in the fourth order process, (b) in the sine-Gordon system it never occurs, and (c) in the TLM model it occurs in the second order. As a result, the friction in each system shows different temperature dependence; (a) $\Gamma \propto T^2$, (b) $\Gamma = 0$, and (c) $\Gamma \propto T$, respectively. We expect that any other nonlinear system would be classified into one of the above three types. It is also interesting that the kink (soliton)-phonon collision yields the kink (soliton) shift in the second order processes in any system of the three. This phenomenon seems to be a universal feature of the kink-type excitations. It leads to the random walk of the kink ($D \propto (k_B T)^2$), when the frequency is not zero and the temperature is low enough.

We have restricted ourselves to the classical low temperature region. It is important to study the quantum effect in polyacetylene, because the optical phonon frequency is of $10^3 K$. Quantum correction is discussed in §3.5.

It is also significant to take account of the lattice

pinning effect on the soliton motion. In Chapter IV, the lattice pinning energy (or Peierls potential barrier) is estimated in the Su, Schrieffer, and Heeger's model. It is shown that the pinning energy is almost negligible when the parameters in the Hamiltonian are the values proposed for polyacetylene. Furthermore the pinning energy for different parameters is calculated. As expected, it increases as the soliton width becomes narrower.

Chapter V is devoted to summary, future problems, and discussion.

References

- 1) N.J. Zabusky and M.D. Kruskal: Phys. Rev. Lett. 15 (1965) 240.
- 2) D.J. Korteweg and G. de Vries: Phil. Mag. 39 (1895) 422.
- 3) J.K. Perring and T.H.R. Skyrme: Nucl. Phys. 31 (1962) 550.
- 4) A.C. Scott, F.Y.F. Chu and D.W. McLaughlin: Proc. IEEE 61 (1973) 1443.

For a review see, G. Eilenberger: "Solitons, Mathematical Methods for Physicists" (Springer, Berlin, 1981).

See also "Solitons", ed. by R.K. Bullough and P.J. Caudrey (Springer, Berlin, 1980).
- 5) C.S. Gardner, J.M. Greene, M.D. Kruskal and R.M. Miura: Phys. Rev. Lett. 19 (1967) 1095.
- 6) P.D. Lax: Commun. Pure Appl. Math. 21 (1968) 467.
- 7) M.J. Ablowitz, D.J. Kaup, A.C. Newell and H. Segur: Studies in Appl. Math. 53 (1974) 249.
- 8) V.E. Zakharov and A.B. Shabat: Soviet Phys. JETP 34 (1972) 62.
- 9) For a review see, M. Toda: Phys. Rep. 18C (1975) 1.
- 10) see refs. 5-7.
- 11) L.A. Takhtadzhyan and L.D. Faddeev: Theor. Math. Phys. 21 (1974) 1046.
- 12) R. Hirota: Phys. Rev. Lett. 27 (1971) 1192.
- 13) See for example, G.L. Lamb: Rev. Mod. Phys. 43 (1971) 99.
- 14) R. Jackiw: Rev. Mod. Phys. 49 (1977) 681.
- 15) D.K. Campbell, J.F. Schonfeld and C.A. Wingate: Physica 9D (1983) 1; and references therein.

- 16) For a review see, "Solitons and Condensed Matter Physics",
ed. by A.R. Bishop and T. Schneider (Springer, Berlin,
1978).
"Physics in One Dimension", ed. by J. Bernasconi and
T. Schneider (Springer, Berlin, 1981).
A.R. Bishop, J.A. Krumhansl and S.E. Trullinger: *Physica* **1D**
(1980) 1.
- 17) A.C. Scott, F.Y.F. Chu and S.A. Reible: *J. Appl. Phys.* **47**
(1976) 3272.
A. Matsuda and T. Kawakami: *Phys. Rev. Lett.* **51** (1983) 694.
J. Nitta, A. Matsuda and T. Kawakami: *J. Appl. Phys.* **55**
(1984) 2758.
- 18) H.J. Mikeska: *J. Phys.* **C11** (1978) L29.
J. Villain: *Physica* **79B** (1975) 1.
A.R. Bishop and T.F. Lewis: *J. Phys.* **C12** (1978) 3811.
- 19) W.P. Su, J.R. Schrieffer and A.J. Heeger: *Phys. Rev. Lett.*
42 (1979) 1698; *Phys. Rev.* **B22** (1980) 2099; **B28** (1983)
1138(E).
- 20) M.J. Rice, A.R. Bishop, J.A. Krumhansl and S.E. Trullinger:
Phys. Rev. Lett. **36** (1976) 432.
- 21) A.S. Davidov: "Solitons in Molecular Systems" (D. Reidel,
Dordrecht and Boston, 1985)
- 22) For a review, see, R. Rajaraman: "Solitons and Instantons"
(North-Holland, 1982). See also ref. 14.
- 23) J.A. Krumhansl and J.R. Schrieffer: *Phys. Rev.* **B11** (1975)
3535.
- 24) J.F. Currie, J.A. Krumhansl, A.R. Bishop and
S.E. Trullinger: *Phys. Rev.* **B22** (1980) 477.

- 25) D.J. Scalapino, M. Sears and R.A. Ferrell: Phys. Rev. B6 (1972) 3409.
- 26) For recent developments, see also; K. Sasaki: Prog. Theor. Phys. 68 (1982) 411, ibid. 71 (1984) 1169.
H. Takayama and G. Sato: J. Phys. Soc. Jpn. 51 (1982) 3120.
N. Theodorakopoulos: Z. Phys. B46 (1982) 367; Phys. Rev. B30 (1984) 4071.
K. Sasaki: Phys. Rev. B33 (1986) 2214.
- 27) Bethe ansatz approach; M. Fowler and X. Zotos: Phys. Rev. B24 (1981) 2634, B25 (1982) 5806, B26 (1982) 2519.
M. Imada, K. Hida and M. Ishikawa: Phys. Lett. 90A (1982) 79; J. Phys. C16 (1983) 35, 4945.
H. Takayama and M. Ishikawa: Prog. Theor. Phys. 74 (1985) 479.
- 28) Path integral approach; K. Maki and H. Takayama: Phys. Rev. B20 (1979) 3223, 5002; H. Takayama and K. Maki: Phys. Rev. B20 (1979) 5009, B21 (1980) 4558.
- 29) T. Miyashita and K. Maki: Phys. Rev. B28 (1983) 6733, B31 (1985) 1836.
M. Fukuma and S. Takada: J. Phys. Soc. Jpn. 55 (1986) 2701, 3123.
- 30) K. Kawasaki: Prog. Theor. Phys. 55 (1976) 2029.
H.J. Mikeska: J. Phys. C11 (1978) L29, C13 (1980) 2913.
K.M. Leung and D.L. Huber: Solid State Commun. 32 (1979) 127.
K. Maki: J. Low Temp. Phys. 41 (1980) 327.
A.R. Bishop: J. Phys. A14 (1981) 1417.
- 31) P.S. Sahni and G.F. Mazenko: Phys. Rev. B20 (1979) 4674.

- E. Allroth and H.J. Mikeska: J. Phys. C13 (1980) L725; Z. Phys. B43 (1981) 209.
- H. J. Mikeska: J. Appl. Phys. 52 (1981) 1950.
- 32) T.R. Koehler, A.R. Bishop, J.A. Krumhansl and J.R. Schrieffer: Solid State Commun. 17 (1975) 1515.
- 33) T. Schneider and E. Stoll: Phys Rev. B22 (1980) 5317, B23 (1981) 4631: For a review see, T. Schneider and E. Stoll in "Physics in One Dimension", (ref. 16) p.75
- 34) For recent developments, see also, D.K. Campbell and M. Peyrard: Physica 18D (1986) 47; D.K. Campbell, M. Peyrard and P. Sodano: Physica 19D (1986) 165; M. Peyrard and D.K. Campbell: Physica 9D (1983) 33.
- 35) M. Peyrard and M.D. Kruskal: Physica 14D (1984) 88.
M. Peyrard, S. Pnevmatikos and N. Flytzanis: Physica 19D (1986) 268.
- 36) J.A. Combs and S. Yip: Phys. Rev. B28 (1983) 6873, B29 (1984) 438.
C. Kunz and J.A. Combs: Phys. Rev. B31 (1985) 527.
- 37) Y. Wada and J.R. Schrieffer: Phys. Rev. B18 (1978) 3897.
- 38) There is another perturbation method utilizing the ISM. Time evolution is derived from the equation of motion for the scattering data. See, for example, D.J. Kaup and A.C. Newell: Proc. Roy. Soc. A361 (1978) 413.
- 39) J. Goldstone and R. Jackiw: Phys. Rev. D11 (1975) 1486.
- 40) N. Theodorakopoulos: Z. Phys. B33 (1979) 385.
- 41) H. Ishiuchi and Y. Wada: Prog. Theor. Phys. Suppl. 69 (1980) 242.
- 42) M. Ogata and Y. Wada: J. Phys. Soc. Jpn. 53 (1984) 3855.

- 43) See, for instance, various reports in
J. de Phys. (Colloque) C3, 44 (1983).
Mol. Cryst. Liq. Cryst. 117, 118, (1985).
and Synth. Metals 13 (1986).
- 44) See also, M.J. Rice: Phys. Lett. A71 (1979) 152.
- 45) R.E. Peierls: "Quantum Theory of Solids" (Clarendon Press,
Oxford, 1955) p.108.
- 46) B.R. Weinberger, J. Kaufer, A.J. Heeger, A. Pron and
A.G. MacDiarmid: Phys. Rev. B20 (1979) 223.
- 47) S. Ikehata, J. Kaufer, T. Woerner, A. Pron, M.A. Druy,
A. Sivak, A.J. Heeger and A.G. MacDiarmid: Phys. Rev. Lett.
45 (1980) 1123.
K. Kume, K. Mizuno, K. Mizoguchi, K. Nomura, H. Takayama,
S. Ishihara, J. Tanaka, M. Tanaka, H. Fujimoto and
H. Shirakawa: J. de Phys. (Colloque) C3, 44 (1983) 353.
- 48) J.D. Flood, E. Ehrenfreund, A.J. Heeger and A.G. MacDiarmid:
Solid State Commun. 44 (1982) 1055;
J.D. Flood and A.J. Heeger: J. de Phys.(Colloque) C3, 44
(1983) 397; Phys. Rev. B28 (1983) 2356.
F. Moraes, Y.W. Park and A.J. Heeger: Synth. Metals 13
(1986) 113.
- 49) G.B. Blanchet, C.R. Fincher, T.C. Chung and A.J. Heeger:
Phys. Rev. Lett. 50 (1983) 1938.
Z. Vardeny, J. Orenstein and G.L. Baker: Phys. Rev. Lett. 50
(1983) 2032.
- 50) R. Ball, W.P. Su and J.R. Schrieffer: J. de Phys. (Colloque)
C3, 44 (1983) 429.
W.P. Su: Phys. Rev. B34 (1986) 2988.

- 51) I.B. Goldberg, H.R. Crowe, P.R. Newman, A.J. Heeger and A.G. MacDiarmid: J. Chem. Phys. 70 (1979) 1132.
- 52) B.R. Weinberger, E. Ehrenfreund, A. Pron, A.J. Heeger and A.G. MacDiarmid: J. Chem. Phys. 72 (1980) 4749.
- 53) N.S. Shiren, Y. Tomkiewicz, T.G. Kazyaka, A.R. Taranko, H. Thomann, L. Dalton and T.C. Clarke: Solid State Commun. 44 (1982) 1157.
- 54) M. Nechtschein, F. Devreux, R.L. Greene, T.C. Clarke and G.B. Street: Phys. Rev. Lett. 44 (1980) 356.
- 55) K. Holczer, J.P. Boucher, F. Devreux and M. Nechtschein: Phys. Rev. B23 (1981) 1051.
- 56) K. Holczer, F. Devreux, M. Nechtschein and J.P. Travers: Solid State Commun. 39 (1981) 881.
- 57) W.G. Clark, K. Glover, G. Mozurkewich, C.T. Murayama, J. Sanny, S. Etemad and M. Maxfield: J. de Phys. (Colloque) C3, 44 (1983) 239.
- 58) A. Abragam: "The Principles of Nuclear Magnetism" (Oxford, 1961).
- 59) M. Nechtschein, F. Devreux, F. Genoud, M. Guglielmi and K. Holczer: Phys. Rev. B27 (1983) 61.
- 60) N.S. Shiren, Y. Tomkiewicz, H. Thomann, L. Dalton and T.C. Clarke: J. de Phys. (Colloque) C3, 44 (1983) 223.
- 61) J.C. Scott and T.C. Clarke: J. de Phys. (Colloque) C3, 44 (1983) 365.
- 62) K. Mizoguchi, K. Kume and H. Shirakawa: Solid State Commun. 50 (1984) 213.
- 63) K. Mizoguchi and K. Kume: Mol. Cryst. Liq. Cryst. 117 (1985)

- 459; K. Kume and K. Mizoguchi: *Mol. Cryst. Liq. Cryst.* 117 (1985) 469.
- 64) M. Mehring, H. Seidel, W. Müller, and G. Wegner: *Solid State Commun.* 45 (1983) 1075; *J. de Phys. (Colloque)* C3, 44 (1983) 217.
- 65) K. Ishida, K. Nagamine, T. Matsuzaki, Y. Kuno, T. Yamazaki, E. Torikai, H. Shirakawa and J.H. Brewer: *Phys. Rev. Lett.* 55 (1985) 2009.
- 66) Z. Vardeny, J. Strait, D. Moses, T.-C. Chung and A.J. Heeger: *Phys. Rev. Lett.* 49 (1982) 1657.
- 67) C.V. Shank, R. Yen, R.L. Fork, J. Orenstein and G.L. Baker: *Phys. Rev. Lett.* 49 (1982) 1660.
- 68) H. Takayama, Y.R. Lin-Liu and K. Maki: *Phys. Rev.* B21 (1980) 2388.
- 69) M. Nakahara and K. Maki: *Phys. Rev.* B25 (1982) 7789.
- 70) H. Ito, A. Terai, Y. Ono and Y. Wada: *J. Phys. Soc. Jpn.* 53 (1984) 3520.
- 71) A. Terai, H. Ito, Y. Ono and Y. Wada: *J. Phys. Soc. Jpn.* 54 (1985) 4468.
- 72) J.C. Hicks and G.A. Blaisdell: *Phys. Rev.* B31 (1985) 919.
- 73) Y. Ono, A. Terai and Y. Wada: *J. Phys. Soc. Jpn.* 55 (1986) 1656.
- 74) G. Barton: *J. Phys.* A18 (1985) 479.
- 75) A. Terai, M. Ogata and Y. Wada: *J. Phys. Soc. Jpn.* 55 (1986) 2296.
- 76) H. Mori: *Prog. Theor. Phys.* 33 (1965) 423.

Chapter II. Brownian-like Motion of Kinks in One-Dimensional ϕ^4 System

§2.1 Introduction

As discussed in §1.5, we propose that there are two mechanisms for Brownian-like motion of kinks:

- (1) One is a random walk whose basic steps are shifts of the kink due to collisions with thermally excited phonons.
- (2) The other is ordinary Brownian motion, where the kink moves in viscous field. The origin of the friction is momentum exchange between the kink and the phonons.

In this chapter, friction and diffusion constant of the ϕ^4 -kink are calculated in the form of low temperature expansion. The relation between the above two mechanisms is also clarified.

In order to study the motion of the kink, we use the collective coordinate method. This method was developed first in the field theory to quantize kink solutions.^{1,2)} The position of the kink is treated as a new dynamical variable called the collective coordinate. In this method the Hamiltonian is highly nonlinear and the perturbation procedure to solve the equation of motion becomes complicated. However, since the collective coordinate is not involved in the Hamiltonian, thermal averages of various quantities can be calculated in a straightforward way. Recently it has been shown that calculations by means of this method reproduce the exact free energy obtained by the transfer integral method.^{3,4)}

We calculate the friction with the help of Mori's formula.⁵⁾ It gives a generalized Langevin equation for the kink motions, dividing the force term into two parts; one part being the friction term and the other the random force. In this formula, the friction is given as a function of time $\gamma(t)$. We calculate its Fourier-Laplace transform $\Gamma(\omega)$ in the low temperature expansion.

At first, we discuss the static limit of $\Gamma(\omega)$, which represents the friction of the ordinary Brownian motion in the mechanism (2). It is to be shown that, in the lowest order proportional to $k_B T$, $\gamma(t)$ has the form of $[\Omega \exp(i\Omega t) + \text{the complex conjugate term}]$, where Ω is a sum of frequencies of thermally excited phonons. The static limit of its Fourier-Laplace transform is given by $\Omega \delta(\Omega)$. This shows that $\Gamma(\omega=0)$ vanishes in the lowest order. In the next order proportional to $(k_B T)^2$, there appear many terms. Most of them are shown to have the time dependence $[\Omega \exp(i\Omega t) + \text{complex conjugate}]$ and thus they have no contribution to $\Gamma(\omega=0)$. Only a few terms contribute to the static limit. These terms turn out to be related to the generation of higher harmonics of two thermally excited phonons, which is consistent with the mechanism of the kink-phonon collision discussed in §1.2.

The relation between the two mechanisms is clarified by investigating the fluctuation-dissipation theorem for the kink motion. We calculate a dynamical diffusion constant $D(\omega)$ in the low temperature and the low frequency region. In the static limit, $(\omega \rightarrow 0)$, $D(\omega)$ becomes an ordinary diffusion constant connected with the friction through the Einstein relation. In

this case the static limit of $\Gamma(\omega)$ due to the second mechanism (2) is playing a dominant role. On the other hand, when the frequency is not zero and the temperature is low enough, the dynamical component of the friction, $\Gamma(\omega)$, becomes dominant. In this case, the diffusion constant becomes proportional to $(k_B T)^2$ and the Brownian-like motion of the first mechanism (1) (random walk) shows up. As the temperature increases, however, the diffusion constant approaches to the curve of $D = k_B T / M \Gamma(0)$. Thus we conclude that there occurs a cross-over from the random walk ($D \propto (k_B T)^2$) to the ordinary Brownian motion ($D = k_B T / M \Gamma(0) \propto (k_B T)^{-1}$), when ω is not zero.

In section 2.2, we introduce the ϕ^4 model and apply the collective coordinate method to it. A diagrammatic representation of the perturbation procedure is also developed in order to solve the equation of motion. In section 2.3, we first review Mori's formula and perform the calculation of the friction in the lowest order. The next order terms are studied in §2.4 and the static limit of $\Gamma(\omega)$ is calculated. The dynamical diffusion constant is obtained in §2.5 with the help of the fluctuation-dissipation theorem of the first kind. Discussion is given in §2.6, where some remarks on the obtained friction in association with the elementary processes of the collision are included.

It is also an interesting problem to study the friction in perfectly integrable systems. In §2.6 and Appendix 2.A, we perform similar calculations in the sine-Gordon system and show, as expected, that there is no friction in that system.

The dynamical diffusion constant is also obtained from the

velocity autocorrelation function. It is shown in Appendix 2.B. For completeness, in Appendix 2.C we compare our results with those of Wada and Schrieffer⁶⁾ to show that the diffusion constant in the latter is to be multiplied by a factor of four. Explicit forms of the interaction Hamiltonians are included in Appendix 2.D. In Appendix 2.E details of the calculations are summarized.

§2.2 The ϕ^4 Model and the Collective Coordinate Method

In the continuum approximation, the model of a ϕ^4 chain can be described in terms of displacement field $\phi(x)$ and momentum field $P(x)$, by the following Hamiltonian,

$$H = A \int \frac{dx}{\ell} \left\{ \frac{P(x)^2}{2mA} + \frac{\omega^2}{2} \left(\frac{\partial \phi}{\partial x} \right)^2 - \frac{\omega_0^2}{4} \phi^2 + \frac{\omega_0^2}{8\phi_0^2} \phi^4 \right\}, \quad (2.2.1)$$

with ℓ being lattice constant, c_0 coupling strength between neighboring ions with mass m , and A is defined by $A = m\ell^2$. This system has a double-well local potential, whose minima are at $\phi = \pm \phi_0$. The constant ω_0 characterizes the frequency of small vibrations at one of the potential minima. A stationary kink solution in the system is given by

$$\phi_K(x) = \phi_0 \tanh(x/2d), \quad (2.2.2)$$

where $d = c_0/\omega_0$.

A new dynamical variable $Q_0(t)$, which represents the location of the kink, is introduced by a point canonical transformation,^{1,7,8)}

$$\phi(x,t) = \phi_K(x - Q_0(t)) + \chi(x - Q_0(t), t), \quad (2.2.3a)$$

$$P(x,t) = - \frac{P_0 + \int \pi \chi' dx}{M_0(1 + \xi(t)/M_0)} \phi_K'(x - Q_0(t)) + \pi(x - Q_0(t), t), \quad (2.2.3b)$$

with constraints

$$\int \chi(x,t) \phi_K'(x) dx = 0, \quad (2.2.4a)$$

$$\int \pi(x,t) \phi_K'(x) dx = 0. \quad (2.2.4b)$$

where $\xi(t)$ and M_0 are defined by

$$\begin{aligned}\xi(t) &= \int \phi_K'(x) \chi'(x, t) dx, \\ M_0 &= \int (\phi_K')^2 dx = 2\phi_0^2/3d, \end{aligned} \tag{2.2.5}$$

and primes on ϕ_K and χ imply spatial derivatives. Unless we indicate otherwise, all integral signs in this chapter denote one-dimensional unrestricted integrations over x . The variable $Q_0(t)$ is called "the collective coordinate".*

As shown in §1.2, the eigenvalue problem for linear modes around a single kink can be solved analytically.⁹⁾ The complete set of eigenfunctions contains the Goldstone mode (zero frequency mode) of the form, $\varphi_0(x) = \phi_K'(x)/\sqrt{M_0}$. In terms of this complete set, the fields χ and π can be expanded as

$$\begin{aligned}\chi(x, t) &= Q_1(t) \varphi_1(x) + \sum_k Q_k(t) \varphi_k(x), \quad (Q_{-k} = Q_k^*) \\ \pi(x, t) &= P_1(t) \varphi_1(x) + \sum_k P_k^*(t) \varphi_k(x), \quad (P_{-k} = P_k^*)\end{aligned} \tag{2.2.6}$$

where the Goldstone mode is excluded because of the constraints (2.2.4). The functions $\varphi_1(x)$ and $\varphi_k(x)$ represent the amplitude

*) Gervais and Jevicki⁸⁾ investigated a point canonical transformation in the path integral formula and showed that careful treatment of the transformation leads to additional potential terms in the action. In the present chapter, however, we discuss only the classical limit where their additional terms are not necessary.

oscillation mode and the phonon mode, respectively. Their explicit forms are shown in §1.2.

With the help of eqs. (2.2.3) and the expansion in (2.2.6), the Hamiltonian in terms of the new variables becomes

$$H = H_0 + H_I, \quad (2.2.7a)$$

$$H_0 = -A \int \frac{dx}{\ell} \frac{\phi_0^2 \omega_0^2}{8} + E_K + \frac{1}{2m\ell} \left(\frac{P_0^2}{M_0} + P_1^2 + \sum_k P_k^* P_k \right) + \frac{m\ell}{2} \left(\omega_1^2 Q_1^2 + \sum_k \omega_k^2 Q_k^* Q_k \right), \quad (2.2.7b)$$

$$H_I = \frac{1}{2m\ell} \left\{ \frac{(P_0 + \int \pi X' dx)^2}{M_0 (1 + 3/M_0)^2} - \frac{P_0^2}{M_0} \right\} + H_\Theta, \quad (2.2.7c)$$

where E_K and M are the excitation energy of the kink, $E_K = M c_0^2$, and the kink mass, $M = m\ell M_0$, respectively. The eigenfrequencies are $\omega_1^2 = 3\omega_0^2/4$ and $\omega_k^2 = \omega_0^2 + c_0^2 k^2$. The interaction Hamiltonian H_Q is composed of nine terms which are cubic or quartic in the variables Q . They are included in the twenty-one interaction Hamiltonians which were calculated without using the collective coordinate.¹⁰⁾ We show the explicit forms of these interaction Hamiltonians in Appendix 2.D.

We will calculate thermal averages at an initial time $t=0$ according to the canonical ensemble distribution. From now on, a variable which is not indicated to be a function of time represents the value at the initial time. Since the transformation in eqs. (2.2.3) and (2.2.5) is canonical⁸⁾, the functional integrals over $\phi(x)$ and $P(x)$ can be replaced by

integrals over Q_0 , P_0 , Q_n , and P_n ($n=1,k$) with a constant Jacobian. (From now on, the suffix n always represents both 1 and k .) Thermal averages with respect to the distribution determined by H_0 are

$$\begin{aligned}\langle P_0^2 \rangle_0 &= m\ell M_0 k_B T, \\ \langle P_n^* P_{n'} \rangle_0 &= \delta_{n,n'} m\ell k_B T, \\ \langle Q_n^* Q_{n'} \rangle_0 &= \delta_{n,n'} k_B T / m\ell \omega_n^2,\end{aligned}\tag{2.2.8}$$

where k_B is the Boltzmann constant, and $\delta_{n,n'}$ is the Kronecker's δ function.

Using the explicit form of the Hamiltonian (2.2.7), we obtain the equations of motion

$$\frac{dQ_0(t)}{dt} = \frac{P_0 + \int \pi x' dx}{m\ell M_0 (1 + \xi(t)/M_0)^2},\tag{2.2.9a}$$

$$\frac{dP_0(t)}{dt} = 0,\tag{2.2.9b}$$

$$\frac{dQ_n(t)}{dt} = \frac{1}{m\ell} P_n^*(t) + \frac{P_0 + \int \pi x' dx}{m\ell M_0 (1 + \xi(t)/M_0)^2} \sum_{n'} C_{-n,n'} Q_{n'}(t),\tag{2.2.9c}$$

$$\begin{aligned}\frac{dP_n^*(t)}{dt} &= -m\ell \omega_n^2 Q_n(t) - \frac{\partial H_0}{\partial \theta_n^*}(t) \\ &+ \frac{P_0 + \int \pi x' dx}{m\ell M_0 (1 + \xi(t)/M_0)^2} \sum_{n'} C_{-n,n'} P_{n'}^*(t) - \frac{(P_0 + \int \pi x' dx)^2}{m\ell M_0^2 (1 + \xi(t)/M_0)^3} C_{0,-n}.\end{aligned}\tag{2.2.9d}$$

The variable P_0 is constant, because the Hamiltonian does not depend on the variable Q_0 owing to the translational symmetry of

the system. It represents the total momentum of the system as readily seen from the expression for the total momentum, $-\int \phi'(x,t)P(x,t)dx$. The function $C_{n,n'}$ is defined by $\int \phi_n(x)\phi_{n'}'(x)dx$, whose explicit form is given in Appendix 2.D. Note that $C_{k,k'}$ can be divided into a δ function part $C_{k,k'}^D$ and a normal part $C_{k,k'}^N$ which has no singularity.

Since we are interested in the nonlinear interactions between the kink and the small deviations around it, we solve the equation of motion using perturbation method. The time evolution operator $\exp(-it\mathcal{L})$ satisfies an integral equation

$$e^{-it\mathcal{L}} = e^{-it\mathcal{L}_0} + \int_0^t dt_1 e^{-i(t-t_1)\mathcal{L}_0} (-i\mathcal{L}_I) e^{-it_1\mathcal{L}}, \quad (2.2.10)$$

where \mathcal{L} is the Liouville operator defined by

$$-i\mathcal{L} = \sum_i \left(-\frac{\partial H}{\partial \theta_i} \frac{\partial}{\partial p_i} + \frac{\partial H}{\partial p_i} \frac{\partial}{\partial \theta_i} \right), \quad (2.2.11)$$

\mathcal{L}_0 being similarly defined in terms of H_0 instead of H , and $\mathcal{L}_I = \mathcal{L} - \mathcal{L}_0$. Equation (2.2.10) leads to the following integral equation of $Q_n(t)$,

$$\begin{aligned} Q_n(t) &= e^{-it\mathcal{L}} Q_n \\ &= e^{-it\mathcal{L}_0} Q_n + \int_0^t dt_1 e^{-i(t-t_1)\mathcal{L}_0} (-i\mathcal{L}_I) Q_n(t_1), \end{aligned} \quad (2.2.12)$$

which is solved iteratively. We can thus obtain a perturbation expansion of $Q_n(t)$ in terms of P_0 , Q_n , and P_n . Each term of this

iteration is represented by a diagram.

Before discussing the details of the perturbation procedure, it is useful to begin with a few remarks. We consider that the system is in equilibrium at the initial time. In the low temperature region, the amplitudes of thermally excited phonons at $t=0$ are small and thus the perturbative calculation is justified. It gives a low temperature expansion, because the square of the amplitude of the phonon is proportional to the temperature.

Let us now return to the perturbation procedure. The first term on the right-hand side of eq. (2.2.12), gives the non-interacting time evolution. For example,

$$\begin{aligned}\bar{Q}_k(t) &= \frac{1}{2} \left(Q_k + \frac{P_k^*}{i m \ell \omega_k} \right) \exp(i \omega_k t) + \frac{1}{2} \left(Q_k - \frac{P_k^*}{i m \ell \omega_k} \right) \exp(-i \omega_k t) \\ &= \frac{1}{\sqrt{2}} \sum_{\pm} a_{k\pm} \exp(\pm i \omega_k t),\end{aligned}\tag{2.2.13a}$$

$$\bar{P}_k^*(t) = \frac{m \ell}{\sqrt{2}} \sum_{\pm} (\pm i \omega_k) a_{k\pm} \exp(\pm i \omega_k t),\tag{2.2.13b}$$

where summation over \pm means the sum over two signs, one of which corresponds to upper signs of symbols \pm and the other to the lower signs. The quantity $a_{k\pm}$ is defined by

$$a_{k\pm} = \frac{1}{\sqrt{2}} \left(Q_k \pm \frac{P_k^*}{i m \ell \omega_k} \right).\tag{2.2.14}$$

The thermal averages of eq. (2.2.8) give

$$\begin{aligned}
\langle a_{1\varepsilon}^* a_{1\varepsilon'} \rangle_0 &= \delta_{\varepsilon, \varepsilon'} k_B T / m \ell \omega_1^2, \\
\langle a_{k\varepsilon}^* a_{k'\varepsilon'} \rangle_0 &= \langle a_{-k-\varepsilon} a_{k'\varepsilon'} \rangle_0 = \delta_{k, k'} \delta_{\varepsilon, \varepsilon'} k_B T / m \ell \omega_k^2, \\
&\equiv \delta_{k, k'} \delta_{\varepsilon, \varepsilon'} \langle a_k^* a_k \rangle_0,
\end{aligned} \tag{2.2.15}$$

where ε and ε' take \pm .

With the help of (2.2.7c) and (2.2.11), we find the lowest order terms in $(-i\mathcal{L}_I)$ to be,

$$\begin{aligned}
-i\mathcal{L}_I^{(1)} &= - \sum_n \frac{\partial H_Q^{(3)}}{\partial Q_n} \frac{\partial}{\partial P_n} - \frac{P_0}{m \ell M_0} \sum_{n, n'} C_{n', n} (P_n^* \frac{\partial}{\partial P_n} + Q_{n'} \frac{\partial}{\partial Q_{n'}^*}) \\
&\quad + \frac{P_0^2}{m \ell M_0^{3/2}} \sum_n C_{0, n} \frac{\partial}{\partial P_n},
\end{aligned} \tag{2.2.16}$$

where $H_Q^{(3)}$ is a part of H_Q cubic in Q_n 's. Substitution of (2.2.16) into (2.2.12) gives the integral equation for $Q_n(t)$ in the lowest order. Its diagrammatic representation is depicted in Fig. 2.1, where time axis is taken in such a way that the left-hand side of the diagram corresponds to the past: A solid triangle represents $\overline{Q}_n(t)$ or $\overline{P}_n(t)$ and an open one represents $Q_n(t)$ or $P_n(t)$, ($n=1, k$): The wavy line which is not connected directly to a triangle corresponds to the integral in (2.2.12): A solid circle connected to a straight line indicates the variable P_0 : Vertices mean the Liouville operator, $-i\mathcal{L}_I^{(1)}$. Note that there are many other terms in the higher order, which are not shown in Fig. 2.1. The dynamical variable $Q_n(t)$ can be obtained by iteratively substituting the left-hand side of Fig. 2.1 into the open triangles on the right-hand side. In the

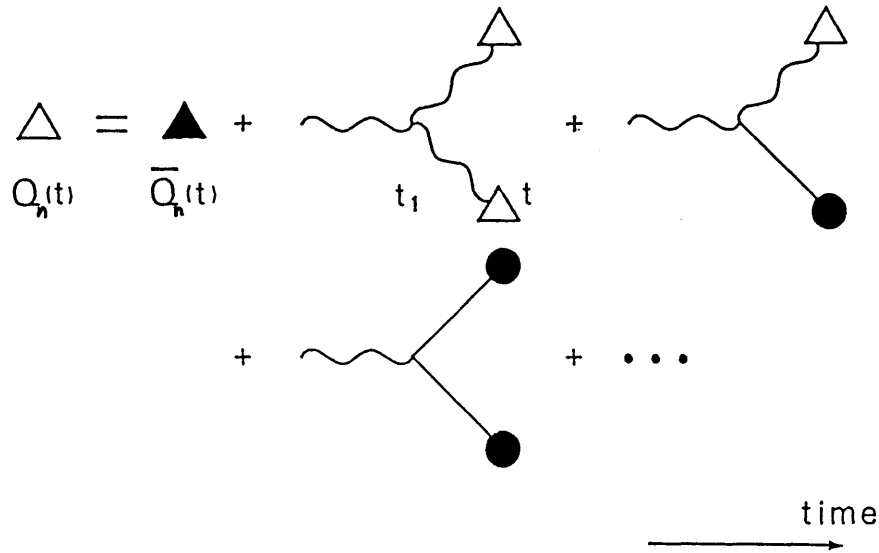


Fig. 2.1 Diagrammatic representation of the integral equation for $Q_n(t)$, ($n=1,k$). Time axis is horizontal, the left-hand side being the past and the right-hand side the future. A solid triangle represents $Q_n(t)$ or $P_n(t)$ and a solid circle indicates P_0 . The wavy line which is not connected directly to a triangle corresponds to the integral in (2.2.12). Vertices mean the interaction Liouville operator.

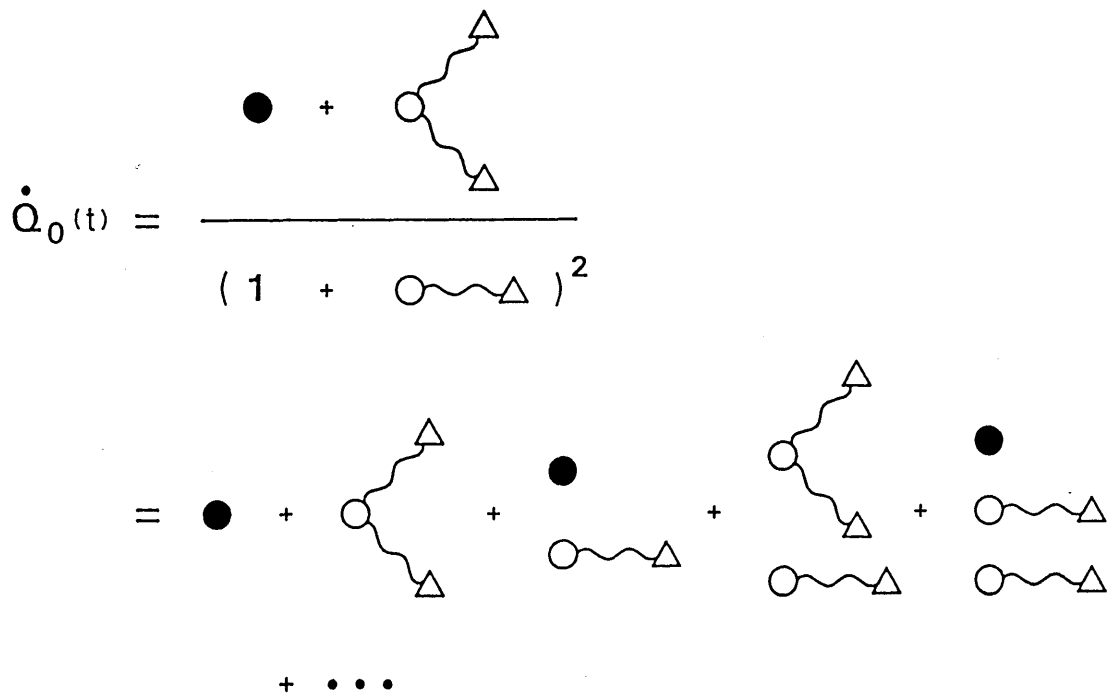


Fig. 2.2 Diagrammatic representation of $dQ_0(t)/dt$, eq. (2.2.9a). The denominator is expanded in a power series. An open circle with two incoming wavy lines indicates the vertex $C_{nn'}$ and an open circle with a wavy line represents $C_{0,n}$. A solid circle is P_0 .

same way, the variable $P_n(t)$ is obtained.

Equation (2.2.9a) gives the velocity of the kink $dQ_0(t)/dt$ with the help of $Q_n(t)$ and $P_n(t)$ obtained above. A diagrammatic representation is shown in Fig. 2.2, where an open circle with two incoming wavy lines indicates the vertex $C_{n,n'}$ which comes from $\int \pi \chi' dx = \sum C_{n,n'} P_n^* Q_{n'}$; an open circle connected to a wavy line represents the vertex $C_{0,n}$ which comes from $\xi = \sum C_{0,n} Q_n$ in the denominator of eq. (2.2.9a).

§2.3. Friction of the Lowest Order

In order to calculate the friction of the ϕ^4 kink, we shall use the method developed by Mori.⁵⁾ It is to be briefly summarized.

A projection of a real variable $g(t)$ onto a real variable a is defined by

$$Pg(t) \equiv \frac{\langle g(t), a \rangle}{\langle a, a \rangle} a, \quad (2.3.1)$$

where a is an initial value of a dynamical variable $a(t)$ and the inner product, \langle , \rangle , represents the canonical ensemble average with respect to the initial distribution. It is shown that the equation of motion for the dynamical variable $a(t)$ becomes⁵⁾

$$da(t)/dt = - \int_0^t \gamma(t-\tau) a(\tau) d\tau + R(t), \quad (2.3.2)$$

where $R(t)$ represents the random force acting on $a(t)$ and $\gamma(t)$ is the friction term defined by

$$\gamma(t) = \langle R(t), R(0) \rangle / \langle a, a \rangle, \quad (2.3.3a)$$

$$R(t) = \exp(-itP' \mathcal{L}) \dot{a}, \quad (2.3.3b)$$

where $P' = 1 - P$. We have used the self-adjoint property of the Liouville operator $\langle i\mathcal{L}a, b \rangle = \langle a, -i\mathcal{L}b \rangle$, for real variables a and b . It leads to the relations $\langle \dot{a}, b \rangle = -\langle a, \dot{b} \rangle$ and $\langle \dot{a}, a \rangle = \langle a, \dot{a} \rangle = 0$.

Equation (2.3.2) gives a generalized Langevin equation for kink motions, when we take the velocity of the kink $dQ_0(t)/dt$ as

the dynamical variable $a(t)$. We calculate Fourier-Laplace transform of $\gamma(t)$,

$$\Gamma(\omega) \equiv \int_0^{\infty} \gamma(t) \exp(-i\omega t) dt. \quad (2.3.4)$$

The fluctuation-dissipation theorem of the first kind is obtained from the Langevin equation (2.3.2). The inner product of \dot{Q}_0 and the equation becomes ($a(t)$ being replaced by $\dot{Q}_0(t)$)

$$\frac{d}{dt} \langle \dot{Q}_0(t), \dot{Q}_0 \rangle = - \int_0^t \gamma(t-\tau) \langle \dot{Q}_0(\tau), \dot{Q}_0 \rangle d\tau, \quad (2.3.5)$$

where the relation $\langle \dot{Q}_0, R(t) \rangle = 0$ has been used. Fourier-Laplace transform of (2.3.5) and integration by parts lead to the fluctuation-dissipation theorem;

$$D(\omega) \equiv \int_0^{\infty} \langle \dot{Q}_0(t), \dot{Q}_0 \rangle \exp(-i\omega t) dt = \frac{\langle \dot{Q}_0, \dot{Q}_0 \rangle}{i\omega + \Gamma(\omega)}. \quad (2.3.6)$$

Instead of (2.3.4), it is convenient to calculate

$$\gamma_t(t) = \frac{\langle \ddot{Q}_0(t), \ddot{Q}_0 \rangle}{\langle \dot{Q}_0, \dot{Q}_0 \rangle},$$

$$\Gamma_t(\omega) = \int_0^{\infty} \gamma_t(t) \exp(-i\omega t) dt, \quad (2.3.7)$$

which is essentially the Fourier-Laplace transform of the total force correlation. Some intriguing discussions are necessary to

identify $\Gamma(\omega)$ with $\Gamma_t(\omega)$, when the latter is estimated using perturbation approximations. We shall summarize them in §2.6. Here, the structure of $\Gamma_t(\omega)$, (2.3.7), is to be studied.

Since the friction is generated by the momentum transfer between the kink and the thermally excited phonons, $\Gamma_t(\omega)$ would diminish as the temperature decreases. It can be expanded with respect to the temperature,

$$\Gamma_t(\omega) = \Gamma_t^{(0)}(\omega) + \Gamma_t^{(1)}(\omega) + \dots \quad (2.3.8)$$

In the present section, we calculate $\Gamma_t^{(0)}(\omega)$. The next order term, $\Gamma_t^{(1)}(\omega)$ is to be calculated in the following section.

The quantity $\ddot{Q}_0(t)$ is obtained by differentiating $dQ_0(t)/dt$ with respect to time. From eq. (2.2.9a), the first order term of $dQ_0(t)/dt$ is

$$\dot{Q}_0^{(1)}(t) = \frac{P_0}{M}, \quad (2.3.9)$$

which vanishes in $\ddot{Q}_0(t)$, (see Fig. 2.2). The second order term is given by

$$\begin{aligned} \dot{Q}_0^{(2)}(t) = & \frac{1}{m\ell M_0} \sum_{n,n'} C_{n,n'} \bar{P}_n^*(t) \bar{Q}_{n'}(t) \\ & - \frac{2P_0}{m\ell M_0^{3/2}} \sum_n C_{0,n} \bar{Q}_n(t), \end{aligned} \quad (2.3.10)$$

which is shown in Fig. 2.3. The quantities $\bar{P}_n(t)$ and $\bar{Q}_n(t)$ are defined in eqs. (2.2.13). Differentiating (2.3.10) with respect to time, we obtain

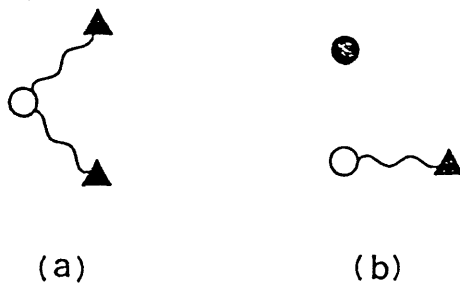


Fig. 2.3 The second order term of $dQ_0(t)/dt$, obtained from Figs. 2.1 and 2.2. It corresponds to eq. (2.3.10).

$$\ddot{Q}_0^{(2)}(t) = -\frac{1}{2M_0} \sum_{n \pm, n' \pm} C_{n, n'} (\pm \omega_n) (\pm \omega_n \pm \omega_{n'}) a_{n \pm} a_{n' \pm} \exp(\pm i \omega_n t \pm i \omega_{n'} t) - \frac{\sqrt{2} P_0}{m \lambda M_0^{3/2}} \sum_{n \pm} C_{0, n} (\pm i \omega_n) a_{n \pm} \exp(\pm i \omega_n t), \quad (2.3.11)$$

where the summations over \pm , one for n and the other for n' are performed independently according to the rule below (2.2.13). Functions $C_{i, j}$ ($i, j=0, 1, k$) are defined by $C_{i, j} \equiv \int \varphi_i(x) \varphi_j'(x) dx$, which appear in the quantities $\int \pi \chi' dx$ and ξ . Substitution into (2.3.7) gives

$$\begin{aligned} \Gamma_t^{(0)}(\omega) &= \int_0^\infty \langle \ddot{Q}_0^{(2)}(t), \ddot{Q}_0^{(2)} \rangle_0 e^{-i\omega t} dt / \langle \dot{Q}_0^{(1)}, \dot{Q}_0^{(1)} \rangle_0 \\ &= \frac{k_B T}{4M} \sum_{n, n'} C_{n, n'} C_{-n, -n'} \frac{(\omega_n^2 - \omega_{n'}^2)^2}{\omega_n^2 \omega_{n'}^2} \\ &\quad \times \left\{ \frac{i\omega}{(\omega_n + \omega_{n'})^2 - (\omega - i\varepsilon)^2} + \frac{i\omega}{(\omega_n - \omega_{n'})^2 - (\omega - i\varepsilon)^2} \right\} \\ &\quad + \frac{4k_B T}{M} \sum_n C_{0, n} C_{0, -n} \frac{i\omega}{\omega_n^2 - (\omega - i\varepsilon)^2}, \quad (2.3.12) \end{aligned}$$

where we have used the relation $C_{n, n'} = -C_{n', n}$ and ε is an infinitesimal positive constant.

It is now clear that $\Gamma_t^{(0)}(\omega)$ vanishes as ω goes to zero. In the low frequency expansion, we find

$$\Gamma_t^{(0)}(\omega) = i\omega \Gamma_1^{(0)} + \omega^2 \Gamma_2^{(0)} + O(\omega^3), \quad (2.3.13)$$

$$\begin{aligned}
\Gamma_1^{(0)} &= \frac{k_B T}{2M} \sum_{n,n'} C_{n,n'} C_{-n,-n'} \frac{\omega_n^2 + \omega_{n'}^2}{\omega_n^2 \omega_{n'}^2} \\
&\quad + \frac{4k_B T}{M} \sum_n C_{0,n} C_{0,-n} / \omega_n^2 \\
&= \frac{93}{40} \tilde{T},
\end{aligned} \tag{2.3.14}$$

$$\begin{aligned}
\Gamma_2^{(0)} &= \frac{k_B T}{4M} \sum_{k,k'} C_{k,k'} C_{-k,-k'} \frac{(\omega_k + \omega_{k'})^2}{\omega_k^2 \omega_{k'}^2} \pi \delta(\omega_k - \omega_{k'}) \\
&= (7 \ln(2 + \sqrt{3}) / \sqrt{3} - 1) \tilde{T} / \pi \omega_0,
\end{aligned} \tag{2.3.15}$$

where the relation

$$\frac{\omega}{\Omega^2 - (\omega - i\varepsilon)^2} = \text{principal part} \frac{\omega}{\Omega^2 - \omega^2} - \frac{i\pi}{2} (\delta(\Omega + \omega) + \delta(\Omega - \omega)), \tag{2.3.16}$$

is used. We have introduced a dimensionless temperature

$$\tilde{T} = k_B T / m \ell d \omega_0^2 \phi_0^2. \tag{2.3.17}$$

Since the denominator of \tilde{T} is equal to $3E_K/2$, \tilde{T} represents the ratio of the energy of the thermally excited phonon to that of the kink. The integrations over k and k' in $\Gamma_1^{(0)}$ and $\Gamma_2^{(0)}$ are carried out in Appendix 2.E(1).

§2.4. Friction of the Next Order

In the previous section we have shown that the static limit of the Fourier-Laplace transform of the friction vanishes in the order of $k_B T$. As mentioned in §1.2, the elementary process of the collision between a kink and a wave packet phonon^{11,12)} tells us that the phonon transfers momentum to the kink in the fourth order processes in the amplitude of the phonon. Therefore we could predict that the friction of the kink is proportional to $(k_B T)^2$ in the low temperature region, if the ϕ^4 -kink would behave as an ordinary Brownian particle. The result in §2.3 is consistent with the above prediction. In the present section, we shall calculate the next order terms.

We begin with a few remarks. First, in the diagrammatic representation developed in §2.2, the wavy lines represent both the phonon modes (indexed by k) and the amplitude oscillation mode (indexed by l). Thus one diagram represents a number of terms which are obtained by attaching the indices k or l to each wavy line. These terms have similar structures and they can be easily obtained from a term containing only the phonon modes according to the following rules:

- (1) If we attach the index l to a wavy line instead of k , we replace the corresponding frequency ω_k by ω_l .
- (2) Each vertex function ($\partial H_I / \partial Q_n$ in the Liouville operator and $C_{n,m}$) is replaced by a relevant function according to incoming wavy lines.

From now on, therefore, we will show expressions which contain

only the phonon modes.

Second, the numerator of $\gamma_t(t)$, eq. (2.3.7), has following seven terms in the next order; $\langle R_0^{(2)}(t), R_0^{(4)} \rangle_0$, $\langle R_0^{(2)}(t), R_0^{(3)} \exp(-\beta H_I) \rangle_0$, two terms in $\langle R_0^{(2)}(t), R_0^{(2)} \exp(-\beta H_I) \rangle_0$, $\langle R_0^{(3)}(t), R_0^{(3)} \rangle_0$, $\langle R_0^{(3)}(t), R_0^{(2)} \exp(-\beta H_I) \rangle_0$, and $\langle R_0^{(4)}(t), R_0^{(2)} \rangle_0$, where $R_0(t)$ represents $\ddot{Q}_0(t)$. Each of the first four terms does not give contributions to $\Gamma(\omega=0)$. It is shown in Appendix 2.E(2).

Let us now proceed to calculate the remaining three terms. Equation (2.2.9a) gives the third order terms (see Fig. 2.2)

$$\begin{aligned} \ddot{Q}_0^{(3)}(t) = & \frac{1}{m\ell M_0} \sum_{k,k'} C_{k,k'} (P_k^{*(2)}(t) \bar{Q}_{k'}(t) + \bar{P}_k^*(t) Q_{k'}^{(2)}(t)) \\ & - \frac{2}{m\ell M_0^{3/2}} \sum_{k,k',p} C_{k,k'} \bar{P}_k^*(t) \bar{Q}_{k'}(t) C_{0,p} \bar{Q}_p(t) \\ & - \frac{2P_0}{m\ell M_0^{3/2}} \sum_k C_{0,k} Q_k^{(2)}(t) + \frac{3P_0}{m\ell M_0^2} \sum_{k,k'} C_{0,k} \bar{Q}_k(t) C_{0,k'} \bar{Q}_{k'}(t), \end{aligned} \quad (2.4.1)$$

On the other hand, the second order phonon is (Fig. 2.1)

$$\begin{aligned} & Q_p^{(2)}(t) \\ = & - \frac{3}{4\ell^{3/2}} \sum_{k,k'(\pm)} \frac{A_{-p,k,k'}}{(\pm i\omega_p)} a_{k\pm} a_{k'\pm} \int_0^t dt_1 \exp(\pm i\omega_p t_1 \pm i\omega_k(t-t_1) \pm i\omega_{k'}(t-t_1)) \\ & + \frac{P_0}{2\sqrt{2} m\ell M_0} \sum_{k(\pm)} C_{-p,k} \left(1 + \frac{\pm\omega_k}{\pm\omega_p}\right) a_{k\pm} \int_0^t dt_1 \exp(\pm i\omega_p t_1 \pm i\omega_k(t-t_1)) \\ & + \frac{P_0^2}{2m^2\ell^2 M_0^{3/2}} \sum_{(\pm)} C_{0,-p} \frac{1}{\pm i\omega_p} \int_0^t dt_1 \exp(\pm i\omega_p t_1), \end{aligned} \quad (2.4.2a)$$

$$\begin{aligned}
& P_p^{(2)*}(t) \\
&= - \frac{3m\ell}{4L^{3/2}} \sum_{k,k'(\pm)} A_{-p,k,k'} a_{k\pm} a_{k'\pm} \int_0^t dt_1 \exp(\pm i\omega_p t_1 \pm i\omega_k(t-t_1) \pm i\omega_{k'}(t-t_1)) \\
&+ \frac{P_0}{2\sqrt{2}M_0} \sum_{k(\pm)} C_{-p,k} (\pm i\omega_p \pm i\omega_k) a_{k\pm} \int_0^t dt_1 \exp(\pm i\omega_p t_1 \pm i\omega_k(t-t_1)) \\
&+ \frac{P_0^2}{2m\ell M_0^{3/2}} \sum_{(\pm)} C_{0,-p} \int_0^t dt_1 \exp(\pm i\omega_p t_1). \tag{2.4.2b}
\end{aligned}$$

The summations over (\pm) are carried out independently with respect to p , k , and k' according to the rule below eq. (2.2.13). Substituting (2.4.2) into (2.4.1) and differentiating with respect to time, we obtain $R_0^{(3)}(t)$. In Fig. 2.4, the diagrammatic representation of $R_0^{(3)}(t)$ is shown and its explicit expression is calculated in Appendix 2.E(3). In particular, a term corresponding to Fig. 2.4(a) is

$$\begin{aligned}
R_0^{(3)}(4a;t) &= - \frac{3}{4\sqrt{2}M_0L^{3/2}} \sum_{k,k',k'',p(\pm)} C_{p,k''} A_{-p,k,k'} \left(1 - \frac{\pm\omega_{k''}}{\pm\omega_p}\right) \frac{a_{k\pm} a_{k'\pm} a_{k''\pm}}{\pm\omega_p \mp \omega_k \mp \omega_{k'}} \\
&\times \left\{ (\pm\omega_p \pm \omega_{k''}) \exp(\pm i\omega_p t \pm i\omega_{k''} t) - (\pm\omega_k \pm \omega_{k'} \pm \omega_{k''}) \exp(\pm i\omega_k t \pm i\omega_{k'} t \pm i\omega_{k''} t) \right\}. \tag{2.4.3}
\end{aligned}$$

The quantity $R_0^{(3)}(t=0)$ is calculated in Appendix 2.E(2) and it is represented by Fig. 2.5, where rules of constructing diagrams are almost the same as those in §2.2. The only difference is that a wavy line which is not connected directly to a triangle does not mean the time integral.

Using these results and after some algebra, we see that the diagrams Fig. 2.4(a) and Fig. 2.5(a) give

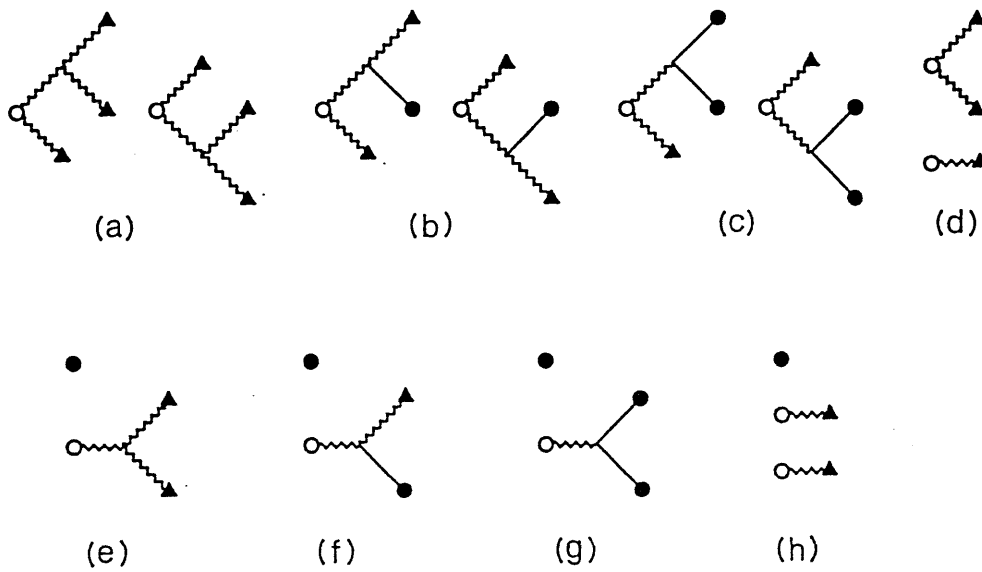


Fig. 2.4 Diagrams representing the third order terms of $R_0(t)$. Their explicit expressions are shown in eqs. (2.4.3) and (2.E.14).

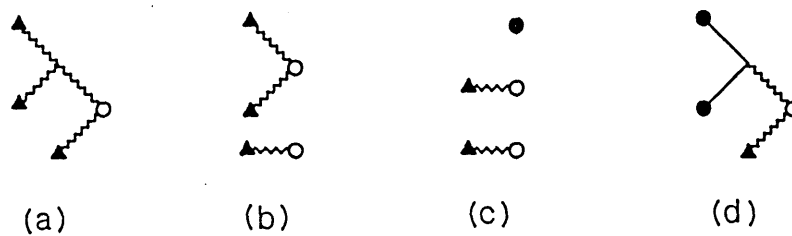


Fig. 2.5 Diagrams representing the quantity $R_0^{(3)}(t=0)$, eq. (2.E.7a). A wavy line which is not connected to a triangle does not mean the time integral.

$$\begin{aligned}
R_0^{(3)}(4a;t) R_0^{(3)}(5a) &= \frac{9}{8M_0^2 L^3} \sum_{k,k',k'',g,g',g'',p,p' \pm} a_{k \pm} a_{k' \pm} a_{k'' \pm} a_g \pm a_{g'} \pm a_{g'' \pm} \\
&\times \left[C_{p,k''}^D A_{k,k',k''} C_{p',g''}^D A_{-p',g,g'} \exp(\pm i\omega_k t \pm i\omega_{k'} t \pm i\omega_{k''} t) \right. \\
&+ C_{p,k''}^D A_{k,k',k''} C_{p',g''}^N A_{-p',g,g'} \exp(\pm i\omega_k t \pm i\omega_{k'} t \pm i\omega_{k''} t) \\
&+ C_{p,k''}^N A_{-p,k,k'} (C_{-p',g''}^D A_{-p',g,g'} + C_{p',g''}^N A_{-p',g,g'}) \\
&\times \left\{ \frac{(\pm\omega_k \pm \omega_{k'})^2 - \omega_{k''}^2}{(\pm\omega_k \pm \omega_{k'})^2 - \omega_p^2} \exp(\pm i\omega_k t \pm i\omega_{k'} t \pm i\omega_{k''} t) \right. \\
&+ \frac{\omega_{k''}^2 - \omega_p^2}{2\omega_p(\pm\omega_k \pm \omega_{k'} - \omega_p)} \exp(\pm i\omega_{k''} t + i\omega_p t) \\
&\left. - \frac{\omega_{k''}^2 - \omega_p^2}{2\omega_p(\pm\omega_k \pm \omega_{k'} + \omega_p)} \exp(\pm i\omega_{k''} t - i\omega_p t) \right\} \Big], \quad (2.4.4)
\end{aligned}$$

where the summation over $\pm\omega_p$ has been carried out. We will first calculate the first term on the right-hand side. Since eq. (2.3.7) gives

$$\begin{aligned}
&\gamma_t(4a, 5a(1); t) \\
&= \frac{9m^2 \ell^2}{4 \langle p_0^2 \rangle_0 L^3} \sum_{k,k',k'' \pm} C_{-k'',k''}^D A_{k,k',k''} (C_{k,-k}^D + C_{k',-k'}^D + C_{k'',-k''}^D) A_{-k,-k',-k''} \\
&\times \langle a_k^* a_k \rangle_0 \langle a_{k'}^* a_{k'} \rangle_0 \langle a_{k''}^* a_{k''} \rangle_0 \exp(\pm i\omega_k t \pm i\omega_{k'} t \pm i\omega_{k''} t),
\end{aligned}$$

and

$$\begin{aligned}
&\Gamma_t(4a, 5a(1); \omega=0) \\
&= \frac{9\pi m^2 \ell^2}{2 \langle p_0^2 \rangle_0 L^3} \sum_{k,k',k''} C_{-k'',k''}^D A_{k,k',k''} (C_{k,-k}^D + C_{k',-k'}^D + C_{k'',-k''}^D) A_{-k,-k',-k''} \\
&\times \langle a_k^* a_k \rangle_0 \langle a_{k'}^* a_{k'} \rangle_0 \langle a_{k''}^* a_{k''} \rangle_0 \left\{ \delta(\omega_k + \omega_{k'} - \omega_{k''}) + \delta(\omega_k - \omega_{k'} + \omega_{k''}) + \delta(-\omega_k + \omega_{k'} + \omega_{k''}) \right\}, \quad (2.4.5.)
\end{aligned}$$

where we have used the formula

$$\lim_{\omega \rightarrow 0} \frac{\omega}{\Omega^2 - (\omega - i\varepsilon)^2} = -i\pi \delta(\Omega). \quad (2.4.6)$$

Using the thermal averages (2.2.8), (2.2.15) and the symmetry relation, $A_{k,k',k''} = A_{k,k'',k'}$, etc., we finally obtain

$$\begin{aligned} & \Gamma_t(4a, 5a(1); \omega=0) \\ &= \frac{9\pi}{2M_0} \left(\frac{k_B T}{m\ell} \right)^2 \frac{1}{L^3} \sum_{k,k',k''} \frac{(k+k'+k'')^2}{\omega_k^2 \omega_{k'}^2 \omega_{k''}^2} A_{k,k',k''} A_{-k,-k',-k''} \delta(\omega_k + \omega_{k'} - \omega_{k''}) \end{aligned} \quad (2.4.7)$$

As discussed before, the diagrams Fig. 2.4(a) and Fig. 2.5(a) have other terms which contain at least one amplitude oscillation mode instead of phonon modes. According to the rules to obtain those terms, they have the form

$$\begin{aligned} & \Gamma_t(4a, 5a(1); \omega=0)_A \\ &= \frac{\pi}{M_0} \left(\frac{k_B T}{m\ell} \right)^2 \frac{1}{L^2} \sum_{k,k'} \frac{(k+k')^2}{\omega_k^2 \omega_{k'}^2 \omega_1^2} A_{1,k,k'} A_{1,-k,-k'} \delta(\omega_k + \omega_{k'} - \omega_1) \\ &+ \frac{\pi}{2M_0} \left(\frac{k_B T}{m\ell} \right)^2 \frac{1}{L} \sum_k \frac{k^2}{\omega_k^2 \omega_1^4} A_{11,k} A_{11,-k} \delta(\omega_k - 2\omega_1). \end{aligned} \quad (2.4.8)$$

The other terms on the right-hand side of (2.4.4) and the contributions from other diagrams are calculated in Appendix 2.E(3), where it is shown that they cancel each other exactly. Thus we conclude that eqs. (2.4.7) and (2.4.8) are the only terms which contribute to the static limit of the friction. It is clear that each of them has a positive value. The integration with respect to k'' in (2.4.7) can be carried out by the formula

$$\delta(\omega_k + \omega_{k'} - \omega_{k''}) = \frac{\omega_k}{c_0^2 \kappa} \left\{ \delta(k'' + k) + \delta(k'' - k) \right\}, \quad (2.4.9)$$

where $\kappa(>0)$ is defined by $\omega_{\kappa} = \omega_k + \omega_{k'}$. Thus we obtain

$$\begin{aligned} \Gamma_t(4a, 5a(1); \omega=0) &= \frac{9}{4M_0} \left(\frac{k_B T}{m\ell} \right)^2 \frac{1}{L^2} \sum_{k, k'} \frac{\omega_k}{c_0^2 \kappa \omega_k^2 \omega_{k'}^2 \omega_{\kappa}^2} \\ &\times \left\{ (k+k'+\kappa)^2 A_{k, k', \kappa} A_{-k, -k'-\kappa} + (k+k'-\kappa)^2 A_{k, k', -\kappa} A_{-k, -k', \kappa} \right\}. \end{aligned} \quad (2.4.10)$$

The other integrations with respect to k and k' are carried out numerically using the explicit form of $A_{k, k', k''}$ in the Appendix D. Note that the δ function part of $A_{k, k', k''}$ does not contribute. The result is

$$\Gamma_t(4a, 5a(1); \omega=0) = 0.02491 \frac{1}{\phi_0^4} \left(\frac{k_B T}{m\ell d \omega_0^2} \right)^2 \omega_0. \quad (2.4.11)$$

In the same way, eq. (2.4.8) gives

$$\Gamma_t(4a, 5a(1); \omega=0)_A = \left(0.05735 + \frac{3\sqrt{6} \pi^2}{\sinh^2(\sqrt{2}\pi)} \right) \frac{1}{\phi_0^4} \left(\frac{k_B T}{m\ell d \omega_0^2} \right)^2 \omega_0, \quad (2.4.12)$$

where the two values correspond to each term in (2.4.8). Finally, the sum of (2.4.11) and (2.4.12) gives the friction of the ϕ^4 -kink

$$\begin{aligned} \Gamma &\equiv \Gamma_t(\omega=0) \\ &= 0.1224 \frac{1}{\phi_0^4} \left(\frac{k_B T}{m\ell d \omega_0^2} \right)^2 \omega_0. \end{aligned} \quad (2.4.13)$$

§2.5 Diffusion Constant and Fluctuation-Dissipation Theorem of the Kink Motion

We define the dynamical diffusion constant by

$$D(\omega) \equiv \int_0^{\infty} \langle \dot{Q}_0(t), \dot{Q}_0 \rangle \exp(-i\omega t) dt = \frac{\langle \dot{Q}_0, \dot{Q}_0 \rangle}{i\omega + \Gamma(\omega)}, \quad (2.5.1)$$

The numerator is calculated up to the order of $(k_B T)^2$ in Appendix 2.B. The result is

$$\langle \dot{Q}_0, \dot{Q}_0 \rangle = \frac{k_B T}{M} (1 + K_1 + O(\tilde{T}^2)), \quad (2.5.2)$$

$$\begin{aligned} K_1 &= \frac{2k_B T \sqrt{M_0}}{M} \sum_{n, n'} N_{n, n'} C_{0, n} A_{-n, n', -n'} / \omega_n^2 \omega_{n'}^2 L^s \\ &\quad + \frac{k_B T}{M} \sum_n C_{0, n} C_{0, -n} / \omega_n^2 \\ &= \frac{113}{40} \tilde{T}, \end{aligned} \quad (2.5.3)$$

where $N_{n, n'} = 3$, if $(n, n') = (1, 1)$ or (k, k') , and unity otherwise. The parameter s is a half of the number of the k modes in (n, n', n'') . The function $A_{n, n', n''}$ comes from the nonlinear interaction Hamiltonian, $m \sum A_{n, n', n''} Q_n Q_{n'} Q_{n''} / L^s$, which is contained in H_Q (Appendix 2.D). The integrations over k and k' in K_1 are also done in Appendix 2.E(1).

Substitution of the results in the preceding sections into the right-hand side of (2.5.1), $\Gamma(\omega)$ being replaced by $\Gamma_t(\omega)$, gives

$$D(\omega) = \frac{k_B T}{M} \frac{1 + K_1 + O(\tilde{T}^2)}{i\omega + \Gamma + i\omega\Gamma_1^{(0)} + \omega^2\Gamma_2^{(0)} + \omega_0 O(\tilde{T}^3, \tilde{\omega}\tilde{T}^2, \tilde{\omega}^3\tilde{T})}, \quad (2.5.4)$$

where the frequency in reduced unit is defined by

$$\tilde{\omega} = \omega/\omega_0. \quad (2.5.5)$$

When we take the static limit $\omega \rightarrow 0$, we obtain the Einstein relation

$$D_0 = \lim_{t \rightarrow \infty} \langle \delta Q_0(t)^2 \rangle / 2t = k_B T / M\Gamma, \quad (2.5.6)$$

It is the diffusion constant proportional to $(k_B T)^{-1}$. Using eq. (2.4.13) we obtain

$$D_0 = 12.25 \tilde{T}^{-1} d^2 \omega_0. \quad (2.5.7)$$

On the other hand, when the frequency is not zero, the temperature dependence of $D(\omega)$ is different. In Fig. 2.6, we show the real part of $D(\omega)/d^2\omega_0$ as a function of the temperature \tilde{T} for several values of $\tilde{\omega}$. When the relation $\Gamma(0) \ll \omega^2\Gamma_2^{(0)}$ holds, (that is $\tilde{T} \ll \tilde{\omega}^2$), the right hand side of (2.5.4) can be expanded as follows:

$$\begin{aligned} D(\omega) = & \frac{k_B T}{iM\omega} \{ 1 + K_1 - \Gamma_1^{(0)} + O(\tilde{T}^2) \} \\ & + \frac{k_B T \Gamma_2^{(0)}}{M} \{ 1 + O(\tilde{T}) \} \\ & + \frac{k_B T \Gamma}{M\omega^2} \{ 1 + O(\tilde{T}) \}. \end{aligned} \quad (2.5.8)$$

In this region, the lowest order term of the real part of $D(\omega)$

becomes

$$D_{\omega} \equiv \frac{k_B T \Gamma_2^{(0)}}{M}, \quad (2.5.9)$$

which is proportional to $(k_B T)^2$. This corresponds to the diffusion constant of the random walk, referred to in Chapter I, whose basic steps are shifts of the kink in the collision with the phonons. In fact, using (2.3.15) we obtain

$$D_{\omega} = 2.06 \tilde{T}^2 d^2 \omega_0. \quad (2.5.10)$$

It is four times as large as the result derived by Wada and Schrieffer.⁶⁾ The difference of the factor 4 is discussed in Appendix 2.C. The present result is equal to the diffusion constant calculated phenomenologically by Theodorakopoulos.¹³⁾

As shown in Fig. 2.6, the real part of $D(\omega)$ approaches to the curve of D_0 as the temperature increases. From the expression in (2.5.4) we can see that $D(\omega)$ is well approximated by D_0 when the static friction coefficient $\Gamma(0)$ is larger than ω . This condition is rewritten as $\tilde{T}^2 \gtrsim \tilde{\omega}$.

The frequency dependence of the real part of $D(\omega)$ is shown in Fig. 2.7 for several values of \tilde{T} . The half-width at the half-maximum of the central peak is determined by $\omega \sim \Gamma(0)$.

In order to check the fluctuation-dissipation theorem, we calculate the velocity autocorrelation function $\langle \dot{Q}_0(t), \dot{Q}_0 \rangle$ in Appendix 2.B. Substituting the result into (2.5.1), we obtain the low temperature expansion of $D(\omega)$ which coincides with (2.5.9).

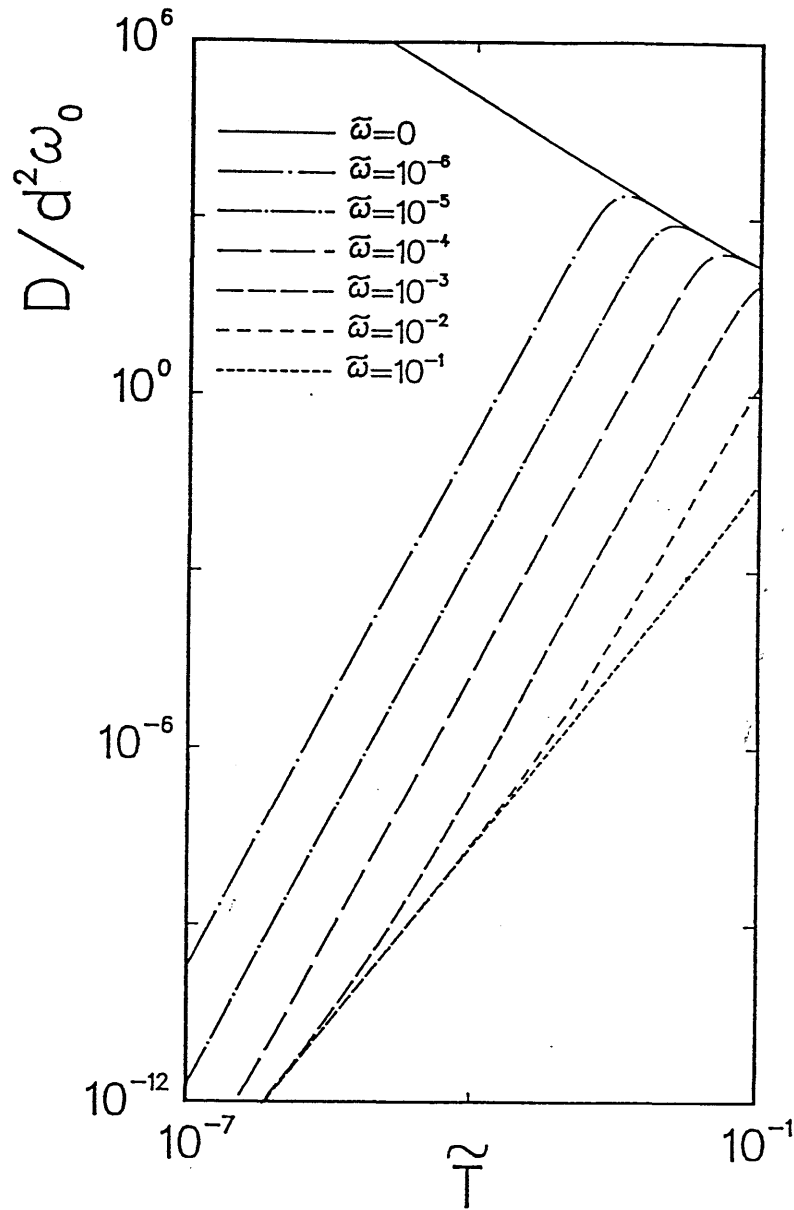


Fig. 2.6 Log-log plot of the real part of $D(\omega)/d^2\omega_0$, (eq. (2.5.4)), as a function of the temperature for several values of the frequency. The reduced temperature and frequency are defined in eqs. (2.3.17) and (2.5.5), respectively. In the region $\tilde{T} < \tilde{\omega}^2$, the diffusion constant is approximately $D\omega$ which is proportional to T^2 , eq. (2.5.10). On the other hand, in the region $\tilde{T} > \tilde{\omega}$, $D(\omega)$ approaches to the curve of D_0 (eq. (2.5.7)) which satisfies the Einstein relation and is proportional to T^{-1} .

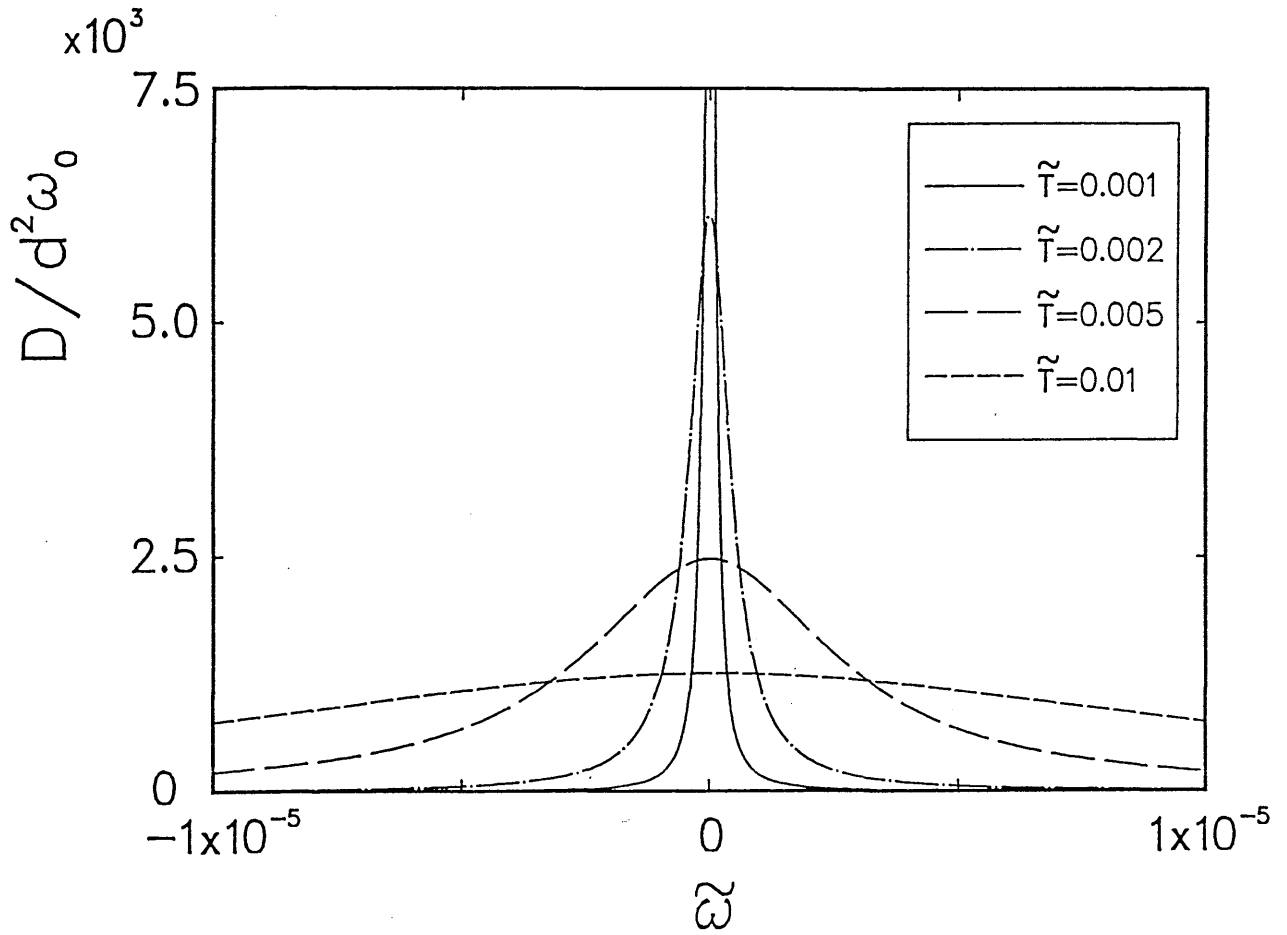


Fig. 2.7 The frequency dependence of the real part of $D(\omega)/d^2\omega_0$, eq. (2.5.4), for several values of the temperature. The half-width at the half-maximum of the central peak is determined by $\omega \sim \Gamma(0)$.

§2.6 Summary and Discussion

Investigating the fluctuation-dissipation theorem for the kink motion, we have shown that the two mechanisms are effective in the Brownian-like motion of the ϕ^4 kink,

One of the two mechanisms is characterized by the friction coefficient $\Gamma(\omega)$. It has been identified with $\Gamma_t(\omega)$. When we substitute the integral equation for $R(t)$

$$\begin{aligned} R(t) &= \ddot{Q}_0(t) + \int_0^t dt_1 \exp\{-i\mathcal{L}(t-t_1)\} (iP\mathcal{L})R(t_1) \\ &= \ddot{Q}_0(t) + \int_0^t dt_1 \dot{Q}_0(t-t_1) \gamma(t_1), \end{aligned} \quad (2.6.1)$$

into the definition of $\Gamma(\omega)$, eq. (2.3.4), the following relation,

$$\Gamma_t(\omega) = \frac{i\omega\Gamma(\omega)}{i\omega + \Gamma(\omega)}, \quad (2.6.2)$$

is obtained.¹⁴⁾ At low frequencies, we generally expect that

$$\Gamma(\omega) \sim \text{finite}, \quad \Gamma_t(\omega) \sim i\omega. \quad (2.6.3)$$

It was, however, pointed out by Kubo¹⁴⁾ that there is a frequency region where $\Gamma_t(\omega)$ is almost frequency independent and identical with $\Gamma(0)$. It is in the region

$$\Gamma(0) \ll \omega \ll \omega_c, \quad (2.6.4)$$

ω_c being the inverse of collision duration time. In the lower frequency region ($\omega < \Gamma(0)$), $\Gamma_t(\omega)$ decreases as $i\omega$ while $\Gamma(\omega) \sim \Gamma(0)$. In the previous sections, we have calculated $\Gamma_t(\omega)$ in the low temperature expansion. As readily seen from

(2.6.2) this expansion has not taken account of higher order terms with respect to $\Gamma(0)/i\omega$. Because of this, the result has not satisfied eq. (2.6.3). It is, however, expected that the perturbation results can be used to obtain $\Gamma(\omega)$, in the sense Kubo discussed. It is worthwhile to make a remark that the lower limit in (2.6.4), $\tilde{\omega} \sim \tilde{T}^2$, is further lower in the frequency region than that for (2.5.9), which is $\tilde{\omega} \sim \tilde{T}^{1/2}$.

We have found that the kink behaves as an ordinary Brownian particle and the Einstein relation $D_0 = k_B T / M\Gamma$ holds in the static limit (long time limit). The diffusion constant is proportional to $(k_B T)^{-1}$. When the frequency is not zero and the temperature is low enough ($\tilde{T} \ll \tilde{\omega}^2$), the dynamical component of $\Gamma(\omega)$ becomes dominant. The diffusion constant turns out to be proportional to $(k_B T)^2$. It is the result of the random walk of the kink, whose basic steps are the shifts of the kink due to the collisions with thermally excited phonons. This mechanism is characteristic for the dynamics of the kinks, in the sense that an ordinary Brownian particle does not suffer a shift of its location from a single collision. As the temperature increases, a crossover takes place from the random walk ($D \propto (k_B T)^2$) to the ordinary Brownian motion ($D = k_B T / M\Gamma \propto (k_B T)^{-1}$), as shown in Fig. 2.6.

Let us discuss the relation between the analysis on the kink-phonon collision process^{11,12)} and the present results.

(1) The temperature dependence of the obtained friction is consistent with the fact that the change of the kink velocity

after the collision is proportional to the fourth order of the incident phonon amplitude.

(2) In the collision process, the higher harmonics of phonons carry the momentum away and thus the kink changes its velocity. It is readily seen that the present friction is also related to the generation of the higher harmonics. The first term on the right-hand side of eq. (2.4.2a) shows that $Q_p^{(2)}(t)$ has a term with a frequency $(\pm\omega_k \pm \omega_{k'})$, which is the higher harmonics of two thermally excited phonons with frequencies ω_k and $\omega_{k'}$. This higher harmonics contributes to the static limit of the friction with another thermally excited phonon, when the frequency of the latter $(\pm\omega_{k''})$ coincides with $(\pm\omega_k \pm \omega_{k'})$, (see eq. (2.4.5)). Note that in the collision process analyzed in ref. 12, one kind of phonon with a typical frequency $\omega_{\bar{q}}$ collided with the kink. Therefore, the momentum transfer was related to the generation of the phonon with a frequency $2\omega_{\bar{q}}$.

(3) It was pointed out¹²⁾ that the effective interaction between the kink and the wave packet phonon is attractive and thus an overtaking phonon reduces the kink velocity, but a head-on colliding phonon accelerates the kink. The magnitude of deceleration surpasses that of acceleration. On the other hand, the number of phonons which collide head-on could be larger than that of overtaking phonons. Therefore the friction of the kink is determined by the competition between the colliding rate and the magnitude of the velocity change. The present calculation has resulted in a positive friction. It is an interesting problem to study the friction from a phenomenological point of view.

(4) Not only the excitations of phonons but also the excitations

of the amplitude oscillation modes are relevant to the friction. In fact, the first term of eq. (2.4.8) comes from a term in $Q_p^{(2)}(t)$ with a frequency $(\pm\omega_k \pm \omega_1)$ which is the higher harmonics of a thermally excited phonon and a thermally excited amplitude oscillation mode. The second term of (2.4.8) comes from two thermally excited amplitude oscillation modes. They were not included in the analysis of kink-phonon collision process in ref. 12.

Next we shall show that the obtained friction can be readily reproduced, except the numerical factor, by a dimensional analysis. It is important to realize that parameters m and ℓ play only the role of a normalization factor of the Hamiltonian (2.2.1) in a form of the product $m\ell$ ($= A/\ell$). Since Γ is proportional to $(k_B T)^2$, it depends on $m\ell$ as $(k_B T/m\ell)^2$. The product $\Gamma(m\ell/k_B T)^2$ has a dimension of $(\text{time})^3(\text{length})^{-2}$. Since there are three additional parameters d , ω_0 , and ϕ_0 , it turns out

$$\Gamma \propto \left(\frac{k_B T}{m\ell} \right)^2 \frac{1}{\omega_0^3 d^2} . \quad (2.6.5)$$

Dependence on ϕ_0 cannot be determined by the dimensional analysis, since ϕ_0 is dimensionless. The acceleration $R_0^{(3)}$, eq. (2.4.3), is proportional to ϕ_0^{-3} , because $M_0 \propto \phi_0^2$ and $A_{\ell, m, n} \propto 1/\phi_0$. On the other hand, the quantity $\langle \dot{Q}_0^{(1)} \dot{Q}_0^{(1)} \rangle_0$ is proportional to ϕ_0^{-2} . Therefore, eq. (2.4.5) gives $\Gamma(0) \propto \phi_0^{-4}$. With eq. (2.6.5), the friction is reproduced except the numerical factor.

In the collective coordinate method the kink location $Q_0(t)$

is defined by¹⁾

$$\int \phi(x,t) \phi_K'(x-Q_0(t)) dx = 0, \quad (2.6.6)$$

as shown from eqs. (2.2.3) and (2.2.4). When the kink is moving at a constant velocity v , the field can be expressed as

$$\phi(x,t) = \phi_K((x-vt)\gamma) + \text{no Goldstone mode around it}, \quad (2.6.7)$$

where $\gamma \equiv 1/\sqrt{1-(v/c_0)^2}$. In this case, eq. (2.6.6) does not give $Q_0(t)=vt$ as discussed in ref. 12. It is because the phonon modes around a moving kink is not orthogonal to $\phi_K'(x-vt)$ and thus $\int \phi(x,t) \phi_K'(x-vt) dx \neq 0$. The difference between $Q_0(t)$ and vt is, however, in the order of $(v/c_0)^2$. We believe that this difference gives to the friction a correction higher than $O(k_B T)^2$.

Next let us briefly discuss the sine-Gordon system. In completely integrable systems a soliton (kink) never changes its velocity. Therefore, we can predict that there is no friction of the soliton due to the soliton-phonon collisions. The method to obtain the friction in the present chapter can be immediately applied to the sine-Gordon system if only the vertex functions are changed. Since there is no amplitude oscillation mode,¹⁵⁾ the friction is given by (2.4.7). The explicit form of the vertex function in the sine-Gordon system is shown in Appendix 2.A. It is readily seen that the vertex $A_{k,k',\kappa}^{SG}$ vanishes for any values k and k' . Therefore the friction of the sine-Gordon soliton is zero up to the order of $(k_B T)^2$. We believe that any higher order calculations do not give friction.

It is one of the characteristics of the completely integrable systems. Even if the friction $\Gamma(0)$ is equal to zero, the static limit ($\omega \rightarrow 0$) of the real part of $D(\omega)$ does not diverge but has a finite value $D_\omega \propto (k_B T)^2$. The imaginary part of $D(\omega)$ diverges as $\omega \rightarrow 0$. It is of course a special case, where the solitons behave as non-interacting particles. There exists only the shift of their locations as a result of the collisions. Therefore, the diffusion constant D_ω due to the random walk of the soliton can be calculated.^{16,17)} In real systems, there would be some perturbations which destroy the complete integrability and the divergence of the diffusion constant would be suppressed.

Recently Kunz and Combs performed the calculation of $\Gamma(0)$ ($\hat{K}(0)$ by their notation) for highly discrete ϕ^4 systems.¹⁸⁾ One of their results was that the diffusion constant goes to zero as the temperature decreases, owing to the discreteness effect. When the temperature is low enough and the kinetic energy of the kink is less than the lattice pinning energy, the kink can not move freely any longer and the diffusion constant decreases. The lattice pinning energy was found to be approximately¹⁹⁾

$$U(Q_0) = \frac{E_a}{2} \cos(2\pi Q_0/\ell), \quad (2.6.8)$$

where E_a is in the present notation

$$E_a = \frac{3\ell E_K}{16d} \exp(-9.68 d^2/\ell^2). \quad (2.6.9)$$

Therefore, the effect of the discreteness on the diffusion constant would become significant in the region

$$\tilde{T} \lesssim \frac{\ell}{d} \exp(-9.68 d^2/\ell^2). \quad (2.6.10)$$

It would also be important to compare (2.6.9) with the uncertainty principle energy for the soliton being located within a given period of the potential.²⁰⁾

Another result of Kunz and Combs¹⁸⁾ was that a component of $\Gamma(0)$ ($\tilde{K}_7(0)$) is proportional to $(k_B T)$ in the low temperature region, even if the continuum limit is taken. In §2.3, however, we concluded that $\Gamma(0)$ is equal to zero in the order of $(k_B T)$. Our result is due to the fact that eq. (2.3.12) has an integrand proportional to $(\omega_k^2 - \omega_{k'}^2)^2 C_{k,k'} C_{-k,-k'}$, which vanishes at $k = \pm k'$. On the other hand, the corresponding expression for $K_7(t)$, (A26) of ref. 18, has an integrand which vanishes at $q = -q'$ but does not vanish at $q = q'$. This difference gives rise to $\tilde{K}_7(0) \propto k_B T$. We can show that it comes from their assumption (A13) that the extended phonon modes could be treated as undistorted plane waves. If we use the distorted phonon ($\varphi_k(x)$) correctly, the relevant expression (in the notation of ref. 18)

$$\sum_k \frac{\partial u_k}{\partial x} u_k \xi^2, \quad (2.6.11)$$

would not be estimated by

$$\frac{1}{\ell} \int dx \frac{\partial u_k}{\partial x} u_k \exp\{i(q+q')x\}, \quad (2.6.12)$$

but by

$$\frac{1}{\ell} \int dx \frac{\partial u_K}{\partial X} u_K^\ell \varphi_q(x) \varphi_{q'}(x). \quad (2.6.13)$$

Equation (2.6.13) does reproduce the factor $(\omega_k^2 - \omega_{k'}^2) C_{k,k'}$, because

$$\begin{aligned} & \frac{1}{\ell} \int dx \phi_K(x) \phi_{K'}(x) \varphi_q(x) \varphi_{q'}(x) \\ &= \frac{1}{2\ell} \int dx \{ \phi_0^2 - \phi_K(x)^2 \} \frac{d}{dx} \{ \varphi_q(x) \varphi_{q'}(x) \} \\ &= - \frac{\phi_0^2}{3\ell \omega_0^2} (\omega_q^2 - \omega_{q'}^2) C_{q,q'}, \end{aligned} \quad (2.6.14)$$

where the eigenvalue equation for the linear modes, eq. (1.2.2) has been used. In summary, it is very important to take account of the correct form of phonons. Otherwise, the kink-phonon coupling could be misinterpreted and the temperature variation of various quantities would be mistaken.

Appendix 2.A. The Sine-Gordon Case

The Hamiltonian of the sine-Gordon system has the form

$$H^{SG} = A \int \frac{dx}{2} \left\{ \frac{1}{2} \left(\frac{\partial \phi}{\partial t} \right)^2 + \frac{c_0^2}{2} \left(\frac{\partial \phi}{\partial x} \right)^2 + \omega_0^2 (1 - \cos \phi) \right\}. \quad (2.A.1)$$

It has the soliton solution

$$\phi_K^{SG}(x) = 4 \tan^{-1} \left\{ \exp(x/d) \right\}, \quad (2.A.2)$$

with $d=c_0/\omega_0$. The phonon mode around the soliton is

$$\varphi_K^{SG}(x) = \frac{1}{\sqrt{L(1+k^2d^2)}} e^{ikx} (kd + i \tanh(x/d)). \quad (2.A.3)$$

Therefore, the three phonon interaction Hamiltonian part in H^{SG} is calculated to be

$$\begin{aligned} H_0^{SG(3)} &= \frac{A}{2L^{3/2}} \sum_{k,k',k''} A_{k,k',k''}^{SG} Q_K Q_{K'} Q_{K''}, \\ A_{K,K',K''}^{SG} &= -\frac{\omega_0^2 L^{3/2}}{6} \int dx \sin \phi_K(x) \varphi_K^{SG}(x) \varphi_{K'}^{SG}(x) \varphi_{K''}^{SG}(x) \\ &= \frac{i\omega_0^2 d}{\sqrt{(1+k^2d^2)(1+k'^2d^2)(1+k''^2d^2)}} \frac{\pi}{24 \cosh(\pi\theta_1/2)} (-3-2\theta_2-\theta_2^2+2\theta_4) \\ &= -\frac{id}{\omega_0^2 \sqrt{(1+k^2d^2)(1+k'^2d^2)(1+k''^2d^2)}} \frac{\pi}{24 \cosh(\pi\theta_1/2)} \\ &\quad \times (\omega_K + \omega_{K'} + \omega_{K''})(\omega_K + \omega_{K'} - \omega_{K''})(\omega_K - \omega_{K'} + \omega_{K''})(-\omega_K + \omega_{K'} + \omega_{K''}), \end{aligned} \quad (2.A.4)$$

with $Q_n = (k^n + k'^n + k''^n) d^n$. Since the relation $A_{k,k',k''}^{SG} = 0$ holds, the friction is zero up to the order of $(k_B T)^2$, as discussed in §2.6. This is associated with no higher harmonics generation at the phonon-soliton collision, which was pointed out in ref. 17.

Appendix 2.B: Velocity Autocorrelation Function

We will calculate the velocity autocorrelation function, $\langle \dot{Q}_0(t), \dot{Q}_0 \rangle$, up to the order of $(k_B T)^2$. The lowest order terms of the kink velocity are

$$\dot{Q}_0^{(1)}(t) = P_0/M, \quad (2.B.1a)$$

$$\begin{aligned} \dot{Q}_0^{(2)}(t) = & \frac{1}{2M_0} \sum_{n, n' \pm} C_{n, n'} (\pm i \omega_n) a_{n \pm} a_{n' \pm} \exp(\pm i \omega_n t \pm i \omega_{n'} t) \\ & - \frac{\sqrt{2} P_0}{m \ell M_0^{3/2}} \sum_{n \pm} C_{0, n} a_{n \pm} \exp(\pm i \omega_n t). \end{aligned} \quad (2.B.1b)$$

First, we will verify the relation

$$\langle \dot{Q}_0(t), \dot{Q}_0^{(1)} \rangle = k_B T/M. \quad (2.B.2)$$

The left-hand side of (2.B.2) can be transformed as

$$\begin{aligned} \langle \dot{Q}_0(t), \dot{Q}_0^{(1)} \rangle &= \langle e^{-it\mathcal{L}} (-i\mathcal{L}) Q_0, P_0/M \rangle \\ &= \left\langle \frac{\partial H}{\partial P_0}, e^{it\mathcal{L}} P_0/M \right\rangle \\ &= \left\langle \frac{\partial H}{\partial P_0}, P_0/M \right\rangle, \end{aligned} \quad (2.B.3)$$

where the self-adjoint property of the Liouville operator and $-i\mathcal{L}P_0=0$ are used. From the definition of the inner product, the final expression in (2.B.3) becomes

$$\begin{aligned} & \int dP_0 dQ_0 \prod_n dP_n dQ_n \frac{\partial H}{\partial P_0} \frac{P_0}{M} e^{-\beta H} / Z \\ &= \int dP_0 dQ_0 \prod_n dP_n dQ_n \left(-\frac{1}{\beta} \frac{\partial}{\partial P_0} e^{-\beta H} \right) \frac{P_0}{M} / Z = \frac{k_B T}{M}. \end{aligned} \quad (2.B.4)$$

With the help of this relation, we find that the low temperature expansion of the velocity autocorrelation function is

$$\begin{aligned}
 \langle \dot{Q}_0(t), \dot{Q}_0 \rangle &= \langle \dot{Q}_0^{(2)}(t), \dot{Q}_0^{(2)} \rangle_0 + \langle \dot{Q}_0^{(1)}(t), \dot{Q}_0 \rangle \\
 &\quad + \langle \dot{Q}_0(t), \dot{Q}_0^{(1)} \rangle - \langle \dot{Q}_0^{(1)}(t), \dot{Q}_0^{(1)} \rangle + O(\tilde{T}^3) \\
 &= \langle \dot{Q}_0^{(2)}(t), \dot{Q}_0^{(2)} \rangle_0 + \frac{2k_B T}{M} - \frac{\langle P_0^2 \rangle}{M^2} + O(\tilde{T}^3).
 \end{aligned}
 \tag{2.B.5}$$

From (2.B.1b), the first term on the right-hand side is

$$\begin{aligned}
 \langle \dot{Q}_0^{(2)}(t), \dot{Q}_0^{(2)} \rangle_0 &= \frac{(k_B T)^2}{4M^2} \sum_{n,n'} C_{n,n'} C_{-n,-n'} / \omega_n^2 \omega_{n'}^2 \\
 &\quad \times \left\{ (\omega_n - \omega_{n'})^2 \cos(\omega_n + \omega_{n'})t + (\omega_n + \omega_{n'})^2 \cos(\omega_n - \omega_{n'})t \right\} \\
 &\quad + \frac{4(k_B T)^2}{M^2} \sum_n C_{0,n} C_{0,-n} \cos \omega_n t / \omega_n^2,
 \end{aligned}
 \tag{2.B.6}$$

where we have used the relation $C_{n,n'} = -C_{n',n}$. To calculate the third term in (2.B.5), we must take account of the effect of the nonlinear Hamiltonian on the thermal average. Using the explicit forms of H_I , (2.2.7c), we obtain

$$\begin{aligned}
 \langle P_0^2 \rangle / M^2 &= \frac{k_B T}{M} - \frac{\beta}{M^2} \langle P_0^2 H_I^{(4)} \rangle_c + \frac{\beta^2}{2M^2} \langle P_0^2 H_I^{(3)^2} \rangle_c + O(\tilde{T}^3) \\
 &= \frac{k_B T}{M} + \frac{3(k_B T)^2}{M^2} \sum_n C_{0,n} C_{0,-n} / \omega_n^2 \\
 &\quad - \frac{2(k_B T)^2 \sqrt{M_0}}{M^2} \sum_{n,n'} N_{n,n'} C_{0,n} A_{-n,n',-n'} / \omega_n^2 \omega_{n'}^2 L^5 \\
 &\quad + \frac{(k_B T)^2}{M^2} \sum_{n,n'} C_{n,n'} C_{-n,-n'} / \omega_n^2 + O(\tilde{T}^3),
 \end{aligned}
 \tag{2.B.7}$$

where $\langle \rangle_c$ indicates the thermal average of the connected diagram. $H_I^{(4)}$ and $H_I^{(3)}$ are the quartic- and the cubic terms in H_I , respectively. Substitution of (2.B.6) and (2.B.7) into (2.B.5) gives

$$\begin{aligned}
\langle \dot{Q}_0(t), \dot{Q}_0 \rangle &= \frac{k_B T}{M} \\
&+ \frac{(k_B T)^2}{4M^2} \sum_{n, n'} C_{n, n'} C_{-n, -n'} / \omega_n^2 \omega_{n'}^2 \\
&\times \left[(\omega_n - \omega_{n'})^2 \cos \{(\omega_n + \omega_{n'})t\} + (\omega_n + \omega_{n'})^2 \cos \{(\omega_n - \omega_{n'})t\} \right. \\
&\quad \left. - 2\omega_n^2 - 2\omega_{n'}^2 \right] \\
&+ \frac{2(k_B T)^2 \sqrt{M_0}}{M^2} \sum_{n, n'} N_{n, n'} C_{0, n} A_{-n, n', -n'} / \omega_n^2 \omega_{n'}^2 L^S \\
&+ \frac{(k_B T)^2}{M^2} \sum_n C_{0, n} C_{0, -n} (4 \cos \omega_n t - 3) / \omega_n^2 + O(\tilde{T}^3). \quad (2.B.8)
\end{aligned}$$

It is readily seen that $\langle Q_0, Q_0 \rangle$ (eq. (2.5.2)) is obtained from (2.B.8). After some algebra, Fourier-Laplace transform of (2.B.8) becomes

$$\int_0^\infty \langle \dot{Q}_0(t), \dot{Q}_0 \rangle e^{-i\omega t} dt = \frac{k_B T (1 + K_1)}{iM\omega} + \frac{k_B T \Gamma^{(0)}(\omega)}{M\omega^2} + O(\tilde{T}^3), \quad (2.B.9)$$

which coincides with $D(\omega)$, up to the order of T^2 .

Appendix 2.C. Diffusion Constant D_ω

We will reproduce the diffusion constant D_ω using the formula

$$D = \lim_{t \rightarrow \infty} \langle \delta Q_0(t)^2 \rangle / 2t, \quad (2.C.1)$$

to compare the present result with that of Wada and Schrieffer.⁶⁾ Here $\delta Q_0(t)$ is the shift of the kink position.

With the help of the relation (2.B.2), we obtain

$$\begin{aligned} \langle \delta \theta_0(t), \delta \theta_0^{(1)}(t) \rangle &= \int_0^t d\tau \langle \dot{\theta}_0(\tau), p_0 \tau / M \rangle \\ &= \frac{k_B T t^2}{M}. \end{aligned} \quad (2.C.2)$$

Therefore, the low temperature expansion of $\langle \delta Q_0(t)^2 \rangle$ becomes

$$\begin{aligned} \langle \delta \theta_0(t)^2 \rangle &= 2 \langle \delta \theta_0(t), \delta \theta_0^{(1)}(t) \rangle \\ &\quad + \langle \delta \theta_0^{(2)}(t)^2 \rangle_0 - \langle \delta \theta_0^{(1)}(t)^2 \rangle + O(\tilde{T}^3). \end{aligned} \quad (2.C.3)$$

The second and third terms are calculated in the same way as eqs. (2.B.6) and (2.B.7). Finally we obtain

$$\begin{aligned} \langle \delta \theta_0(t)^2 \rangle &= \frac{(k_B T)^2}{2M^2} \sum_{n, n'} C_{n, n'} C_{-n, -n'} / \omega_n^2 \omega_{n'}^2 \\ &\quad \times \left[\left(\frac{\omega_n - \omega_{n'}}{\omega_n + \omega_{n'}} \right)^2 \{ 1 - \cos(\omega_n + \omega_{n'}) t \} \right. \\ &\quad \left. + \left(\frac{\omega_n + \omega_{n'}}{\omega_n - \omega_{n'}} \right)^2 \{ 1 - \cos(\omega_n - \omega_{n'}) t \} \right] \\ &\quad + \frac{8(k_B T)^2}{M^2} \sum_n C_{0, n} C_{0, -n} (1 - \cos \omega_n t) / \omega_n^4 \end{aligned}$$

$$+ \frac{k_B T}{M} (1 + K_1 - \Gamma_1^{(0)}) t^2. \quad (2.C.4)$$

Note that the last term proportional to t^2 diverges in the formula (2.C.1). This term corresponds to the first term of $D(\omega)$ in (2.5.8), which diverges when $\omega \rightarrow 0$. To remove this divergence, we must proceed to calculate the next order terms (proportional to T^3) and renormalize the divergence into the denominator in the form, $D(\omega) = k_B T / M \{i\omega + \Gamma(\omega)\}$.

For large t , the first term in (2.C.4) becomes

$$\frac{(k_B T)^2}{2M^2} \sum_{k, k'} C_{k, k'} C_{-k, -k'} \frac{(\omega_k + \omega_{k'})^2}{\omega_k^2 \omega_{k'}^2} \pi t \delta(\omega_k - \omega_{k'}), \quad (2.C.5)$$

where we have used the formula

$$\lim_{t \rightarrow \infty} \frac{1 - \cos \Omega t}{t \Omega^2} \cong \pi \delta(\Omega). \quad (2.C.6)$$

Substitution of (2.C.5) into (2.C.1) reproduces the diffusion constant D_ω (eq. (2.5.10)).

Now we compare the above discussions with previous ones of Wada and Schrieffer,⁶⁾ who calculated the diffusion constant using the same formula, (2.C.1). There are several differences. In ref. 6, the collective coordinate was not introduced. The kink position was calculated from the coefficient of the Goldstone mode.

The second difference is that the previous discussions were confined in the sector where the kink was initially at rest. This is the reason why the divergent term was not obtained.

Thirdly, the adiabatic hypothesis was used; that is, the initial time was taken at the negative infinity and the adiabatic constant ε was introduced. The time t , in the denominator of (2.C.1), was replaced by

$$\int_{-\infty}^0 e^{\varepsilon t} dt = \frac{1}{\varepsilon} . \quad (2.C.7)$$

This approximation is reasonable as far as the order of magnitude is concerned. However, the numerical prefactor of \tilde{T}^2 of D_ω can not be determined precisely. This is the reason why the diffusion constant obtained in ref. 6 is different from ours by a factor 4. We consider that the correct prefactor is 2.06 as shown in §2.5, which is identical with the phenomenological estimation of Theodorakopoulos.¹³⁾

Next, we shall show that D_ω can be reproduced in the formula of ref. 6, without introducing the adiabatic hypothesis, if a small frictional force is supposed to be working against the Goldstone mode. The strength of the force would be reduced to zero later.

Equation of motion for the Goldstone mode q_0 was given by (4.9) of ref. 6 and (2.13a) of ref. 12

$$\ddot{q}_0 = - \frac{1}{m\ell} \frac{\partial H_I}{\partial q_0} , \quad (2.C.8)$$

in the notation of the latter. It is modified to

$$\ddot{q}_0 + \lambda \dot{q}_0 = - \frac{1}{m\ell} \frac{\partial H_I}{\partial q_0} , \quad (2.C.9)$$

λ being the strength of the frictional force. This has the solution

$$q_0(t) = \frac{1}{\lambda m \ell} \int_0^t dt_1 (e^{-\lambda(t-t_1)} - 1) \frac{\partial H_I(t_1)}{\partial q_0}, \quad (2.C.10)$$

for initial conditions $q_0(0) = \dot{q}_0(0) = 0$. Retaining only the relevant H_6 for H_I , we rewrite (2.C.10)

$$q_0(t) = \frac{1}{2L} \sum_{k,k' \pm} A_{6k,k'} a_{k\pm} a_{k'\pm} \times \left\{ - \frac{e^{\pm i\omega_k t \pm i\omega_{k'} t} - 1}{(\lambda \pm i\omega_k \pm i\omega_{k'}) (\pm i\omega_k \pm i\omega_{k'})} + \frac{1 - e^{-\lambda t}}{\lambda (\lambda \pm i\omega_k \pm i\omega_{k'})} \right\}, \quad (2.C.11)$$

where $A_{6k,k'}$ is defined by (A.1) of ref. 12. Using the relation

$$\theta_0(t) = -\sqrt{\frac{3d}{2}} \frac{q_0(t)}{\phi_0}, \quad (2.C.12)$$

which is obtained from (1.2.3) and (1.2.4), we get

$$\begin{aligned} \langle \theta_0(t)^2 \rangle &= 3d \left(\frac{k_B T}{m \ell \phi_0 L} \right)^2 \sum_{k,k'} A_{6k,k'} A_{6-k,-k'} / \omega_k^2 \omega_{k'}^2 \\ &\times \left[\frac{1 - \cos(\omega_k \pm \omega_{k'}) t}{(\lambda^2 + (\omega_k \pm \omega_{k'})^2) (\omega_k \pm \omega_{k'})^2} \right. \\ &\quad \left. - \frac{(1 - e^{-\lambda t}) \sin(\omega_k \pm \omega_{k'}) t}{\lambda (\lambda^2 + (\omega_k \pm \omega_{k'})^2) (\omega_k \pm \omega_{k'})} + \frac{(1 - e^{-\lambda t})^2}{2\lambda^2 (\lambda^2 + (\omega_k \pm \omega_{k'})^2)} \right]. \end{aligned} \quad (2.C.13)$$

We take the limit

$$\lambda t \gg \omega_0/\lambda \gg 1. \quad (2.C.14)$$

Using (2.C.6) and

$$\lim_{t \rightarrow \infty} \frac{\sin \Omega t}{\Omega} \cong \pi \delta(\Omega), \quad (2.C.15)$$

we obtain

$$\begin{aligned} \langle \theta_0(t)^2 \rangle = & 3d \left(\frac{k_B T}{m l \phi_0 L} \right)^2 \sum_{k, k'} \frac{A_{6k, k'} A_{6-k, -k'}}{\omega_k^2 \omega_{k'}^2 (\omega_k - \omega_{k'})^2} \\ & \times \left\{ \pi t \delta(\omega_k - \omega_{k'}) - \frac{\pi}{\lambda} \delta(\omega_k - \omega_{k'}) + \frac{1}{2\lambda^2} \right\}. \end{aligned} \quad (2.C.16)$$

The last two terms can be neglected by the condition (2.C.14). The first term gives the same expression with (2.C.5), as seen easily with the help of the relation

$$A_{6k, k'} = - \frac{\sqrt{3d} L}{2\sqrt{2} \phi_0} (\omega_k^2 - \omega_{k'}^2) C_{k, k'}, \quad (2.C.17)$$

which is obtained from the equality (2.6.14):

Furthermore, it can be shown that equation (2.C.4) is again obtained by the discussions in ref. 6, without introducing the adiabatic hypothesis and the frictional force, if the thermal distribution of the initial momentum of the Goldstone mode is taken into account.²¹⁾ It is thus considered that the method developed in ref. 6 is equivalent to the collective coordinate method. Difference is a matter of convenience.

Appendix 2.D. Interaction Hamiltonians and Vertex Function $C_{n,m}$

Here, the explicit forms of the nine interaction Hamiltonians of H_Q in eq. (2.2.7c) are shown. They were included in the twenty-one interaction Hamiltonians in ref.10. Notations and expressions are simplified and some errors are corrected. The vertex functions $C_{i,j}$ ($i,j=0,1,k$) defined by, $\int \varphi_i(x) \varphi_j'(x) dx$, are also shown. The function $C_{k,k'}$ was first calculated by Gervais, Jevicki, and Sakita, eq.(A3) in ref. 22.

$$H_0 = H_{111} + H_{11k} + H_{1kh} + H_{khh} + H_{1111} + H_{111k} + H_{11kh} + H_{1khh} + H_{khhh},$$

$$H_{111} = m\ell A_{111} \theta_1^3, \quad A_{111} = \frac{3\sqrt{3} \pi \omega_0^2}{128 \phi_0 \sqrt{d}}, \quad (2.D.1)$$

$$H_{11k} = \frac{m\ell}{\sqrt{L}} \sum_k A_{11k} \theta_1^2 \theta_k,$$

$$A_{11k} = \frac{i \omega_0^2}{\phi_0 \sqrt{(1+k^2)(1+4k^2)}} \frac{3\pi}{4 \sinh \pi K} K^2 (K^2+1)(2K^2-1), \quad (2.D.2)$$

with $K = kd$,

$$H_{1kh} = \frac{m\ell}{L} \sum_{k,k'} A_{1k,k'} \theta_1 \theta_k \theta_{k'},$$

$$A_{1k,k'} = \frac{\omega_0^2 \sqrt{d}}{\phi_0 \sqrt{(1+k^2)(1+4k^2)(1+k'^2)(1+4k'^2)}} \frac{3\sqrt{3} \pi}{2 \cosh \pi(K+K')}$$

$$\times \left\{ -(K^2-K'^2)^2(K^2+K'^2) - \frac{1}{4}(K^4+K'^4) + \frac{5}{2}K^2K'^2 + \frac{17}{16}(K^2+K'^2) + \frac{17}{64} \right\}, \quad (2.D.3)$$

$$H_{kkk} = \frac{m\ell}{L^{3/2}} \sum_{k,k',k''} A_{k,k',k''} \Theta_k \Theta_{k'} \Theta_{k''},$$

$$A_{k,k',k''} = A_{k,k',k''}^D \delta(k+k'+k'') + A_{k,k',k''}^P \frac{\text{principal part}}{\sinh \pi (k+k'+k'')},$$

$$A_{k,k',k''}^D = \frac{i\pi\omega_0^2 d}{\phi_0 \sqrt{(1+k^2)(1+4k^2)(1+k'^2)(1+4k'^2)(1+k''^2)(1+4k''^2)}} \\ \times (k^3 + k'^3 + k''^3) \{ 3 + 2(k^2 + k'^2 + k''^2) \}, \quad (2.D.4a)^*$$

$$A_{k,k',k''}^P = \frac{i\pi\omega_0^2 d}{2\phi_0 \sqrt{(1+k^2)(1+4k^2)(1+k'^2)(1+4k'^2)(1+k''^2)(1+4k''^2)}} \\ \times \{ 2 + 5(k^2 + k'^2 + k''^2) + 8(k^2 k'^2 + k'^2 k''^2 + k''^2 k^2) \\ + 3(k^2 k'^4 + k^2 k''^4 + k'^2 k''^4 + k'^2 k^4 + k''^2 k^4 + k''^2 k'^4) \\ - 3(k^6 + k'^6 + k''^6) + 2k^2 k'^2 k''^2 \}, \quad (2.D.4b)$$

$$H_{iiii} = m\ell A_{iiii} \Theta_i^4, \quad A_{iiii} = \frac{9\omega_0^2}{560\phi_0^2 d}, \quad (2.D.5)$$

$$H_{iiik} = \frac{m\ell}{\sqrt{L}} \sum_k A_{iiik} \Theta_i^3 \Theta_k,$$

$$A_{iiik} = \frac{i\omega_0^2}{\phi_0^2 \sqrt{d(1+k^2)(1+4k^2)}} \frac{\sqrt{3}\pi}{140 \cosh \pi k} K(1+k^2)(1+4k^2)(-5+4k^2), \quad (2.D.6)$$

$$H_{iikk} = \frac{m\ell}{L} \sum_{k,k'} A_{iikk,k'} \Theta_i^2 \Theta_k \Theta_{k'},$$

$$A_{iikk,k'} = \frac{\omega_0^2}{\phi_0^2 \sqrt{(1+k^2)(1+4k^2)(1+k'^2)(1+4k'^2)}} \frac{\pi}{\sinh \pi P_1} \\ \times \left(\frac{33}{140} P_1 + \frac{3}{10} P_2 P_1 + \frac{3}{4} P_3 + \frac{3}{2} P_3 P_2 - \frac{6}{5} P_5 + \frac{6}{5} P_5 P_2 - \frac{12}{7} P_7 \right), \quad (2.D.7)^*$$

$$\text{with } P_n = (k^n + k'^n) d^n,$$

*) These are the corrected forms of the corresponding equations in Ref. 10.

$$H_{1k,k',k''} = \frac{m\ell}{L^{3/2}} \sum_{k,k',k''} A_{1k,k',k''} Q_1 Q_k Q_{k'} Q_{k''},$$

$$A_{1k,k',k''} = \frac{i \omega_0^2 \sqrt{d}}{\phi_0^2 \sqrt{(1+K^2)(1+4K^2)(1+K'^2)(1+4K'^2)(1+K''^2)(1+4K''^2)}} \frac{\sqrt{3} \pi}{\cosh \pi \Theta_1} \\ \times \left(\frac{29}{140} \Theta_1 + \frac{1}{5} \Theta_2 \Theta_1 + \frac{3}{4} \Theta_3 + \Theta_3 \Theta_2 - \frac{3}{5} \Theta_5 + \frac{4}{5} \Theta_5 \Theta_2 - \frac{8}{7} \Theta_7 \right),$$

(2.D.8)*

$$\text{with } Q_n = (k^n + k'^n + k''^n) d^n,$$

$$H_{kkkk} = \frac{m\ell}{L^2} \sum_{k,k',k'',k'''} A_{k,k',k'',k'''} Q_k Q_{k'} Q_{k''} Q_{k'''}$$

$$A_{k,k',k'',k'''} = A_{k,k',k'',k'''}^D \delta(R_1) + A_{k,k',k'',k'''}^P \frac{\text{principal part}}{\sinh \pi R_1},$$

$$A_{k,k',k'',k'''}^D = \frac{\pi \omega_0^2 d}{8 \phi_0^2 \sqrt{(1+K^2)(1+4K^2)(1+K'^2)(1+4K'^2)(1+K''^2)(1+4K''^2)(1+K'''^2)(1+4K'''^2)}} \\ \times \left(2 + 5R_2 + \frac{25}{4} R_2^2 - \frac{17}{2} R_4 + \frac{5}{2} R_2^3 - 5R_4 R_2 - \frac{16}{9} R_3^2 + \frac{1}{2} (R_2^2 - 2R_4)^2 \right),$$

(2.D.9a)*

$$A_{k,k',k'',k'''}^P = \frac{\pi \omega_0^2 d}{8 \phi_0^2 \sqrt{(1+K^2)(1+4K^2)(1+K'^2)(1+4K'^2)(1+K''^2)(1+4K''^2)(1+K'''^2)(1+4K'''^2)}} \\ \times \left(-\frac{54}{35} R_1 - \frac{6}{5} R_2 R_1 - 6R_3 - 6R_3 R_2 + \frac{12}{5} R_5 - \frac{24}{5} R_5 R_2 + \frac{48}{7} R_7 \right),$$

(2.D.9b)*

$$\text{with } R_n = (k^n + k'^n + k''^n + k'''^n) d^n,$$

$$C_{11} = 0,$$

(2.D.10)

$$C_{k,1} = -C_{1,k} = -\frac{1}{\sqrt{Ld(1+K^2)(1+4K^2)}} \frac{\sqrt{3} \pi}{16 \cosh \pi K} (1+4K^2)(3+4K^2),$$

(2.D.11)

$$C_{k,k'} = C_{k,k'}^D + C_{k,k'}^N ,$$

$$C_{k,k'}^D = \frac{2\pi i k'}{L} \delta(k+k') = i k' \delta_{k+k', 0} ,$$

(2.D.12a)

$$C_{k,k'}^N = - \frac{i}{L \sqrt{(1+k^2)(1+4k^2)(1+k'^2)(1+4k'^2)}} \frac{3\pi}{\sinh \pi(k+k')} \\ \times (k^2 - k'^2)(k^2 + k'^2 + 1) ,$$

(2.D.12b)

$$C_{0,1} = - C_{1,0} = \frac{3\sqrt{2}\pi}{32d} ,$$

(2.D.13)

$$C_{0,k} = - C_{k,0} = - \frac{i}{\sqrt{Ld(1+k^2)(1+4k^2)}} \sqrt{\frac{3}{2}} \frac{\pi k^2(1+k^2)}{\sinh \pi k} .$$

(2.D.14)

Appendix 2.E: Details of Calculations

(1) Numerical factors of $\Gamma_1^{(0)}$, $\Gamma_2^{(0)}$ and K_1

With the help of the explicit forms of $C_{n,n'}$ given in Appendix 2.D, the first term of $\Gamma_1^{(0)}$ becomes

$$\begin{aligned}
 & \frac{3}{8} \tilde{T} \left[\iint dk dk' \frac{9(k^2 - k'^2)^2 (k^2 + k'^2 + 1)^2}{(1+k^2)^2 (1+4k^2)(1+k'^2)(1+4k'^2) \sinh^2 \pi(k+k')} \right. \\
 & \quad \left. + \int dk \frac{\pi (1+4k^2)(3+4k^2)^2 (7+4k^2)}{128 (1+k^2)^2 \cosh^2 \pi k} \right] \\
 & = \frac{3}{8} \tilde{T} \int dk \left\{ \frac{12k^2 + \frac{12}{5}}{\pi (1+k^2)^2 (1+4k^2)} - \frac{3\pi k^4}{(1+4k^2) \sinh^2 \pi k} + \frac{\pi (1+4k^2)(3+4k^2)^2}{32 (1+k^2) \cosh^2 \pi k} \right\} \\
 & = \frac{33}{40} \tilde{T}, \tag{2.E.1}
 \end{aligned}$$

where we have used the formulae^{12,23)}

$$\int_{-\infty}^{\infty} dk' \frac{(k^2 - k'^2)^2}{(1+k'^2) \sinh^2 \pi(k+k')} = \frac{\pi (1+k^2)^2}{\sinh^2 \pi k} + \frac{4k^2 - 3}{3\pi k^2}, \tag{2.E.2a}$$

$$\int_{-\infty}^{\infty} dk' \frac{(k^2 - k'^2)^2}{(1+4k'^2) \sinh^2 \pi(k+k')} = -\frac{\pi (1+4k^2)^2}{32 \cosh^2 \pi k} + \frac{1}{3\pi}, \tag{2.E.2b)*}$$

$$\int_{-\infty}^{\infty} dk \frac{1}{(1+k^2) \cosh^2 \pi k} = \pi - \frac{8}{\pi}, \tag{2.E.2c}$$

*) The formula (2.E.2b) corresponds to (E.2b) in ref.12. However, the expression of (E.2b) had a typing mistake. The second term has to be $1/3\pi$.

$$\int_{-\infty}^{\infty} dk \frac{k^{2n}}{\sinh^2 \pi k} = \frac{2}{\pi} |B_{2n}|, \quad (n \geq 1)$$

$$\int_{-\infty}^{\infty} dk \frac{k^{2n}}{\cosh^2 \pi k} = \frac{2^{2n} - 2}{\pi 2^{2n-1}} |B_{2n}|, \quad (2.E.2d)$$

with B_n Bernoulli number. In the same way, the second term of $\Gamma_1^{(0)}$ is

$$\begin{aligned} 6 \tilde{T} \left[\frac{3\pi}{4} \int dk \frac{k^4}{(1+4k^2) \sinh^2 \pi k} + \frac{3\pi^2}{128} \right] \\ = \frac{3}{2} \tilde{T} \end{aligned} \quad (2.E.3)$$

Equations (2.E.1) and (2.E.3) lead to $\Gamma_1^{(0)}$, eq. (2.3.14).

The integration in $\Gamma_2^{(0)}$ is identical with that carried out in ref. 6, (4.19).

$$\begin{aligned} \Gamma_2^{(0)} &= \frac{27 \tilde{T}}{2\pi \omega_0} \int dk \frac{|k| (2k^2+1)^2}{(1+k^2)^{5/2} (1+4k^2)^2} \\ &= \frac{\tilde{T}}{\pi \omega_0} \left(\frac{7}{\sqrt{3}} \ln(2+\sqrt{3}) - 1 \right). \end{aligned} \quad (2.E.4)$$

Next the numerical factor of K_1 is calculated. Note that the δ function part of $A_{k,k',k''}$ does not contribute. The first term of K_1 , (2.5.3), becomes

$$\begin{aligned}
& -\frac{9}{8} \tilde{T} \iint dk dk' \frac{k^2}{(1+k^2)(1+4k^2)(1+k'^2)^2(1+4k'^2) \sinh^2 \pi k} \\
& \quad \times \left\{ 2+10k'^2+8k'^4 + (5+16k'^2+8k'^4)k^2 + 6k'^2k^4 - 3k^6 \right\} \\
& + \frac{9\pi}{16} \tilde{T} \int dk \frac{2k^4 + \frac{17}{8}k^2 + \frac{17}{64}}{(1+k^2)^2(1+4k^2)} \\
& - \frac{3\pi}{2} \tilde{T} \int dk \frac{k^4(2k^2-1)}{(1+4k^2) \sinh^2 \pi k} + \frac{9\pi^2}{128} \tilde{T} \\
& = \frac{49}{20} \tilde{T}.
\end{aligned}$$

(2.E.5)

The second term of K_1 gives $3\tilde{T}/8$, which is readily seen from (2.E.3). Finally we obtain the result of (2.5.3).

(2) Calculations of Terms of the Friction with $R_0^{(2)}(t)$

It is shown that the terms of $\langle R_0^{(2)}(t), R_0^{(2)} \exp(-\beta H_I) \rangle_0$, $\langle R_0^{(2)}(t), R_0^{(3)} \exp(-\beta H_I) \rangle_0$, and $\langle R_0^{(2)}(t), R_0^{(4)} \rangle_0$ do not contribute to the static friction. First, we calculate $R_0(t=0)$ up to the fourth order. Estimating eqs. (2.2.9c) and (2.2.9d) at the initial time, we obtain

$$\dot{\Theta}_n^{(1)} = \frac{1}{m\ell} P_n^*,$$

$$\dot{\Theta}_n^{(2)} = \frac{P_0}{m\ell M_0} \sum_{n'} C_{-n,n'} \Theta_{n'},$$

$$\begin{aligned} \dot{\Theta}_n^{(3)} = & -\frac{2P_0}{m\ell M_0^{3/2}} \sum_{n',n''} C_{-n,n'} \Theta_{n'} C_{0,n''} \Theta_{n''} \\ & + \frac{1}{m\ell M_0} \sum_{n',n'',n'''} C_{-n,n'} \Theta_{n'} C_{n'',n'''} P_{n'''}^* \Theta_{n'''}, \end{aligned}$$

$$\dot{P}_n^{*(1)} = -m\ell \omega_n^2 \Theta_n,$$

$$\begin{aligned} \dot{P}_n^{*(2)} = & -\frac{3m\ell}{L^{3/2}} \sum_{n',n''} A_{-n,n',n''} \Theta_{n'} \Theta_{n''} \\ & + \frac{P_0}{m\ell M_0} \sum_{n'} C_{-n,n'} P_{n'}^* + \frac{P_0^2}{m\ell M_0^{3/2}} C_{0,-n}, \end{aligned}$$

$$\begin{aligned} \dot{P}_n^{*(3)} = & -\frac{4m\ell}{L^2} \sum_{n',n'',n'''} A_{-n,n',n'',n'''} \Theta_{n'} \Theta_{n''} \Theta_{n'''} \\ & + \frac{1}{m\ell M_0} \sum_{n',n'',n'''} C_{-n,n'} P_{n'}^* C_{n'',n'''} P_{n'''}^* \Theta_{n'''} \\ & - \frac{2P_0}{m\ell M_0^{3/2}} \sum_{n',n''} C_{-n,n'} P_{n'}^* C_{0,n''} \Theta_{n''} \\ & + \frac{2P_0}{m\ell M_0^{3/2}} \sum_{n',n''} C_{0,-n} C_{n',n''} P_{n'}^* \Theta_{n''} \\ & - \frac{3P_0^2}{m\ell M_0^2} \sum_{n'} C_{0,-n} C_{0,n'} \Theta_{n'}. \end{aligned} \quad (2.E.6)$$

Substitution into eq. (2.2.9a) gives

$$\begin{aligned} \ddot{\Theta}_0^{(3)}(0) = R_0^{(3)}(0) = & -\frac{3}{2\sqrt{2}M_0 L^{3/2}} \sum_{q,q',q'',p' \pm} C_{p',q''} A_{-p',q,q'} a_{q \pm} a_{q' \pm} a_{q'' \pm} \\ & + \frac{1}{\sqrt{2}M_0^{3/2}} \sum_{q,q',q'' \pm} C_{q,q'} C_{0,q''} (\pm\omega_q)(\pm\omega_q \pm \omega_{q'} \pm \omega_{q''}) a_{q \pm} a_{q' \pm} a_{q'' \pm} \\ & + \frac{3P_0}{2m\ell M_0^2} \sum_{q,q', \pm} C_{0,q} C_{0,q'} (\pm i\omega_q \pm i\omega_{q'}) a_{q \pm} a_{q' \pm} \\ & - \frac{P_0^2}{\sqrt{2}m^2\ell^2 M_0^{5/2}} \sum_{p',q \pm} C_{0,p'} C_{-p',q} a_{q \pm}, \end{aligned} \quad (2.E.7a)$$

$$\begin{aligned}
\ddot{Q}_0^{(4)}(0) &= R_0^{(4)}(0) \\
&= -\frac{1}{M_0 L^2} \sum_{p', q, q', q'' \pm} C_{p', q''} A_{-p', q, q', q''} a_{q \pm} a_{q' \pm} a_{q'' \pm} a_{q'' \pm} \\
&\quad + \frac{3}{2 M_0^{3/2} L^{3/2}} \sum_{p', q, q', q'' \pm} C_{p', q''} A_{-p', q, q'} C_{0, q''} a_{q \pm} a_{q' \pm} a_{q'' \pm} a_{q'' \pm} \\
&\quad - \frac{3}{4 M_0^2} \sum_{q, q', q'', q''' \pm} C_{q, q'} C_{0, q''} C_{0, q'''} (\pm \omega_q) (\pm \omega_q \pm \omega_{q''} \pm \omega_{q'''}) a_{q \pm} a_{q' \pm} a_{q'' \pm} a_{q''' \pm} \\
&\quad - \frac{P_0}{\sqrt{2} m \ell M_0^{5/2}} \sum_{p, q, q', q'' \pm} C_{0, p} C_{-p, q} C_{q', q''} (\pm i \omega_{q'}) a_{q \pm} a_{q' \pm} a_{q'' \pm} \\
&\quad - \frac{6 P_0}{\sqrt{2} m \ell M_0^{5/2}} \sum_{q, q', q'' \pm} C_{0, q} C_{0, q'} C_{0, q''} (\pm i \omega_q) a_{q \pm} a_{q' \pm} a_{q'' \pm} \\
&\quad + \frac{5 P_0^2}{2 m^2 \ell^2 M_0^3} \sum_{p', q, q' \pm} C_{0, p'} C_{-p', q} C_{0, q'} a_{q \pm} a_{q' \pm} . \quad (2.E.7b)
\end{aligned}$$

The quantity $R_0^{(2)}(t=0)$ can be easily obtained from eq. (2.3.11).

Next, the interaction Hamiltonians up to the fourth order are

$$\begin{aligned}
H_I^{(3)} &= H_0^{(3)} + \frac{P_0}{m \ell M_0} \int \pi x' dx - \frac{P_0^2}{m \ell M_0^2} \mathcal{Z} , \\
H_I^{(4)} &= H_0^{(4)} + \frac{1}{2 m \ell M_0} \left(\int \pi x' dx \right)^2 \\
&\quad - \frac{2 P_0}{m \ell M_0^2} \int \pi x' dx \cdot \mathcal{Z} \\
&\quad + \frac{3 P_0^2}{2 m \ell M_0^3} \mathcal{Z}^2 . \quad (2.E.8)
\end{aligned}$$

With these results and $R_0^{(2)}(t)$, we can calculate each term of $\langle R_0^{(2)}(t), R_0^{(2)} \exp(-\beta H_I) \rangle_0$, $\langle R_0^{(2)}(t), R_0^{(3)} \exp(-\beta H_I) \rangle_0$, and $\langle R_0^{(2)}(t), R_0^{(4)} \rangle_0$. Almost all of them have a time dependence of $[\Omega \exp(i \Omega t) + \text{c.c.}]$, and thus do not contribute to the static friction. The only exceptional case is a term in $\langle R_0^{(2)}(t), R_0^{(4)} \rangle_0$, which comes from the first term in eq. (2.E.7b).

$$\begin{aligned}
& \langle R_0^{(2)}(t), R_0^{(4)}(7Eb(1)) \rangle_0 \\
&= \frac{3}{2M_0^2 L^2} \sum_{k, k', k'' \pm} C_{k, k'}^N (C_{k, -k}^D + C_{k', -k'}^D + 2 C_{k'', -k''}^D) A_{-k, -k', k'', -k''} \\
&\times (\omega_k^2 - \omega_{k'}^2) \langle a_k^* a_k \rangle_0 \langle a_{k'}^* a_{k'} \rangle_0 \langle a_{k''}^* a_{k''} \rangle_0 \exp(\pm i \omega_k t \pm i \omega_{k'} t). \quad (2.E.9)
\end{aligned}$$

Substituting this into (2.3.7) we obtain

$$\begin{aligned}
& \Gamma_t(2, 7Eb(1); \omega=0) \\
&= \frac{3\pi}{M_0^2 L^2} \sum_{k, k', k''} C_{k, k'}^N (C_{k, -k}^D + C_{k', -k'}^D + 2 C_{k'', -k''}^D) A_{-k, -k', k'', -k''} \\
&\times (\omega_k^2 - \omega_{k'}^2) \langle a_k^* a_k \rangle_0 \langle a_{k'}^* a_{k'} \rangle_0 \langle a_{k''}^* a_{k''} \rangle_0 \delta(\omega_k - \omega_{k'}), \quad (2.E.10)
\end{aligned}$$

where the zero point at $k = -k'$ vanishes owing to the hyperbolic sine function in $A_{-k, -k', k'', -k''}$. However, eq. (2.E.10) vanishes because the first two terms cancel each other and the third term is antisymmetric with respect to k'' . Thus we conclude that each term in $\langle R_0^{(2)}(t), R_0^{(2)} \exp(-\beta H_I) \rangle_0$, $\langle R_0^{(2)}(t), R_0^{(3)} \exp(-\beta H_I) \rangle_0$, and $\langle R_0^{(2)}(t), R_0^{(4)} \rangle_0$, does not contribute to $\Gamma_t(0)$.

(3) Cancellations of Remaining Terms of the Friction

We shall show that other terms, not calculated in §2.4, cancel each other exactly.

First, we calculate the remaining terms in eq. (2.4.4), which corresponds to the diagrams in Fig. 2.4(a) and Fig. 2.5(a). The contribution from the second term in (2.4.4) can be easily estimated in the same way as the first term. It gives

$$\Gamma_t(4a, 5a(2); \omega = 0)$$

$$= \frac{q\pi m^2 \ell^2}{2 \langle p_0^2 \rangle_0 L^3} \sum_{k, k', k'', p} (C_{-k, k}^D + C_{-k', k'}^D + C_{-k'', k''}^D) C_{p, -k''}^N \\ \times A_{k, k', k''} A_{-p, -k, -k'} \langle a_k^* a_k \rangle_0 \langle a_{k'}^* a_{k'} \rangle_0 \langle a_{k''}^* a_{k''} \rangle_0 \\ \times \left\{ \delta(\omega_k + \omega_{k'} - \omega_{k''}) + \delta(\omega_k - \omega_{k'} + \omega_{k''}) + \delta(-\omega_k + \omega_{k'} + \omega_{k''}) \right\}, \quad (2.E.11)$$

which is to be cancelled in eq. (2.E.30). Second we will show that the first component in the third term in (2.4.4), with $C_{p', q''}^D A_{-p', q, q'}$, does not contribute to the static friction. Its explicit form is

$$\Gamma_t(4a, 5a(3); \omega = 0)$$

$$= \frac{q\pi m^2 \ell^2}{2 \langle p_0^2 \rangle_0 L^3} \sum_{k, k', k'', p} C_{p, k''}^N (C_{k, -k}^D + C_{k', -k'}^D + C_{k'', -k''}^D) \\ \times A_{-p, k, k'} A_{-k, -k', -k''} \langle a_k^* a_k \rangle_0 \langle a_{k'}^* a_{k'} \rangle_0 \langle a_{k''}^* a_{k''} \rangle_0 \\ \times \left[\frac{(\omega_k + \omega_{k'})^2 - \omega_{k''}^2}{(\omega_k + \omega_{k'})^2 - \omega_p^2} \delta(\omega_k + \omega_{k'} - \omega_{k''}) \right. \\ \left. + \frac{(\omega_k - \omega_{k'})^2 - \omega_{k''}^2}{(\omega_k - \omega_{k'})^2 - \omega_p^2} \left\{ \delta(\omega_k - \omega_{k'} + \omega_{k''}) + \delta(-\omega_k + \omega_{k'} + \omega_{k''}) \right\} \right. \\ \left. + \left\{ \frac{1}{(\omega_k + \omega_{k'})^2 - \omega_p^2} + \frac{1}{(\omega_k - \omega_{k'})^2 - \omega_p^2} \right\} (\omega_{k''}^2 - \omega_p^2) \delta(\omega_{k''} - \omega_p) \right]. \quad (2.E.12)$$

As far as a term has the form of $\Omega \delta(\Omega)$, it does not give a contribution to the static friction. The only exceptional case is the third term when one of the vertex functions $A_{k, k', k''}$ is the δ function part (2.D.4a) and the other is the principal part

(2.D.4b). In this case, it becomes

$$\begin{aligned}
 & \Gamma_t (4a, 5a(3); \omega = 0) \\
 &= - \frac{9\pi m^2 \ell^2}{2 \langle P_0^2 \rangle_0 L^3} \sum_{k, k', k''} \frac{\omega_{k''}^2 - \omega_{k+k'}^2}{\sinh \pi(k+k'+k'')d} C_{k+k', k''}^N \\
 & \times \langle a_k^* a_k \rangle_0 \langle a_{k'}^* a_{k'} \rangle_0 \langle a_{k''}^* a_{k''} \rangle_0 \delta(\omega_{k''} - \omega_{k+k'}) \\
 & \times \left[(C_{k, -k}^D + C_{k', -k'}^D + C_{k'', -k''}^D) A_{-k+k', k, k'}^D A_{-k, -k', -k''}^P \left\{ \frac{1}{(\omega_k + \omega_{k'})^2 - \omega_{k+k'}^2} + \frac{1}{(\omega_k - \omega_{k'})^2 - \omega_{k+k'}^2} \right\} \right. \\
 & \left. + (C_{k, k}^D + C_{k', k'}^D + C_{-k+k', k+k'}^D) A_{k, k', k''}^P A_{-k, -k', k+k'}^D \left\{ \frac{1}{(\omega_k + \omega_{k'})^2 - \omega_{k''}^2} + \frac{1}{(\omega_k - \omega_{k'})^2 - \omega_{k''}^2} \right\} \right],
 \end{aligned}
 \tag{2.E.13}$$

where the zero points vanish owing to the hyperbolic sine functions in the denominators. However the two terms in (2.E.13) cancel each other because the relations $A_{k, k', k''}^D = -A_{-k, -k', -k''}^D$ and $A_{k, k', k''}^P = A_{-k, -k', -k''}^P$ hold.* The second component in the third term in (2.4.4), with $C_{p', q''}^N A_{-p', q', q''}$, does not have this exceptional case, each term having a time dependence of $[\Omega \exp(i\Omega t) + \text{c.c.}]$. Therefore, it makes no contribution to the static friction.

*) We may consider that these terms in (2.E.13) are contributions from higher harmonics with momentum $(k+k')$ which emerges through the three phonon interaction $A_{k, k', k''}$. The fact that they give no contributions to the friction is consistent with the analysis of kink-phonon collision where only the higher harmonics with frequency $2\omega_{\bar{q}}$ played an important role in the momentum transfer.

Next, we calculate the other contributions in $\langle R_0^{(3)}(t), R_0^{(3)} \rangle_0$. The explicit forms of $R_0^{(3)}(t)$, represented in Figs .2.4(b)-2.4(h), are

$$\begin{aligned}
R_0^{(3)}(4b;t) &= \frac{P_0}{4m\ell M_0^2} \sum_{k,k',p\pm} C_{-p,k}^N C_{p,k'} \left(1 - \frac{\pm\omega_{k'}}{\pm\omega_p}\right) \frac{\pm\omega_p \pm \omega_k}{\pm\omega_p \mp \omega_k} a_{k\pm} a_{k'\pm} \\
&\quad \times \left\{ (\pm i\omega_p \pm i\omega_{k'}) \exp(\pm i\omega_p t \pm i\omega_{k'} t) - (\pm i\omega_k \pm i\omega_{k'}) \exp(\pm i\omega_k t \pm i\omega_{k'} t) \right\} \\
&\quad + \frac{P_0}{2m\ell M_0^2} \sum_{k,k'\pm} C_{-k,k}^D C_{k,k'} (\pm i\omega_k \mp i\omega_{k'}) a_{k\pm} a_{k'\pm} \\
&\quad \times \left\{ \exp(\pm i\omega_k t \pm i\omega_{k'} t) + (\pm i\omega_k \pm i\omega_{k'}) t \exp(\pm i\omega_k t \pm i\omega_{k'} t) \right\}, \\
R_0^{(3)}(4c;t) &= \frac{P_0^2}{2\sqrt{2} m^2 \ell^2 M_0^{5/2}} \sum_{k,p,\pm} C_{p,k} C_{0,-p} \frac{1}{\pm\omega_p} \left(1 - \frac{\pm\omega_k}{\pm\omega_p}\right) a_{k\pm} \\
&\quad \times \left\{ (\pm\omega_p \pm \omega_k) \exp(\pm i\omega_p t \pm i\omega_k t) - (\pm\omega_k) \exp(\pm i\omega_k t) \right\}, \\
R_0^{(3)}(4d;t) &= \frac{1}{\sqrt{2} M_0^{3/2}} \sum_{k,k',k'',\pm} C_{k,k'} C_{0,k''} (\pm\omega_k) (\pm\omega_k \pm \omega_{k'} \pm \omega_{k''}) a_{k\pm} a_{k'\pm} a_{k''\pm} \\
&\quad \times \exp(\pm i\omega_k t \pm i\omega_{k'} t \pm i\omega_{k''} t), \\
R_0^{(3)}(4e;t) &= - \frac{3P_0}{2m\ell M_0^{3/2} \ell^{3/2}} \sum_{p,k,k'\pm} C_{0,p} A_{-p,k,k'} \frac{a_{k\pm} a_{k'\pm}}{(\pm\omega_p)(\pm\omega_p \mp \omega_k \mp \omega_{k'})} \\
&\quad \times \left\{ (\pm i\omega_p) \exp(\pm i\omega_p t) - (\pm i\omega_k \pm i\omega_{k'}) \exp(\pm i\omega_k t \pm i\omega_{k'} t) \right\}, \\
R_0^{(3)}(4f;t) &= - \frac{P_0^2}{\sqrt{2} m^2 \ell^2 M_0^{5/2}} \sum_{p,k\pm} C_{-p,k}^N C_{0,p} \left(1 + \frac{\pm\omega_k}{\pm\omega_p}\right) \frac{a_{k\pm}}{\pm\omega_p \mp \omega_k} \\
&\quad \times \left\{ (\pm\omega_p) \exp(\pm i\omega_p t) - (\pm\omega_k) \exp(\pm i\omega_k t) \right\} \\
&\quad - \frac{\sqrt{2} P_0^2}{m^2 \ell^2 M_0^{5/2}} \sum_{k\pm} C_{-k,k}^D C_{0,k} a_{k\pm} \left\{ \exp(\pm i\omega_k t) \pm i\omega_k t \exp(\pm i\omega_k t) \right\}, \\
R_0^{(3)}(4g;t) &= - \frac{P_0^3}{m^3 \ell^3 M_0^3} \sum_{p,\pm} C_{0,p} C_{0,-p} \frac{1}{\pm i\omega_p} \exp(\pm i\omega_p t), \\
R_0^{(3)}(4h;t) &= \frac{3P_0}{2m\ell M_0^2} \sum_{k,k'\pm} C_{0,k} C_{0,k'} a_{k\pm} a_{k'\pm} (\pm i\omega_k \pm i\omega_{k'}) \\
&\quad \times \exp(\pm i\omega_k t \pm i\omega_{k'} t),
\end{aligned} \tag{2.E.14}$$

where $R_0^{(3)}(4a;t)$ corresponding to Fig. 2.4(a) has been shown in eq. (2.4.3). Using these terms and $R_0^{(3)}(0)$ obtained in eq. (2.E.7a), we can calculate the remaining terms of $\langle R_0^{(3)}(t), R_0^{(3)} \rangle_0$. Almost all of them have a time dependence of $[\Omega \exp(i\Omega t) + \text{c.c.}]$, and thus do not contribute to the static friction. One of the two exceptional cases is a term

$$\begin{aligned} \langle R_0^{(3)}(4b;t), R_0^{(3)}(5c) \rangle_0 &= \frac{3 \langle P_0^2 \rangle_0}{2m^2 l^2 M_0^4} \sum_{k, k' \pm} C_{-k, k}^D C_{k, k'} (w_k^2 - w_{k'}^2) C_{0, -k} C_{0, -k'} \\ &\times \langle a_k^* a_k \rangle_0 \langle a_{k'}^* a_{k'} \rangle_0 (\pm i w_k \pm i w_{k'}) t \exp(\pm i w_k t \pm i w_{k'} t). \end{aligned} \quad (2.E.15a)$$

However, its contribution to $\Gamma_t(0)$ turns out to be

$$\begin{aligned} \Gamma_t(4b, 5c; \omega=0) &= - \frac{3\pi \langle P_0^2 \rangle_0}{m^2 l^2 M_0^4} \sum_{k, k'} C_{-k, k}^D C_{k, k'} (w_k^2 - w_{k'}^2) \\ &\times C_{0, -k} C_{0, -k'} \langle a_k^* a_k \rangle_0 \langle a_{k'}^* a_{k'} \rangle_0 \delta(w_k - w_{k'}) \\ &= 0, \end{aligned} \quad (2.E.15b)$$

where we have used the formula

$$\lim_{\omega \rightarrow 0} \int_0^\infty i\Omega t (e^{i\Omega t} - e^{-i\Omega t}) e^{-i\omega t} dt = -2\pi \delta(\Omega). \quad (2.E.16)$$

The same discussion applies to the other case $\langle R_0^{(3)}(4f;t), R_0^{(3)}(5d) \rangle_0$ to see that it does not give the contribution either.

Finally, the various terms in $\langle R_0^{(3)}(t) R_0^{(2)} \exp(-\beta H_I) \rangle_0$ and $\langle R_0^{(4)}(t), R_0^{(2)} \rangle_0$ are similarly investigated. In Fig. 2.8, we show all the diagrams which contribute to the friction.

[Figs. 2.8(a,b)] Using $R_0^{(3)}(t)$ in eq. (2.4.3) and the third order interaction Hamiltonian in (2.E.8), we find that Figs. 2.8(a) and 2.8(b) give

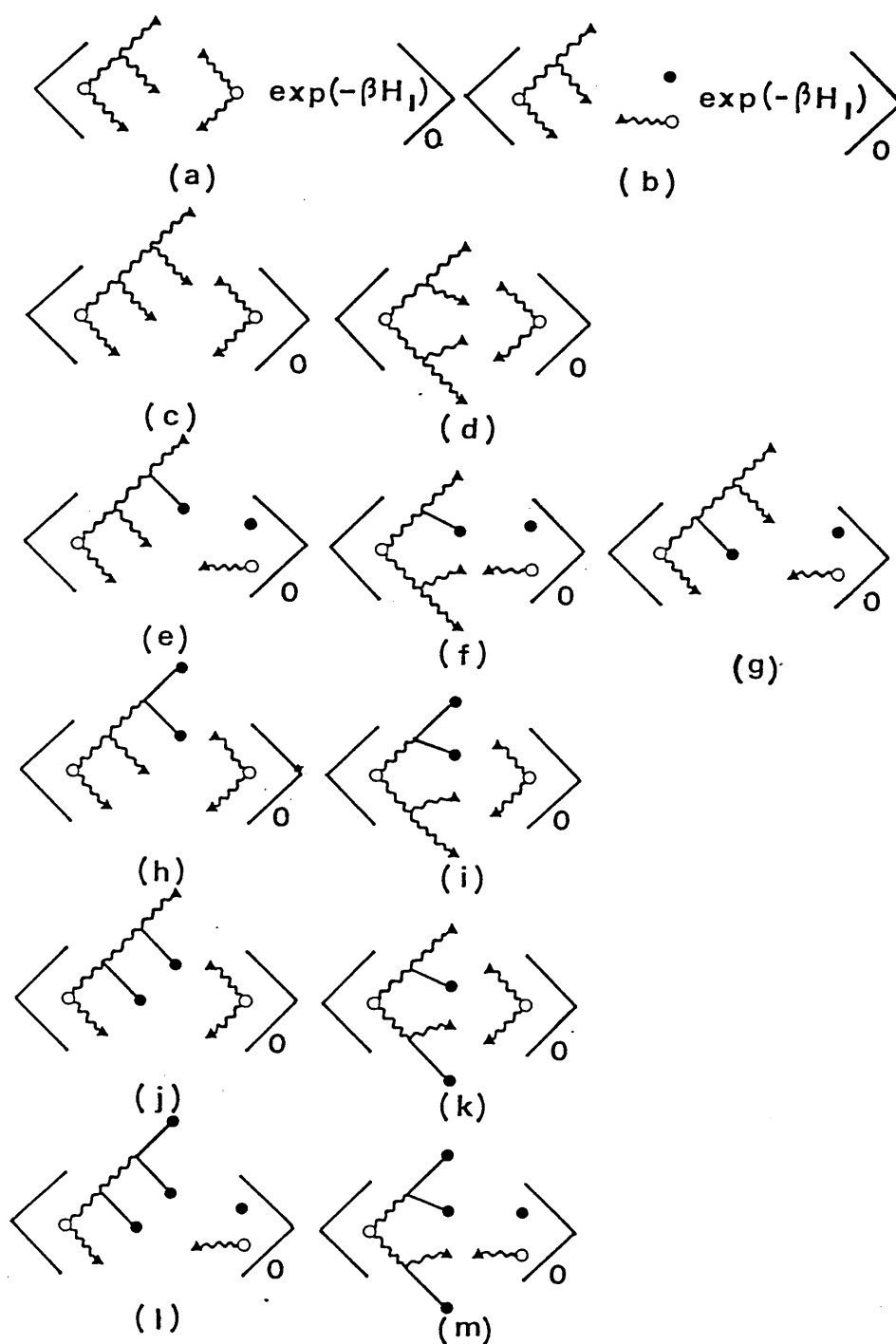


Fig. 2.8 Diagrams in $\langle R_0^{(3)}(t), R_0^{(2)} \exp(-\beta H_I) \rangle_0$ and $\langle R_0^{(4)}(t), R_0^{(2)} \rangle_0$, which contribute to the friction. They are calculated in Appendix 2.E(3). The total sum of $\Gamma(4a, 5a(2))$ and their contributions is shown to be zero in eq. (2.E.30).

$$\begin{aligned}
\Gamma_t^{(8a)}(\omega=0) = & - \frac{9\pi m^3 \ell^3 \beta}{2 \langle P_0^2 \rangle_0 L^3} \sum_{k, k', k'', q} (C_{-k, k}^D + C_{-k', k'}^D + C_{-k'', k''}^D) \\
& \times \left\{ C_{q, -k''}^N A_{k, k', k''} A_{-q, -k, -k'} (\omega_q^2 - \omega_{k''}^2) + C_{-k', -k''}^N A_{k, k', k''} A_{-k, q, -q} \omega_{k'}^2 \right\} \\
& \times \langle a_k^* a_k \rangle_0 \langle a_{k'}^* a_{k'} \rangle_0 \langle a_{k''}^* a_{k''} \rangle_0 \langle a_q^* a_q \rangle_0 \\
& \times \left\{ \delta(\omega_k + \omega_{k'} - \omega_{k''}) + \delta(\omega_k - \omega_{k'} + \omega_{k''}) + \delta(-\omega_k + \omega_{k'} + \omega_{k''}) \right\} \\
& + \frac{3\pi m \ell \beta}{2 M_0^{3/2} L^{3/2}} \sum_{k, k', k''} (C_{-k, k}^D + C_{-k', k'}^D + C_{-k'', k''}^D) A_{k, k', k''} C_{0, -k''} C_{-k, -k'}^N \\
& \times \omega_k^2 \langle a_k^* a_k \rangle_0 \langle a_{k'}^* a_{k'} \rangle_0 \langle a_{k''}^* a_{k''} \rangle_0 \\
& \times \left\{ \delta(\omega_k + \omega_{k'} - \omega_{k''}) + \delta(\omega_k - \omega_{k'} + \omega_{k''}) + \delta(-\omega_k + \omega_{k'} + \omega_{k''}) \right\}, \quad (2.E.17)
\end{aligned}$$

and

$$\begin{aligned}
\Gamma_t^{(8b)}(\omega=0) = & - \frac{3\pi m \ell \beta}{M_0^{3/2} L^{3/2}} \sum_{k, k', k''} (C_{-k, k}^D + C_{-k', k'}^D + C_{-k'', k''}^D) A_{k, k', k''} C_{0, -k''} C_{-k, -k'}^N \\
& \times \omega_k \omega_{k''} \langle a_k^* a_k \rangle_0 \langle a_{k'}^* a_{k'} \rangle_0 \langle a_{k''}^* a_{k''} \rangle_0 \\
& \times \left\{ \delta(\omega_k + \omega_{k'} - \omega_{k''}) - \delta(\omega_k - \omega_{k'} + \omega_{k''}) + \delta(-\omega_k + \omega_{k'} + \omega_{k''}) \right\}. \quad (2.E.18)
\end{aligned}$$

[Fig. 2.8(c)] In order to calculate the diagram in Fig. 2.8(c), we need the third order phonon. According to the diagrammatic perturbation procedure, we obtain

$$\begin{aligned}
Q_p^{(3)}(p; t) = & - \frac{9}{4\sqrt{2} L^3} \sum_{k, k', k'', p'(\pm)} \frac{A_{-p', k, k'} A_{-p, p', k''}}{(\pm \omega_p)(\pm \omega_{p'}) (\pm i \omega_p \mp i \omega_{p'} \mp i \omega_{k''})} a_k \pm a_{k'} \pm a_{k''} \pm \\
& \times \int_0^t dt_1 \left\{ \exp(\pm i \omega_p t_1 + (\pm i \omega_k \pm i \omega_{k'} \pm i \omega_{k''})(t - t_1)) \right. \\
& \left. - \exp(\pm i \omega_{k''} t \pm i \omega_{p'} t_1 + (\pm i \omega_k \pm i \omega_{k'}) (t - t_1)) \right\}, \quad (2.E.19)
\end{aligned}$$

and

$$\begin{aligned}
R_0^{(4)}(\mathbf{c}; t) = & \frac{9}{4M_0L^3} \sum_{\mathbf{k}, \mathbf{k}', \mathbf{k}'', \mathbf{k}''', \mathbf{p}, \mathbf{p}' \pm} C_{\mathbf{p}, \mathbf{k}'''} A_{-\mathbf{p}', \mathbf{k}, \mathbf{k}'} A_{-\mathbf{p}, \mathbf{p}', \mathbf{k}''} a_{\mathbf{k} \pm} a_{\mathbf{k}' \pm} a_{\mathbf{k}'' \pm} a_{\mathbf{k}''' \pm} \\
& \times \left[\frac{\omega_p^2 - \omega_{\mathbf{k}'''}^2}{\omega_p \{(\omega_p \mp \omega_{\mathbf{k}''})^2 - \omega_{\mathbf{p}'}^2\} (\pm \omega_{\mathbf{k}} \pm \omega_{\mathbf{k}'} \pm \omega_{\mathbf{k}''} - \omega_p)} \exp(i\omega_p t \pm i\omega_{\mathbf{k}'''} t) \right. \\
& - \frac{\omega_p^2 - \omega_{\mathbf{k}'''}^2}{\omega_p \{(\omega_p \pm \omega_{\mathbf{k}''})^2 - \omega_{\mathbf{p}'}^2\} (\pm \omega_{\mathbf{k}} \pm \omega_{\mathbf{k}'} \pm \omega_{\mathbf{k}''} + \omega_p)} \exp(-i\omega_p t \pm i\omega_{\mathbf{k}'''} t) \\
& + \frac{(\omega_{\mathbf{p}'} \pm \omega_{\mathbf{k}''})^2 - \omega_{\mathbf{k}'''}^2}{\omega_{\mathbf{p}'} \{(\omega_{\mathbf{p}'} \pm \omega_{\mathbf{k}''})^2 - \omega_p^2\} (\pm \omega_{\mathbf{k}} \pm \omega_{\mathbf{k}'} - \omega_{\mathbf{p}'})} \exp(i\omega_{\mathbf{p}'} t \pm i\omega_{\mathbf{k}''} t \pm i\omega_{\mathbf{k}'''} t) \\
& - \frac{(\omega_{\mathbf{p}'} \mp \omega_{\mathbf{k}''})^2 - \omega_{\mathbf{k}'''}^2}{\omega_{\mathbf{p}'} \{(\omega_{\mathbf{p}'} \mp \omega_{\mathbf{k}''})^2 - \omega_p^2\} (\pm \omega_{\mathbf{k}} \pm \omega_{\mathbf{k}'} + \omega_{\mathbf{p}'})} \exp(-i\omega_{\mathbf{p}'} t \pm i\omega_{\mathbf{k}''} t \pm i\omega_{\mathbf{k}'''} t) \\
& \left. - 2 \frac{(\pm \omega_{\mathbf{k}} \pm \omega_{\mathbf{k}'} \pm \omega_{\mathbf{k}''})^2 - \omega_{\mathbf{k}'''}^2}{\{(\pm \omega_{\mathbf{k}} \pm \omega_{\mathbf{k}'} \pm \omega_{\mathbf{k}''})^2 - \omega_p^2\} \{(\pm \omega_{\mathbf{k}} \pm \omega_{\mathbf{k}'} \pm \omega_{\mathbf{k}''})^2 - \omega_{\mathbf{p}'}^2\}} \exp(\pm i\omega_{\mathbf{k}} t \pm i\omega_{\mathbf{k}'} t \pm i\omega_{\mathbf{k}''} t \pm i\omega_{\mathbf{k}'''} t) \right] \quad (2.E.20)
\end{aligned}$$

where the summations over $\pm \omega_p$ and $\pm \omega_{\mathbf{p}'}$ are carried out.

Finally Fig. 2.8(c) gives

$$\begin{aligned}
\Gamma_t(\mathbf{c}; \omega=0) = & -\frac{9\pi m^2 \ell^2}{2\langle P_0^2 \rangle_0 L^3} \sum_{\mathbf{k}, \mathbf{k}', \mathbf{k}'', \mathbf{p}} (C_{-\mathbf{k}, \mathbf{k}}^D + C_{-\mathbf{k}'', \mathbf{k}''}^D) A_{\mathbf{k}, \mathbf{k}'', \mathbf{p}} A_{-\mathbf{p}, -\mathbf{k}, -\mathbf{k}'} C_{\mathbf{k}', -\mathbf{k}''}^N \\
& \times \frac{(\omega_{\mathbf{k}}^2 - \omega_{\mathbf{k}''}^2)}{\omega_p} \langle a_{\mathbf{k}}^* a_{\mathbf{k}} \rangle_0 \langle a_{\mathbf{k}'}^* a_{\mathbf{k}'} \rangle_0 \langle a_{\mathbf{k}''}^* a_{\mathbf{k}''} \rangle_0 \\
& \times \left[-\frac{\omega_{\mathbf{k}} + \omega_p}{(\omega_{\mathbf{k}} + \omega_p)^2 - \omega_{\mathbf{k}'}^2} \delta(\omega_{\mathbf{k}} + \omega_p - \omega_{\mathbf{k}'}) \right. \\
& \left. + \frac{\omega_{\mathbf{k}} - \omega_p}{(\omega_{\mathbf{k}} - \omega_p)^2 - \omega_{\mathbf{k}'}^2} \{ \delta(\omega_{\mathbf{k}} - \omega_p + \omega_{\mathbf{k}'}) + \delta(-\omega_{\mathbf{k}} + \omega_p + \omega_{\mathbf{k}'}) \} \right] \\
& + \frac{9\pi m^2 \ell^2}{2\langle P_0^2 \rangle_0 L^3} \sum_{\mathbf{k}, \mathbf{k}', \mathbf{k}'', \mathbf{p}} (C_{-\mathbf{k}', \mathbf{k}'}^D + C_{-\mathbf{k}'', \mathbf{k}''}^D) A_{\mathbf{k}', \mathbf{k}'', \mathbf{p}} A_{-\mathbf{p}, \mathbf{k}, -\mathbf{k}'} C_{-\mathbf{k}', -\mathbf{k}''}^N \\
& \times \langle a_{\mathbf{k}}^* a_{\mathbf{k}} \rangle_0 \langle a_{\mathbf{k}'}^* a_{\mathbf{k}'} \rangle_0 \langle a_{\mathbf{k}''}^* a_{\mathbf{k}''} \rangle_0 \omega_{\mathbf{k}'}^2 / \omega_p^2 \\
& \times \{ \delta(\omega_{\mathbf{k}'} + \omega_{\mathbf{k}''} - \omega_p) + \delta(\omega_{\mathbf{k}'} - \omega_{\mathbf{k}''} + \omega_p) + \delta(-\omega_{\mathbf{k}'} + \omega_{\mathbf{k}''} + \omega_p) \} \quad (2.E.21)
\end{aligned}$$

[Fig. 2.8(d)] Using the second order phonon in eq. (2.4.2), we obtain the contribution from Fig. 2.8(d). We notice it gives complementary terms to Fig. 2.8(c); that is, a term similar to

the first term in (2.E.21) which has $C_{-p,p}^D$ instead of $(C_{-k,k}^D + C_{-k'',k''}^D)$ and a term similar to the second term with $C_{-p,p}^D$ instead of $(C_{-k',k'}^D + C_{-k'',k''}^D)$. The sum of Figs. 2.8(c) and 2.8(d) is

$$\begin{aligned}
 & \Gamma_t(8c; \omega=0) + \Gamma_t(8d; \omega=0) \\
 &= -\frac{9\pi m^2 \ell^2}{2\langle P_0^2 \rangle_0 L^3} \sum_{k, k', k'', p} (C_{-k,k}^D + C_{-p,p}^D + C_{-k'',k''}^D) A_{k,k',p} A_{-p,k,-k'} C_{k',-k''}^N \frac{\omega_{k''}^2}{\omega_p^2} \\
 & \times \langle a_k^* a_k \rangle_0 \langle a_{k'}^* a_{k'} \rangle_0 \langle a_{k''}^* a_{k''} \rangle_0 \{ \delta(\omega_k + \omega_p - \omega_{k''}) + \delta(\omega_k - \omega_p + \omega_{k''}) + \delta(-\omega_k + \omega_p + \omega_{k''}) \} \\
 & + \frac{9\pi m^2 \ell^2}{2\langle P_0^2 \rangle_0 L^3} \sum_{k, k', k'', p} (C_{-k',k'}^D + C_{-k'',k''}^D + C_{-p,p}^D) A_{k',k'',p} A_{-p,k,-k} C_{-k',-k''}^N \frac{\omega_{k'}^2}{\omega_p^2} \\
 & \times \langle a_k^* a_k \rangle_0 \langle a_{k'}^* a_{k'} \rangle_0 \langle a_{k''}^* a_{k''} \rangle_0 \{ \delta(\omega_{k'} + \omega_{k''} - \omega_p) + \delta(\omega_{k'} - \omega_{k''} + \omega_p) + \delta(-\omega_{k'} + \omega_{k''} + \omega_p) \}
 \end{aligned} \tag{2.E.22}$$

where we have exchanged the variables p and k partially in the first term and used equalities due to the δ functions.

[Figs. 2.8(e-g)] They compose another group. Corresponding to Fig. 2.8(e), we obtain

$$\begin{aligned}
 Q_p^{(3)}(8e; t) &= \frac{3P_0}{4m\ell M_0 L^{3/2}} \sum_{k, k', p'(\pm)} C_{-p',k} A_{-p,p',k'} \left(1 + \frac{\pm\omega_k}{\pm\omega_{p'}}\right) \frac{a_k \pm a_{k'} \pm}{(\pm\omega_p)(\pm\omega_p \mp \omega_{p'} \mp \omega_{k'})} \\
 & \times \int_0^+ dt_1 \{ \exp(\pm i\omega_p t_1 + (\pm i\omega_k \pm i\omega_{k'})(t-t_1)) - \exp(\pm i\omega_{k'} t \pm i\omega_{p'} t_1 \pm i\omega_k(t-t_1)) \},
 \end{aligned} \tag{2.E.23}$$

and

$$\begin{aligned}
 & \Gamma_t(8e; \omega=0) \\
 &= \frac{3\pi}{M_0^{3/2} L^{3/2}} \sum_{k, k', p} (C_{-k,k}^D + C_{-k',k'}^D) A_{k,k',p} C_{-p,-k}^N C_{0,-k'} \frac{\omega_{k'}}{\omega_p} \langle a_k^* a_k \rangle_0 \langle a_{k'}^* a_{k'} \rangle_0 \\
 & \times \left[\frac{\omega_p - \omega_k}{\omega_p + \omega_k} \delta(\omega_k + \omega_p - \omega_{k'}) + \frac{\omega_p + \omega_k}{\omega_p - \omega_k} \{ \delta(\omega_k - \omega_p + \omega_{k'}) - \delta(-\omega_k + \omega_p + \omega_{k'}) \} \right].
 \end{aligned} \tag{2.E.24}$$

Figure 2.8(f) gives two terms. First it has a singular term which diverges,

$$\Gamma_t(8f; \omega=0) = - \frac{6}{M_0^{3/2} L^{3/2}} \sum_{k,k'} C_{-k',k'}^D C_{k',-k'}^D \times (A_{k,k,-k} C_{0,-k'} + 2 A_{k,k',-k'} C_{0,-k}) \langle a_k^* a_k \rangle_0 \langle a_{k'}^* a_{k'} \rangle_0 \int_0^\infty dt. \quad (2.E.25)$$

However, the contribution from Fig. 2.8(g) gives the very counter-term of it. Second, Fig. 2.8(f) has the other term which is complementary to Fig. 2.8(e) with $C_{-p,p}^D$ instead of $(C_{-k,k}^D + C_{-k',k'}^D)$ in (2.E.24). Totally, Figs. 2.8(e)-2.8(g) give

$$\begin{aligned} & \Gamma_t(8e; \omega=0) + \Gamma_t(8f; \omega=0) + \Gamma_t(8g; \omega=0) \\ &= \frac{3\pi}{M_0^{3/2} L^{3/2}} \sum_{k,k',p} (C_{-k,k}^D + C_{-k',k'}^D + C_{-p,p}^D) A_{k,k',p} C_{-p,-k}^N C_{0,-k'} \langle a_k^* a_k \rangle_0 \\ & \times \langle a_{k'}^* a_{k'} \rangle_0 \left\{ \delta(\omega_k + \omega_{k'} - \omega_p) + \delta(\omega_k - \omega_{k'} + \omega_p) + \delta(-\omega_k + \omega_{k'} + \omega_p) \right\}, \quad (2.E.26) \end{aligned}$$

where the antisymmetric property with respect to the exchange of p and k has been used.

[Figs. 2.8(h,i)] Corresponding to Fig. 2.8(h), we obtain

$$\begin{aligned} Q_p^{(3)}(8h; t) &= - \frac{3 i p_0^2}{2\sqrt{2} m^2 l^2 M_0^{3/2} L^{3/2}} \sum_{k,p'(\pm)} C_{0,-p'} A_{-p,p',k} \frac{a_{k\pm}}{(\pm\omega_p)(\pm\omega_{p'}) (\pm\omega_p \mp \omega_k \mp \omega_{p'})} \\ & \times \int_0^t dt_1 \left\{ \exp(\pm i\omega_p t_1 \pm i\omega_k(t-t_1)) - \exp(\pm i\omega_{p'} t_1 \pm i\omega_k t) \right\}, \\ \Gamma_t(8h; \omega=0) &= - \frac{3\pi}{2 M_0^{3/2} L^{3/2}} \sum_{k,k',p} (C_{-k,k}^D + C_{-k',k'}^D) A_{k,k',p} C_{-k,-k'}^N C_{0,-p} \frac{\omega_k^2}{\omega_p^2} \\ & \times \langle a_k^* a_k \rangle_0 \langle a_{k'}^* a_{k'} \rangle_0 \left\{ \delta(\omega_k + \omega_{k'} - \omega_p) + \delta(\omega_k - \omega_{k'} + \omega_p) + \delta(-\omega_k + \omega_{k'} + \omega_p) \right\}. \end{aligned} \quad (2.E.27)$$

Figure 2.8(i) gives a complementary term to this, which has $C_{-p,p}^D$ instead of $(C_{-k,k}^D + C_{-k',k'}^D)$.

[Figs. 2.8(j-m)] Figures 2.8(j) and 2.8(l) give

$$\begin{aligned}
& \Gamma_t(8j; \omega=0) \\
&= -\frac{\pi}{2M_0^2} \sum_{k,k',p} C_{-p,k}^N C_{k',p}^N C_{-k',k'}^D C_{-k,-k'}^N \frac{(\omega_p + \omega_{k'}) (\omega_p^2 + \omega_{k'}^2) (\omega_{k'}^2 - \omega_{k'}'^2)}{\omega_p (\omega_p^2 - \omega_{k'}^2)} \\
&\quad \times \langle a_k^* a_k \rangle_0 \langle a_{k'}'^* a_{k'} \rangle_0 \delta(\omega_p - \omega_{k'}) \\
&+ \frac{\pi}{2M_0^2} \sum_{k,k'} (C_{-k,k}^D + C_{-k',k'}^D) C_{-k',k'}^D C_{k',k}^N C_{-k,-k'}^N (\omega_k + \omega_{k'})^2 \langle a_k^* a_k \rangle_0 \langle a_{k'}'^* a_{k'} \rangle_0 \\
&\quad \times \delta(\omega_k - \omega_{k'}) \\
&+ \frac{1}{M_0^2} \sum_{k,k'} C_{k',-k'}^D C_{-k',k'}^D C_{k',k}^N C_{-k,-k'}^N (\omega_k^2 + \omega_{k'}^2) \int_0^\infty dt, \tag{2.E.28}
\end{aligned}$$

$$\begin{aligned}
& \Gamma(8l; \omega=0) \\
&= -\frac{3\pi \langle p_0^2 \rangle_0}{m^2 l^2 M_0^3} \sum_{k,p} C_{0,-p} C_{k,p}^N C_{-k,k}^D C_{0,-k} \frac{\omega_k (\omega_k + \omega_p)}{\omega_p^2} \langle a_k^* a_k \rangle_0 \delta(\omega_p - \omega_k) \\
&\quad - \frac{3 \langle p_0^2 \rangle_0}{m^2 l^2 M_0^3} \sum_k C_{0,k} C_{k,-k}^D C_{-k,k}^D C_{0,-k} \langle a_k^* a_k \rangle_0 \int_0^\infty dt. \tag{2.E.29}
\end{aligned}$$

We can verify that the contribution from Fig. 2.8(k) exactly cancel with that from Fig. 2.8(j) and so does the contribution from Fig. 2.8(m) with that from Fig. 2.8(l). It is readily seen that the total sum vanishes;

$$\begin{aligned}
& \Gamma(4a; 5a(2)) + \Gamma(8a) + \Gamma(8b) + \Gamma(8c) + \Gamma(8d) + \Gamma(8e) + \Gamma(8f) \\
& + \Gamma(8g) + \Gamma(8h) + \Gamma(8i) + \Gamma(8j) + \Gamma(8k) + \Gamma(8l) + \Gamma(8m) = 0. \tag{2.E.30}
\end{aligned}$$

References

- 1) J.-L. Gervais and B. Sakita: Phys. Rev. D11 (1975) 2943.
- 2) For a review see, R. Jackiw: Rev. Mod. Phys. 49 (1977) 681.
- 3) T. Miyashita and K. Maki: Phys. Rev. B28 (1983) 6733; Phys. Rev. B31 (1985) 1836.
- 4) M. Fukuma and S. Takada: J. Phys. Soc. Jpn. 55 (1986) 2701.
- 5) H. Mori: Prog. Theor. Phys. 33 (1965) 423.
- 6) Y. Wada and J.R. Schrieffer: Phys. Rev. B18 (1978) 3897.
- 7) E. Tomboulis: Phys. Rev. D12 (1975) 1678.
- 8) J.-L. Gervais and A. Jevicki: Nucl. Phys. B110 (1976) 93.
- 9) J. Goldstone and R. Jackiw: Phys. Rev. D11 (1975) 1486.
- 10) Y. Wada: J. Phys. Soc. Jpn. 51 (1982) 2735.
- 11) H. Ishiuchi and Y. Wada: Prog. Theor. Phys. Suppl. 69 (1980) 242.
- 12) M. Ogata and Y. Wada: J. Phys. Soc. Jpn. 53 (1984) 3855.
- 13) N. Theodorakopoulos: Z. Physik B33 (1979) 385.
- 14) R. Kubo: Rep. Prog. Phys. 29 (1966) 255.
- 15) J. Rubinstein: J. Math. Phys. 11 (1970) 258.
- 16) K. Fesser: Z. Physik B39 (1980) 47.
- 17) Y. Wada and H. Ishiuchi: J. Phys. Soc. Jpn. 51 (1981) 1372.
- 18) C. Kunz and J.A. Combs: Phys. Rev. B31 (1985) 527.
- 19) J.A. Combs and S. Yip: Phys. Rev. B28 (1983) 6873.
- 20) J.R. Schrieffer: private communication.
- 21) M. Ogata: unpublished.
- 22) J.-L. Gervais, A. Jevicki and B. Sakita: Phys. Rev. D12 (1975) 1038.
- 23) I.S. Gradshteyn and I.M. Ryzhik: Tables of Integrals, Series and Products (Academic Press, New York, 1980) p.352.

Chapter III Brownian Motion of a Soliton in trans-Polyacetylene

§3.1. Introduction

In the previous chapter, the Brownian motion of the ϕ^4 -kink has been studied. In this chapter, we study diffusive motion of a soliton in trans-polyacetylene, using Takayama, Lin-Liu, and Maki's model (TLM model).¹⁾ As in the ϕ^4 case, there are two mechanisms. One is a random walk and the other is an ordinary Brownian motion.

As discussed in §1.4, the effective potential for phonons in the presence of a soliton is not reflectionless in the TLM model.²⁾ This means that there is momentum transfer between the soliton and the phonons in the lowest order collision process. As a result, it is predicted that the friction is proportional to $k_B T$ in the low temperature region, if the classical ensemble average of the phonon distribution is assumed. In fact, we calculate the friction to show that it is proportional to $k_B T$. Einstein relation gives a diffusion constant which is temperature independent.

The relation between the two mechanisms is also clarified by investigating the fluctuation-dissipation theorem. It is shown that, when the frequency is not zero (finite time region), the mechanism of the random walk coexists with the ordinary Brownian motion. The dynamical diffusion constant, $D(\omega)$, becomes proportional to T^2 , when $\omega \neq 0$ and the temperature is low enough. As the temperature increases, $D(\omega)$ approaches a constant value.

In §3.2 we apply the collective coordinate method³⁻⁶⁾ to

the TLM model within the adiabatic approximation. One of the merits of this method is that the soliton coordinate (collective coordinate) can be introduced from the original field variable by a canonical transformation.⁵⁾ It is remarkable that there are only a few differences between the Hamiltonian in the ϕ^4 model and that in the TLM model, when they are written in terms of the collective coordinates. Especially it is shown that the equations of motion are formally universal. Using Mori's formula,⁷⁾ we calculate the friction in §3.3. In order to take account of the reflection of the phonon, structure of $\Gamma(\omega)$ is carefully studied. In §3.4, the diffusion constant is obtained and the relation between the two mechanisms is clarified. Quantum correction is discussed in §3.5. Section 3.6 is devoted to discussion.

§3.2 Collective Coordinate Method for trans-(CH)_x

For trans-polyacetylene, Takayama, Lin-Liu, and Maki derived a Hamiltonian,¹⁾ (see §1.4),

$$H = \frac{1}{2g^2} \int dx \{ g^4 P^2(x,t) + \omega_Q^2 \Delta^2(x,t) \} \\ + \sum_s \int dx \psi_s^\dagger(x,t) [-iv_F \sigma_3 \partial_x + \sigma_1 \Delta(x,t)] \psi_s(x,t), \quad (3.2.1)$$

with g the coupling constant, ω_Q the bare optical phonon frequency, v_F the Fermi velocity, and σ_1 and σ_3 the Pauli matrices. The order parameter $\Delta(x,t)$ is proportional to the continuum limit of $(-1)^n u_n$, where u_n is the displacement of the n -th (CH) unit from its equilibrium point of non-dimerized state. Its conjugate momentum $P(x,t)$ is defined by $P(x,t) = \dot{\Delta}(x,t)/g^2$. The electron fields $\psi_s^\dagger(x,t)$ and $\psi_s(x,t)$ with the spin index s have two components which represent the right- and left-going waves. We use the unit system where $\hbar=1$.

As one of exact static solutions of (3.2.1), there is a soliton solution in the form

$$\Delta_s(x) = \Delta_0 \tanh(x/\xi), \quad (3.2.2)$$

with $\xi = v_F/\Delta_0$ the soliton width, Δ_0 the magnitude of the order parameter in the dimerized state. The corresponding electronic wave functions and eigenvalues are expressed by $\{\psi_{n,s}^{(0)}(x)\}$ and $\{\varepsilon_n\}$, respectively. The gap in the electronic band is equal to $2\Delta_0$.

In order to investigate the soliton motion, we introduce a transformation of the variables in the form^{5,6)}

$$\Delta(x,t) = \Delta_s(x-Q_0(t)) + \chi(x-Q_0(t),t),$$

$$P(x,t) = - \frac{P_0 + \int \pi \chi' dx}{M_0(1+\zeta(t)/M_0)} \Delta_s'(x-Q_0(t)) + \pi(x-Q_0(t),t), \quad (3.2.3)$$

with constraints

$$\begin{aligned} \int \chi(x,t) \Delta_s'(x) dx &= 0, \\ \int \pi(x,t) \Delta_s'(x) dx &= 0, \end{aligned} \quad (3.2.4)$$

where primes attached on χ and Δ_s indicate the spatial derivatives, M_0 is "mass" of the soliton defined by

$$M_0 = \int (\Delta_s')^2 dx = 4\Delta_0^2/3\xi, \quad (3.2.5)$$

and the function $\zeta(t)$ is

$$\zeta(t) = \int \Delta_s'(x) \chi'(x,t) dx. \quad (3.2.6)$$

As readily seen from (3.2.3), a new dynamical variable Q_0 represents the location of the soliton. It is called the collective coordinate.

As referred to in §1.4, the linear mode analysis around the soliton solution was carried out numerically to show that there are three localized modes, g_0 , g_1 , and g_2 in addition to the extended phonon modes.^{2,8,9)*} The lowest energy mode g_0 with

* Hicks and Blaisdell⁹⁾ concluded that there were two localized modes. Ono, Terai and Wada²⁾ have reinvestigated the linear modes taking account of the correct boundary condition to find that the phase shift analysis of the extended modes has confirmed the existence of the three localized modes. The number of the localized modes, however, does not affect our results qualitatively.

zero eigenfrequency has the form

$$g_0(x) = \text{sech}^2(x/\xi) \propto \Delta_s'(x). \quad (3.2.7)$$

It corresponds to the Goldstone mode. Using these linear modes, we can expand the fields $\chi(x,t)$ and $\pi(x,t)$ as

$$\begin{aligned} \chi(x,t) &= \sum_{n \neq 0} N_n^{-1/2} Q_n(t) g_n(x), \\ \pi(x,t) &= \sum_{n \neq 0} N_n^{-1/2} P_n^*(t) g_n(x). \end{aligned} \quad (3.2.8)$$

Here N_n is the normalization factor defined by $\int g_n^* g_m dx = N_n \delta_{n,m}$. In eq. (3.2.8), the Goldstone mode is excluded because of the constraints (3.2.4). Note that the summation is over the other two localized modes as well as the phonon modes $g_k(x)$ defined by

$$g_k(x) = g_{ek}(x) + i g_{ok}(x), \quad g_{-k}(x) = g_k^*(x), \quad (3.2.9)$$

with $g_{ek}(x)$ and $g_{ok}(x)$ being the even and odd eigenfunctions, respectively. The normalization factor of g_k is $N_k=L$. It can be shown that the transformation from $\{\Delta(x), P(x)\}$ to $\{Q_0, P_0, Q_n, P_n\}$ is canonical.^{5,6)}

Substitution of eqs. (3.2.3) and (3.2.8) into (3.2.1) leads to the following Hamiltonian in terms of the new variables,

$$\begin{aligned} H &= \sum_{n,s} \varepsilon_n C_{n,s}^\dagger C_{n,s} + \sum_m \sum_{n,s} \varphi_{mn}[\chi] C_{m,s}^\dagger C_{n,s} \\ &+ \frac{g^2 (P_0 + \int \pi \chi' dx)^2}{2M_0 (1 + \xi/M_0)^2} + \frac{g^2}{2} \int \pi^2 dx + \frac{\omega_Q^2}{2g^2} \int (\Delta_s + \chi)^2 dx, \end{aligned} \quad (3.2.10)$$

where $C_{n,s}^\dagger$ and $C_{n,s}$ are the creation and annihilation operators of an electron in the state $\psi_n^{(0)}(x-Q_0)$ and

$$\varphi_{mn}[\chi] \equiv \int dx \psi_m^{(0)\dagger}(x) \sigma_1 \chi(x,t) \psi_n^{(0)}(x). \quad (3.2.11)$$

Next, we introduce the electron annihilation operator A_{ns} and the hole annihilation operator B_{ns} by

$$A_{ns} = C_{ns} \quad [n : \text{unoccupied}], \quad (3.2.12a)$$

$$B_{ns} = C_{ns}^\dagger \quad [n : \text{occupied}]. \quad (3.2.12b)$$

The creation operators are defined similarly. Then the Hamiltonian can be rewritten as follows;^{10,11)}

$$H = E_S + H_0 + H_{\text{int}} + H_{\text{ph}},$$

$$H_0 = \sum_{m,s}'' \varepsilon_m A_{m,s}^\dagger A_{m,s} - \sum_{n,s}' \varepsilon_n B_{n,s}^\dagger B_{n,s},$$

$$\begin{aligned} H_{\text{int}} = & \sum_m'' \sum_{n,s}'' \varphi_{mn}[\chi] A_{m,s}^\dagger A_{n,s} - \sum_m' \sum_{n,s}' \varphi_{nm}[\chi] B_{m,s}^\dagger B_{n,s} \\ & + \sum_m'' \sum_{n,s}' \{ \varphi_{mn}[\chi] A_{m,s}^\dagger B_{n,s}^\dagger + \varphi_{nm}[\chi] B_{n,s} A_{m,s} \}, \end{aligned}$$

$$H_{\text{ph}} = \frac{g^2 (P_0 + \int \pi \chi' dx)^2}{2M_0 (1 + \zeta/M_0)^2} + \frac{g^2}{2} \int \pi^2 dx + \frac{\omega_Q^2}{2g^2} \int \chi^2 dx, \quad (3.2.13)$$

where E_S is the excitation energy of the soliton ($E_S = 2\Delta_0/\pi$).

The prime and the double prime attached to the summation symbols indicate the sums over the occupied states and the unoccupied states, respectively.

In the following, we use the adiabatic approximation, i.e., we assume that the occupancy of the electronic states does not

change even if $\Delta(x,t)$ varies with time. Within this approximation, the above Hamiltonian is reduced to

$$H_{ad} = E_S + H_{ph} + V[\chi]. \quad (3.2.14)$$

The quantity $V[\chi]$ is called an adiabatic potential. According to the usual many-body theory,¹²⁾ it is expressed by

$$\begin{aligned} V[\chi(x,t)] &= \sum_{j=0}^{\infty} V^{(j)}[\chi] \\ &= \sum (0 | H_{int} \left(\frac{1}{E_0 - H_0} H_{int} \right)^j | 0)_c, \end{aligned} \quad (3.2.15)$$

where $|0\rangle$ denotes the ground state of the electrons for the unperturbed Hamiltonian H_0 and $E_0 = \sum_{n,s} \epsilon_n$. Only the contributions from connected diagrams are taken into account in (3.2.15). Since the soliton solution gives a minimal value of the energy, the linear term with respect to χ vanishes. It is also readily seen that the bilinear terms with respect to χ , i.e. $V^{(1)}[\chi]$ and $(\omega_Q^2/2g^2) \int \chi^2 dx$, give a simple term $\sum \Omega_n^2 Q_n^* Q_n$, because the field χ has been expanded in terms of the appropriate linear modes. Finally the following Hamiltonian is obtained;

$$\begin{aligned} H &= E_S + \frac{g^2 (P_0 + \int \pi \chi' dx)^2}{2M_0 (1 + \xi/M_0)^2} + \frac{g^2}{2} \sum_{n \neq 0} P_n^* P_n + \frac{1}{2g^2} \sum_{n \neq 0} \Omega_n^2 Q_n^* Q_n + H_Q, \\ H_Q &= \sum_{j=2}^{\infty} V^{(j)}[\chi], \end{aligned} \quad (3.2.16)$$

where H_Q represents nonlinear interactions between the linear modes, which are cubic, quartic, and of the higher orders with respect to Q_n . The explicit expression for $V^{(2)}[\chi]$ is given in

ref. 10 as

$$\begin{aligned}
 V^{(2)}[\chi] &= \sum'_{n,s} \sum''_{m\ell} \frac{\varphi_{n\ell}[\chi] \varphi_{\ell m}[\chi] \varphi_{mn}[\chi]}{(\varepsilon_n - \varepsilon_\ell)(\varepsilon_n - \varepsilon_m)} \\
 &- \sum'_{n,m,s} \sum''_{\ell} \frac{\varphi_{n\ell}[\chi] \varphi_{\ell m}[\chi] \varphi_{mn}[\chi]}{(\varepsilon_\ell - \varepsilon_m)(\varepsilon_\ell - \varepsilon_n)} \\
 &= \sum_{n,n',n''} A_{n,n',n''} Q_n Q_{n'} Q_{n''} / L^S,
 \end{aligned}
 \tag{3.2.17}$$

where the parameter s is a half of the number of the extended phonon modes in (n, n', n'') . Finally the equation of motion for the collective coordinate is

$$\begin{aligned}
 \frac{dQ_0(t)}{dt} &= \frac{g^2(P_0 + \int \pi \chi' dx)}{M_0(1 + \zeta/M_0)^2}, \\
 \frac{dP_0(t)}{dt} &= 0.
 \end{aligned}
 \tag{3.2.18}$$

Since the Hamiltonian (3.2.16) does not depend on Q_0 , owing to the translational symmetry of the system, the variable P_0 is constant.

Before concluding this section, we compare the polyacetylene with the nonlinear Klein-Gordon systems, such as sine-Gordon, ϕ^4 . Although the original Hamiltonian is very different, the collective coordinate Hamiltonian for the nonlinear Klein-Gordon model (see §2.2) is similar to that for the TLM model. The difference is in the linear mode analysis.

In the ϕ^4 model, the complete set of the linear modes around the soliton (kink) contains the phonon modes and two

localized modes with frequencies $\omega=0$ and $\omega=\omega_1 = \sqrt{3/4}\omega_0$. (See eq. (1.2.3) and Ref. 13.) The phonon dispersion is determined by $\omega^2 = \omega_0^2(1+\eta^2)$, with $\eta=k\xi/2$ and $\xi=2d$ the soliton width.

On the other hand, numerical calculation in the TLM model showed that there are three localized modes g_0 , g_1 , and g_2 .^{2,8)} Their eigenfrequencies Ω_i 's are

$$\left(\frac{\Omega_0}{\omega_0}\right)^2 = 0.000, \quad \left(\frac{\Omega_1}{\omega_0}\right)^2 = 0.703, \quad \left(\frac{\Omega_2}{\omega_0}\right)^2 = 0.941, \quad (3.2.21)$$

respectively, in the weak coupling limit.¹⁴⁾ Here ω_0 is the renormalized optical phonon frequency $\omega_0 = \sqrt{2\lambda}\omega_Q$ and $\lambda = g^2/\pi v_F \omega_Q^2 = 0.19$. Concerning the phonon dispersion, it is worthwhile noting that there is an analytic expression in the case of the perfectly dimerized state (i.e. $\Delta(x) = \Delta_0$). The integral equation of the linear mode around the perfectly dimerized state has an eigenfunction of the form $g_k = \exp(ikx)$ and the corresponding eigenfrequency is given by¹⁵⁾

$$\frac{\Omega^2}{\omega_0^2} = \eta^{-1}(1+\eta^2)^{1/2} \operatorname{arcsinh} \eta, \quad (3.2.22)$$

with $\eta = k\xi/2$. Since the soliton is an localized object, it is natural to expect that the extended phonon modes asymptotically approach the plane waves in the region far from the soliton. Therefore, the phonon dispersion in the presence of the soliton is the same as that in the perfectly dimerized case, (3.2.22). In fact, the numerical calculation of the linear mode around the soliton showed that the phonon dispersion coincides exactly with

that without the soliton, if the finite cut-off effect of the momentum integral is taken into account. The phonon dispersion (3.2.22) is depicted in Fig. 3.1 in comparison with that of the ϕ^4 model.

Furthermore, as discussed in §1.4, the effective potential for phonons is not reflectionless in the TLM model, while it is reflectionless in the ϕ^4 model. This difference appears in the explicit form of the phonon mode, $g_k(x)$. In the TLM model, the phase shifts of the even and odd parity phonon modes are different from each other (see Fig. 1.13), while they are the same in the ϕ^4 model.

Except for these points, there is no difference in the structures of the collective coordinate Hamiltonians of the TLM model and the nonlinear Klein-Gordon model. Especially the equation of motion of the collective coordinate, (3.2.18), is universal in these soliton bearing systems. In the following section, we apply to the TLM model the method of calculating the friction and the diffusion constant which has been developed for the ϕ^4 model in Chapter II.

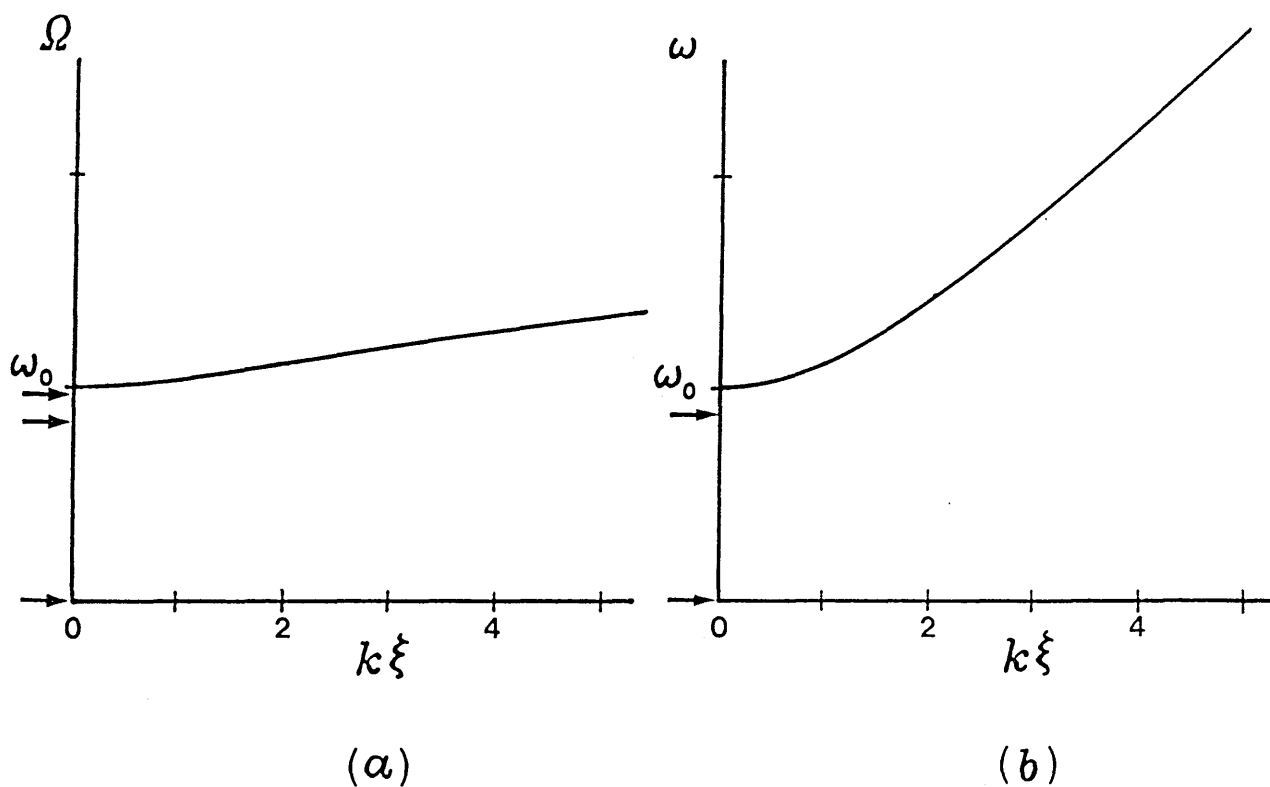


Fig. 3.1 Dispersions of the optical phonon frequencies; (a) in the TLM model and (b) in the ϕ^4 model. For the TLM model, the dispersion is calculated from the analytic form in eq. (3.2.22). The frequencies of the localized modes are indicated by arrows.

§3.3 Friction Function

We use the formula developed by Mori,⁷⁾ which gives the equation of motion for the dynamical variable $Q_0(t)$ in a form of a generalized Langevin equation

$$d^2Q_0(t)/dt^2 = -\int_0^t \gamma(t-\tau) \dot{Q}_0(\tau) d\tau + R(t), \quad (3.3.1)$$

where the random force $R(t)$ is defined by

$$R(t) = \exp(-itP'\mathcal{L}) \ddot{Q}_0, \quad (3.3.2)$$

\mathcal{L} being the Liouville operator and $\ddot{Q}_0 = \ddot{Q}_0(t=0)$. From now on, a variable, which is not indicated to be a function of time, represents its value at the initial time, $t=0$. The projection operator P is defined by

$$Pg(t) \equiv \frac{\langle g(t), \dot{Q}_0 \rangle}{\langle \dot{Q}_0, \dot{Q}_0 \rangle} \dot{Q}_0, \quad (3.3.3)$$

and $P' = 1 - P$, where the inner product \langle , \rangle means the canonical ensemble average with respect to the initial distribution. The function $\gamma(t)$ represents the friction defined by

$$\gamma(t) = \langle R(t), R(0) \rangle / \langle \dot{Q}_0, \dot{Q}_0 \rangle. \quad (3.3.4)$$

Mori's formula gives the fluctuation-dissipation theorem of the first kind for the soliton motion, which relates the diffusion constant with the friction. Taking the inner product of

(3.3.1) and \dot{Q}_0 , we perform the Fourier-Laplace transformation. An integration by parts gives the fluctuation-dissipation theorem:

$$D(\omega) \equiv \int_0^{\infty} \langle \dot{Q}_0(t), \dot{Q}_0 \rangle \exp(-i\omega t) dt = \frac{\langle \dot{Q}_0, \dot{Q}_0 \rangle}{i\omega + \Gamma(\omega)}, \quad (3.3.5)$$

where

$$\Gamma(\omega) = \int_0^{\infty} \gamma(t) \exp(-i\omega t) dt. \quad (3.3.6)$$

In the following, we calculate

$$\Gamma_t(\omega) = \int_0^{\infty} \frac{\langle \ddot{Q}_0(t), \ddot{Q}_0 \rangle}{\langle \dot{Q}_0, \dot{Q}_0 \rangle} \exp(-i\omega t) dt, \quad (3.3.7)$$

which is the Fourier-Laplace transform of the total force correlation. Some discussions have been given to identify $\Gamma(\omega)$ with $\Gamma_t(\omega)$, when the latter is estimated using perturbation approximations. (see §2.6)

We first expand $\Gamma_t(\omega)$ in a power series with respect to the temperature T ,

$$\Gamma_t(\omega) = \Gamma_t^{(0)}(\omega) + \Gamma_t^{(1)}(\omega) + \dots, \quad (3.3.8)$$

the first and second terms being linear and quadratic in T , respectively. Next, a perturbation expansion of $\dot{Q}_0(t)$ is obtained from (3.2.18). Finally, substituting the obtained expressions of $\dot{Q}_0(t)$ into (3.3.7) and making use of the thermal averages of the variables

$$\langle Q_n^* Q_n \rangle_0 = g^2 k_B T / \Omega_n^2,$$

$$\langle P_n^* P_n \rangle_0 = k_B T / g^2,$$

$$\langle P_0^2 \rangle_0 = M_0 k_B T / g^2, \quad (3.3.9)$$

we obtain the low temperature expansion of $\Gamma_t(\omega)$. Here the brackets \langle , \rangle_0 indicate the thermal average with respect to the distribution determined by the bilinear part of the Hamiltonian (3.2.16). In the lowest order, we get,

$$\begin{aligned} \Gamma_t^{(0)}(\omega) = & \frac{g^2 k_B T}{4M_0} \sum_{n,n'} C_{n,n'} C_{-n,-n'} \frac{(\Omega_n^2 - \Omega_{n'}^2)^2}{\Omega_n^2 \Omega_{n'}^2} \\ & \times \left[\frac{i\omega}{(\Omega_n + \Omega_{n'})^2 - (\omega - i\varepsilon)^2} + \frac{i\omega}{(\Omega_n - \Omega_{n'})^2 - (\omega - i\varepsilon)^2} \right] \\ & + \frac{4g^2 k_B T}{M_0} \sum_n C_{0,n} C_{0,-n} \frac{i\omega}{\Omega_n^2 - (\omega - i\varepsilon)^2}, \end{aligned} \quad (3.3.10)$$

where $C_{n,m}$ is defined by

$$C_{n,m} = (N_n N_m)^{-1/2} \int g_n(x) g_m'(x) dx, \quad (n, m = 0, 1, 2, k) \quad (3.3.11)$$

which appears in the quantities $\int \pi \chi' dx$ and ζ .

Using the relation,

$$\frac{\omega}{\Omega^2 - (\omega - i\varepsilon)^2} = \text{principal part} \frac{\omega}{\Omega^2 - \omega^2} - \frac{i\pi}{2} [\delta(\Omega + \omega) + \delta(\Omega - \omega)], \quad (3.3.12)$$

we obtain the static limit of eq. (3.3.10),

$$\Gamma^{(0)} \equiv \lim_{\omega \rightarrow 0} \Gamma_t^{(0)}(\omega) = \frac{g^2 k_B T_L}{8M_0} \sum_q |C_{q,p}|^2 \frac{(\Omega_q^2 - \Omega_p^2)^2}{\Omega_q^2 \Omega_p^2 |v_p|} \Big|_{|p| \rightarrow q}, \quad (3.3.13)$$

where v_q is the group velocity defined by

$$v_q = d\Omega_q/dq. \quad (3.3.14)$$

Note that the second term on the r.h.s. of eq. (3.3.10) does not contribute to the friction. Whether $\Gamma^{(0)}$ remains finite or not depends on the structure of the function $C_{q,p}$. If $C_{q,p}$ has a pole at $|p|=q$, $\Gamma^{(0)}$ has a finite value. Otherwise it is equal to zero. In the following, we calculate $C_{q,p}$ carefully, taking into account the effect of the reflection.

The extended phonon modes approach plane waves in the region far from the soliton. Therefore we rewrite even and odd parity phonons in the form, (see §1.4),

$$\begin{aligned} g_{eq}(x) &= \cos[qx + \delta_e(q)/2] + f_{eq}(x), \\ g_{oq}(x) &= \sin[qx + \delta_o(q)/2] + f_{oq}(x), \end{aligned} \quad (q>0, x>0) \quad (3.3.15)$$

where $f_{eq}(x)$ and $f_{oq}(x)$ are functions localized near the soliton at $x=0$. From the explicit forms of $g_{eq}(x)$ and $g_{oq}(x)$ obtained numerically, the phase shifts have been calculated through the least square method.²⁾ The obtained phase shifts are well approximated by the following forms,

$$\begin{aligned} \delta_e(q) &= 3\pi - 2[\arctan(a_1 q \xi) + \arctan(a_2 \xi) + \arctan(a_1 q \xi)], \\ \delta_o(q) &= 2\pi - 2[\arctan\{(\sqrt{(q\xi)^2 + b_1^2} - b_1)/b_2\} \\ &\quad + \arctan\{(\sqrt{(q\xi)^2 + b_1^2} - b_1)/b_3\}], \end{aligned} \quad (3.3.16)$$

with the coefficients $(a_1, a_2, a_3, b_1, b_2, b_3) = (1.70, 0.895, 0.316, 1.53, 0.551, 3.45)$.*)

Using the above results, we define the normal mode by

$$\begin{aligned} g_q(x) &= g_{eq}(x) + ig_{oq}(x), \\ g_{-q}(x) &= g_q(x)^*. \end{aligned} \quad (3.3.17)$$

Substituting eqs. (3.3.15) and (3.3.17) into the definition of $C_{q,p}$, eq. (3.3.11), we obtain

$$\begin{aligned} C_{q,p} &= (2i/L) \int_0^{L/2} [g_{eq}(x)g'_{op}(x) + g_{oq}(x)g'_{ep}(x)]dx \\ &= \frac{2i}{L} \left[-\frac{p}{2(q+p)} \{ \sin[\delta_e(q)/2 + \delta_o(p)/2] + \sin[\delta_o(q)/2 + \delta_e(p)/2] \} \right. \\ &\quad \left. -\frac{p}{2(q-p)} \{ \sin[\delta_e(q)/2 - \delta_o(p)/2] - \sin[\delta_o(q)/2 - \delta_e(p)/2] \} \right. \\ &\quad \left. + \int_0^{L/2} \{ p f_{eq}(x) \cos[px + \delta_o(p)/2] + f'_{ep}(x) \sin[qx + \delta_o(q)/2] \right. \\ &\quad \left. - p f_{oq}(x) \sin[px + \delta_e(p)/2] + f'_{op}(x) \cos[qx + \delta_e(q)/2] \right. \\ &\quad \left. + f_{eq}(x)f'_{op}(x) + f_{oq}(x)f'_{ep}(x) \} dx \right], \end{aligned} \quad (3.3.18)$$

for $q > 0$ and $p > 0$. The function $C_{q,-p}$ is similarly calculated from

*) In ref. 2, integral in the eigenvalue problem for the linear modes has been replaced by a discrete sum with a uniform mesh dx . Two different values of dx have been taken. In the present paper, we use their data for $dx = 0.1\xi$.

$$C_{q,-p} = (2i/L) \int_0^{L/2} [-g_{eq}(x)g'_{op}(x) + g_{oq}(x)g'_{ep}(x)]dx. \quad (3.3.19)$$

It is readily seen that $C_{q,p}$ has a simple pole at $p=q$, while $C_{q,-p}$ does not. For simplicity we rewrite the function $C_{q,p}$ as

$$C_{q,p} = C_q^S/(q-p) + C_{q,p}^N, \\ C_q^S = -(2iq/L) \sin[\delta_e(q)/2 - \delta_o(q)/2]. \quad (3.3.20)$$

As discussed before, the singular part of $C_{q,p}$ leads to a finite value of the static component, $\Gamma^{(0)}$. Using eqs. (3.3.13) and (3.3.20), we get,

$$\Gamma^{(0)} = \frac{g^2 k_B T}{\pi M_0} \int \frac{q^2 |v_q|}{\Omega_q^2} \sin^2[\delta_e(q)/2 - \delta_o(q)/2] dq. \quad (3.3.21)$$

The integration over q is carried out numerically by using the phase shifts in eq. (3.3.16) and Ω_q in eq. (3.2.22). We finally obtain

$$\Gamma^{(0)} = 0.00087 (\omega_0 k_B T / \Delta_0). \quad (3.3.22)$$

In obtaining eq. (3.3.22), we have used the relations

$$g^2 = \pi v_F \omega_0^2 / 2, \\ M_0 = 4\Delta_0^2 / 3\xi. \quad (3.3.23)$$

The dynamical component of $\Gamma_t^{(0)}(\omega)$ is calculated in Appendix 3.A. The result is, in the low frequency expansion,

$$\begin{aligned}
\Gamma_t^{(0)}(\omega) &= \Gamma^{(0)} + i\omega\Gamma_1^{(0)} + \omega^2\Gamma_2^{(0)} + O(\omega^3), \\
\Gamma_2^{(0)} &= 55 (k_B T / \Delta_0 \omega_0), \\
\Gamma_1^{(0)} &= a (k_B T / \Delta_0), \tag{3.3.24}
\end{aligned}$$

where a is a numerical factor of the imaginary part $\Gamma_1^{(0)}$. It is not calculated, because it has little effect on the diffusion constant as shown in the following section.

§3.4 Diffusion Constant

The diffusion constant of the soliton is obtained from the fluctuation-dissipation theorem, eq. (3.3.5). The numerator is calculated up to the order of $(k_B T)^2$. The result is

$$\langle \dot{Q}_0, \dot{Q}_0 \rangle = \frac{g^2 k_B T}{M_0} (1 + K_1 + O(T^2)), \quad (3.4.1)$$

$$\begin{aligned} K_1 = & \frac{2g^4 k_B T}{\sqrt{M_0}} \sum_{n,n'} N_{n,n'} C_{0,n} A_{-n,n'} / \Omega_n^2 \Omega_{n'}^2 L^5 \\ & + \frac{g^2 k_B T}{M_0} \sum_n C_{0,n} C_{0,-n} / \Omega_n^2, \end{aligned} \quad (3.4.2)$$

where $N_{n,n'} = 3$, if $(n,n') = (1,1)$, $(2,2)$ or (k,k') , and unity otherwise. Substitution of (3.3.24) and (3.4.1) into the right-hand side of (3.3.5), $\Gamma(\omega)$ being replaced by $\Gamma_t(\omega)$, gives

$$D(\omega) = \frac{g^2 k_B T}{M_0} \frac{1 + K_1}{i\omega + \Gamma^{(0)} + i\omega \Gamma_1^{(0)} + \omega^2 \Gamma_2^{(0)}}. \quad (3.4.3)$$

In the static limit, $\omega \rightarrow 0$, we have the Einstein relation,

$$D(0) = \frac{g^2 k_B T}{M_0 \Gamma^{(0)}} + O(T). \quad (3.4.4)$$

It is independent of the temperature in the low temperature limit. Using eq. (3.3.22), we obtain

$$D(0) = 1.4 \times 10^3 \xi^2 \omega_0. \quad (3.4.5)$$

On the other hand, when the frequency is not zero, the real part of $D(\omega)$ becomes

$$\text{Re } D(\omega) = \frac{g^2 k_B T (\Gamma_1^{(0)} + \omega^2 \Gamma_2^{(0)})}{M_0 [\omega^2 + (\Gamma_1^{(0)})^2]}, \quad (3.4.6)$$

where we have used the relations, $\Gamma_1^{(0)} \ll 1$ and $\omega \gg \omega^2 \Gamma_2^{(0)}$. In Fig. 3.2, we show the temperature dependence of eq. (3.4.6) for several values of ω . When the relation $\omega > \Gamma_1^{(0)}$ holds, $\text{Re } D(\omega)$ is proportional to T^2 . This corresponds to the diffusion constant of the "random walk", referred to in §3.1, whose basic steps are the shifts of the soliton in the collisions with the thermal phonons. From the expression in (3.4.6), we can see that the real part of $D(\omega)$ approaches to a constant value as the temperature increases.

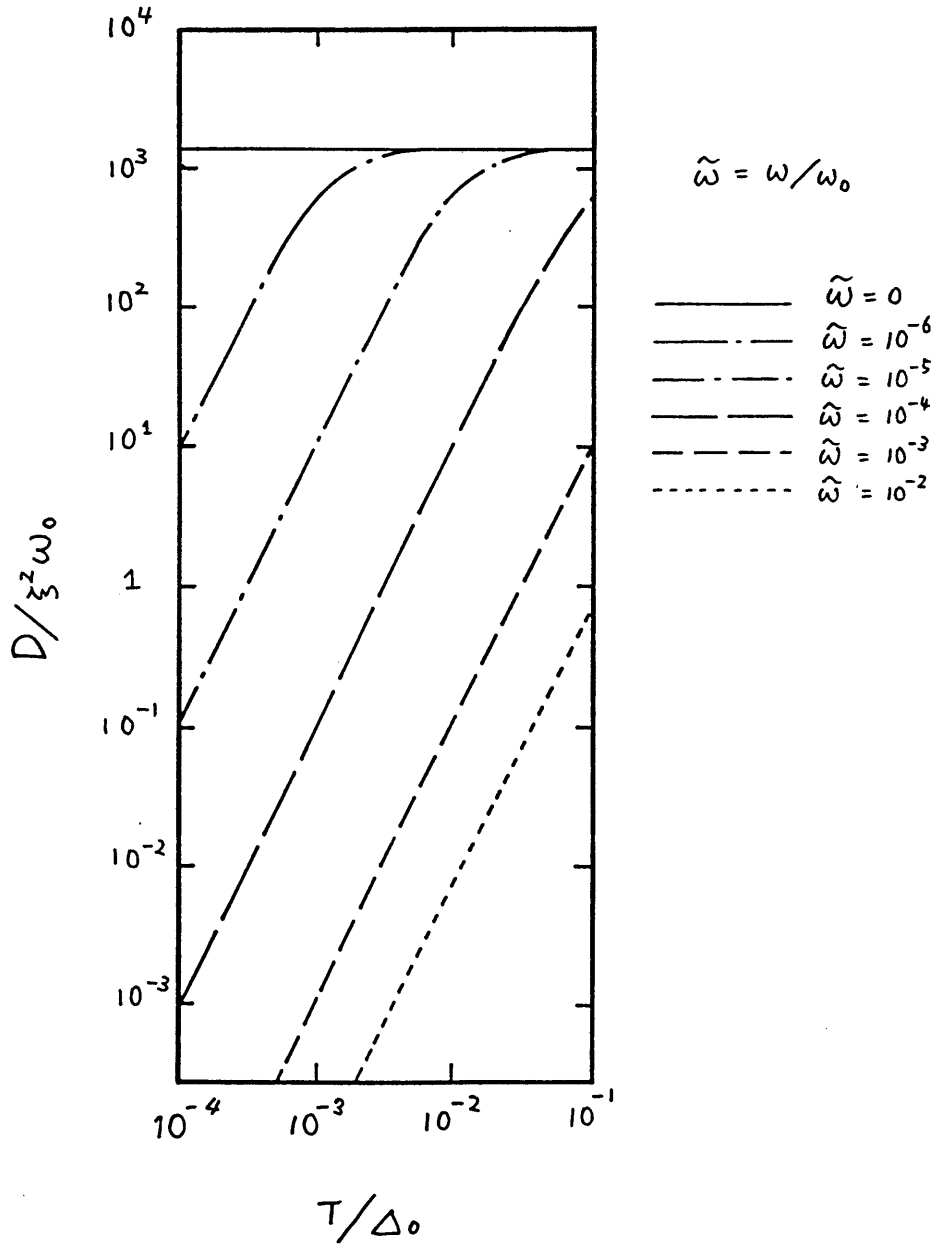


Fig. 3.2 Log-log plot of the real part of $D(\omega)/\xi^2\omega_0$ as a function of the temperature for several values of the frequency. The temperature is normalized by the electronic band gap Δ_0 ($\sim 7000k$). In the region $\omega > \Gamma^{(0)}$, the diffusion constant is proportional to T^2 . On the other hand, in the region $\omega < \Gamma^{(0)}$, it approaches to a constant value in eq. (3.4.5).

§3.5 Quantum Corrections

We have restricted ourselves to the classical low temperature region. It is important to study the quantum effect, since the optical phonon frequency ω_0 is of the order of $10^3 K$ in trans-(CH)_x.¹⁶⁾

Mori's formula for calculating the friction can be easily extended to the quantum case.⁷⁾ In the classical case, the inner product \langle , \rangle is defined by the canonical ensemble average, (see eq. (3.3.3)). In the quantal case, we use

$$(a, b) = \frac{1}{\beta} \int_0^\beta \langle e^{\lambda H} a e^{-\lambda H}, b \rangle d\lambda, \quad (3.5.1)$$

$$\beta = (k_B T)^{-1},$$

where a and b are dynamical variables and the angular brackets denote the average over the canonical ensemble

$$\rho = \exp(-\beta H) / \text{Tr} \exp(-\beta H). \quad (3.5.2)$$

As in the classical case, the friction $\Gamma(\omega)$ is estimated by,

$$\Gamma_t(\omega) = \int_0^\infty (\ddot{Q}_0(t), \ddot{Q}_0) e^{-i\omega t} dt / (\dot{Q}_0, \dot{Q}_0). \quad (3.5.3)$$

Annihilation and creation operators of the linear modes (except the Goldstone mode) are defined by

$$Q_n = \sqrt{\frac{g^2}{2\Omega_n}} (a_n + a_{-n}^\dagger),$$

$$P_n = i \sqrt{\frac{\Omega_n}{2g^2}} (a_n^\dagger - a_{-n}). \quad (n=1), \quad (3.5.4)$$

Substitution into the Hamiltonian, eq. (3.2.16), gives

$$H = E_s + \frac{g^2 (P_0 + \int \pi \chi' dx)^2}{2M_0 (1 + \zeta/M_0)^2} + \sum_{n \neq 0} \Omega_n (a_n^\dagger a_n + \frac{1}{2}) + H_Q,$$

$$H_0 = \sum_{j=2}^{\infty} V^{(j)}[\chi], \quad (3.5.5)$$

where H_Q represents the nonlinear interactions between the linear modes.

Before calculating the friction, it is useful to discuss small parameters which are used in the perturbation. It can be shown that the nonlinear interactions, H_Q , are in the higher order with respect to (ω_0/Δ_0) . Furthermore, the function ζ/M_0 , which appears in the denominator of the Hamiltonian, is also in the order of $(\omega_0/\Delta_0)^{1/2}$. In fact, it is rewritten as,

$$\begin{aligned} \zeta/M_0 &= \sum_{n \neq 0} C_{0,n} Q_n / \sqrt{M_0} \\ &= \frac{\sqrt{3\pi}}{4} \left(\frac{\omega_0}{\Delta_0} \right)^{1/2} \left(\frac{\zeta}{L} \right)^{s'} \sum_{n \neq 0} \left(\frac{\omega_0}{\Omega_n} \right)^{1/2} \tilde{C}_{0,n} (a_n + a_{-n}^\dagger), \end{aligned} \quad (3.5.6)$$

where $\tilde{C}_{0,n}$ is a dimensionless function defined by

$$\tilde{C}_{0,n} = \zeta \left(\frac{L}{\zeta} \right)^{s'} (N_0 N_n)^{-1/2} \int g_0(x) g_n'(x) dx, \quad (3.5.7)$$

and s' is 1/2 if n-mode is the extended phonon mode and $s' = 0$ otherwise.

In addition to (ω_0/Δ_0) , we treat P_0 as a small parameter. Since the Hamiltonian does not depend on Q_0 , we assume the thermal average of P_0 to be the same as in the classical case,

that is,

$$(P_0, P_0) = \frac{M_0 k_B T}{g^2} . \quad (3.5.8)$$

Let us now proceed to calculate the friction, $\Gamma_t(\omega)$. In the lowest order of the perturbation, we find,

$$\begin{aligned} \Gamma_t^{(0)}(\omega) = & \frac{g^2}{4M_0} \sum_{n,n'} C_{n,n'} C_{-n,-n'} i\omega (\Omega_n^2 - \Omega_{n'}^2) / \Omega_n \Omega_{n'} \\ & \times \left[\frac{\Omega_n - \Omega_{n'}}{(\Omega_n + \Omega_{n'})^2 - (\omega - i\varepsilon)^2} \{ (f_n + 1)(f_{n'} + 1) - f_n f_{n'} \} \right. \\ & \left. + \frac{\Omega_n + \Omega_{n'}}{(\Omega_n - \Omega_{n'})^2 - (\omega - i\varepsilon)^2} \{ (f_n + 1)f_{n'} - f_n(f_{n'} + 1) \} \right] \\ & + \frac{4g^2 k_B T}{M_0} \sum_n C_{0,n} C_{0,-n} i\omega / (\Omega_n^2 - (\omega - i\varepsilon)^2), \end{aligned} \quad (3.5.9)$$

where f_n is the thermal distribution function,

$$f_n = \langle a_n^\dagger a_n \rangle = \frac{1}{e^{\Omega_n/k_B T} - 1} . \quad (3.5.10)$$

The first term on the right-hand side of (3.5.9) is in the order of $\omega_0(\omega_0/\Delta_0)$, while the second term is in the order of $\omega_0(k_B T/\Delta_0)$.

Using the explicit form of $C_{q,p}$, discussed in §3.3, we see that the static limit of $\Gamma_t^{(0)}(\omega)$ is,

$$\Gamma_t^{(0)}(\omega \rightarrow 0) = \frac{g^2}{\pi M_0 k_B T} \int dq \, q^2 |v_q| \sin^2 [\delta_e(q)/2 - \delta_0(q)/2] f_q (f_q + 1). \quad (3.5.11)$$

Note that eq. (3.5.11) coincides with the result in §3.3, in the following classical limit,

$$f_g \rightarrow \frac{k_B T}{\Omega_g} . \quad (3.5.12)$$

In Fig. 3.3, the temperature dependence of $\Gamma^{(0)}(0)$ is depicted. In the region $k_B T < \omega_0$, it is an activation type.

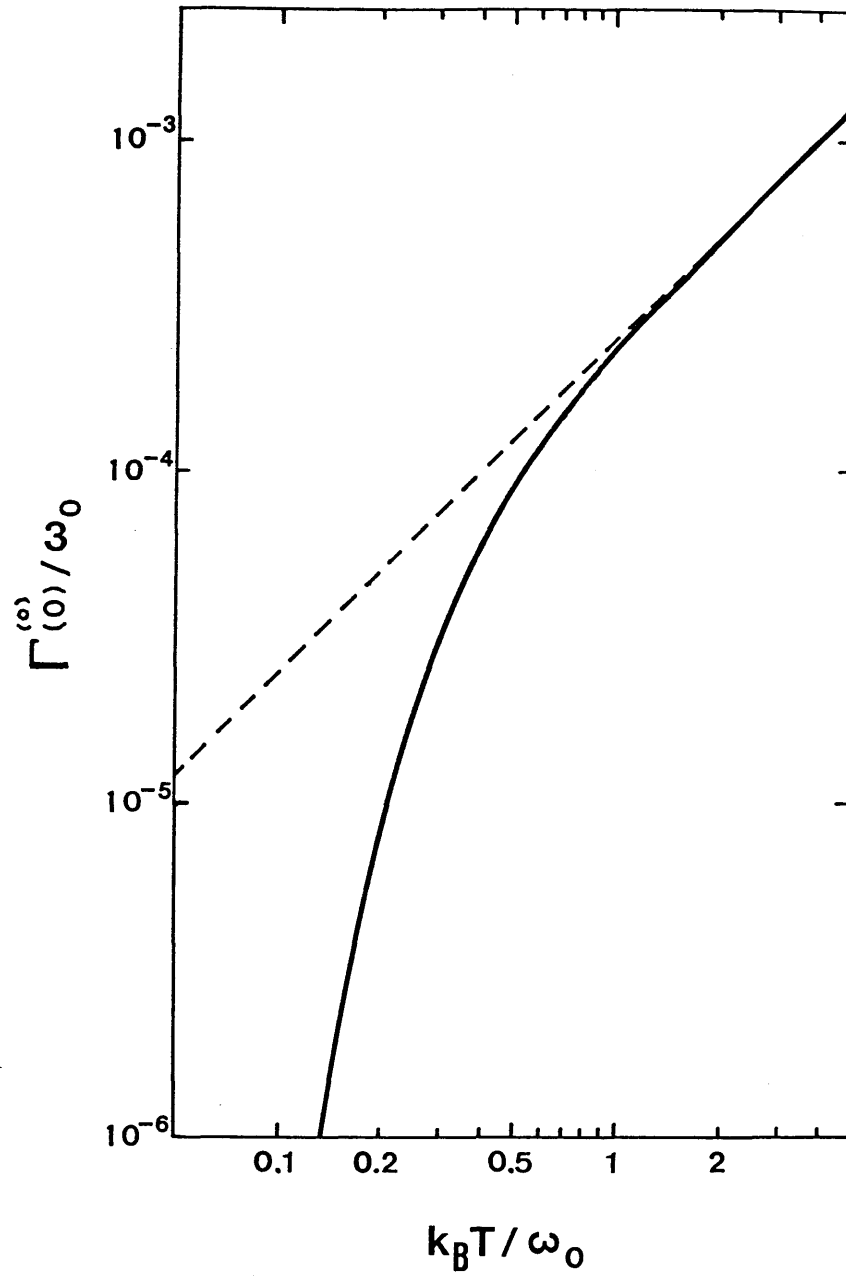


Fig. 3.3 Temperature dependence of the friction in the quantal case. The broken line indicates the classical result proportional to T . The temperature is normalized by the optical phonon frequency ($\omega_0 \sim 2000k$).

§3.6 Summary and Discussion

We have investigated the diffusive motion of the soliton in trans-(CH)_x , using the TLM model and the collective coordinate method. It has been shown that the structure of the soliton-phonon interaction has a remarkable similarity to that in the scalar field theory, such as the ϕ^4 system. Especially the equation of motion for the collective coordinate is universal in these soliton bearing systems. Applying the method developed in the ϕ^4 model, we have calculated the friction of the soliton, $\Gamma(\omega)$, in the low temperatures.

It is found that the diffusive motion is induced by the two mechanisms as in the ϕ^4 system. In the static limit, (long time limit), the soliton behaves as an ordinary Brownian particle and the Einstein relation holds. The diffusion constant is independent of the temperature if we assume the classical ensemble average. In this diffusive motion, the origin of the friction is momentum transfer between the soliton and thermally excited phonons. The other mechanism is related to the shift of the soliton induced by the collision with the phonons. This mechanism, however, does not appear in the static limit (or in the long time limit). It appears only when the frequency is not zero and the temperature is low enough. As shown in Fig. 3.2, the dynamical diffusion constant ($\text{Re}D(\omega)$) becomes proportional to T^2 in this region.

We have also studied the quantum effect on the static limit of $\Gamma_t^{(0)}(\omega)$. The friction has the temperature dependence of an activation type. In the temperature range $k_B T < \omega_0$, therefore, it

is important to take account of acoustic phonons, though their coupling to the soliton is weaker than that of the optical phonons by a factor a/ξ .^{17,18)} It remains a future problem.

In real systems, there may be other mechanisms for the soliton to stop. They would contribute to the friction and modify the temperature dependence of the diffusion constant. Especially the discreteness effect will be studied in the following Chapter.

Appendix 3.A. Dynamical Component of $\Gamma_t^{(0)}(\omega)$

We calculate the real part of $\Gamma_t^{(0)}(\omega)$, eq. (3.3.10), in the low frequency expansion. The integration over $p (=n')$ can be carried out using the relation in eq. (3.3.12). After some algebra we obtain

$$\begin{aligned} \text{Re } \Gamma_t^{(0)}(\omega) = & - \frac{g^2 k_B T}{M_0} \sum_{q>0} \frac{v_q}{\Omega_q^2} \\ & \times \left[C^S(q)^2 + C^S(q)^2 \left\{ -\frac{1}{6} \frac{v_q''}{v_q^3} + \frac{1}{4} \frac{(v_q')^2}{v_q^4} + \frac{5}{4 \Omega_q^2} \right\} \omega^2 \right. \\ & + 2 C^S(q) \left\{ \frac{v_q'}{2 v_q^3} C_2(q) + \frac{1}{v_q \Omega_q} C_2(q) - \frac{1}{v_q^2} C_3(q) \right\} \omega^2 \\ & \left. + \frac{1}{v_q^2} C_2(q)^2 \omega^2 + \frac{1}{v_q^2} C_1(q)^2 \omega^2 \right], \end{aligned} \quad (3.A.1)$$

where functions $C_1(q)$, $C_2(q)$ and $C_3(q)$ are defined by

$$\begin{aligned} C_1(q) &= \lim_{p \rightarrow q} C_{q,-p}, \\ C_2(q) &= \lim_{p \rightarrow q} C_{q,p}^N, \\ C_3(q) &= \lim_{p \rightarrow q} d C_{q,p}^N / dp. \end{aligned} \quad (3.A.2)$$

The function $C_{q,p}^N$ is the normal part of $C_{q,p}$ introduced in eq. (3.3.20). From the definition of $C_{q,p}$, the explicit forms of $C_i(q)$ become,

$$C_1(q) = \frac{i q}{2L} \left(\frac{d\delta e}{dq} + \frac{d\delta o}{dq} \right) \cos [\delta e/2 - \delta o/2] \\ + \frac{2i}{L} \int_0^{L/2} dx \left\{ -q f_{eq}(x) \cos [qx + \delta o/2] + f'_{eq}(x) \sin [qx + \delta o/2] \right. \\ \left. - q f_{oq}(x) \sin [qx + \delta e/2] - f'_{oq}(x) \cos [qx + \delta e/2] \right. \\ \left. - f_{eq}(x) f'_{oq}(x) + f_{oq}(x) f'_{eq}(x) \right\},$$

$$C_2(q) = \frac{i}{L} \sin [\delta e/2 - \delta o/2] + \frac{i q}{2L} \left(\frac{d\delta e}{dq} - \frac{d\delta o}{dq} \right) \cos [\delta e/2 - \delta o/2],$$

$$C_3(q) = -\frac{i}{2qL} \sin [\delta e/2 + \delta o/2] - \frac{i}{4L} \left(\frac{d\delta e}{dq} + \frac{d\delta o}{dq} \right) \cos [\delta e/2 + \delta o/2] \\ + \frac{i}{2L} \left(\frac{d\delta e}{dq} - \frac{d\delta o}{dq} \right) \cos [\delta e/2 - \delta o/2] \\ - \frac{i q}{8L} \left\{ \left(\frac{d\delta e}{dq} \right)^2 + \left(\frac{d\delta o}{dq} \right)^2 \right\} \sin [\delta e/2 - \delta o/2] \\ + \frac{i q}{4L} \left(\frac{d^2\delta e}{dq^2} - \frac{d^2\delta o}{dq^2} \right) \cos [\delta e/2 - \delta o/2] \\ + \frac{2i}{L} \int_0^{L/2} dx \left\{ f_{eq}(x) \cos [qx + \delta o/2] \right. \\ \left. - q f_{eq}(x) \sin [qx + \delta o/2] \left(x + \frac{1}{2} \frac{d\delta o}{dq} \right) \right. \\ \left. + \frac{d f'_{eq}(x)}{dq} \sin [qx + \delta o/2] \right. \\ \left. - f_{oq}(x) \sin [qx + \delta e/2] \right. \\ \left. - q f_{oq}(x) \cos [qx + \delta e/2] \left(x + \frac{1}{2} \frac{d\delta e}{dq} \right) \right. \\ \left. + \frac{d f'_{oq}(x)}{dq} \cos [qx + \delta e/2] \right. \\ \left. + f_{eq}(x) \frac{d f'_{oq}(x)}{dq} + f_{oq}(x) \frac{d f'_{eq}(x)}{dq} \right\}, \quad (3.A.3)$$

where primes on $f_{eq}(x)$ and $f_{oq}(x)$ represent the spatial

derivatives. In obtaining $C_2(q)$, we have performed the integral by part and used the following relation,

$$g_{ok}(0) = \sin[\delta_0(k)/2] + f_{ok}(0) = 0. \quad (3.A.4)$$

Integrations over x and q in eqs. (3.A.1) and (3.A.3) are carried out numerically, using the explicit forms of $f_{ok}(x)$ and $f_{ek}(x)$ obtained in ref. 2. Finally we get eq. (3.3.24).

The imaginary part of $\Gamma_t^{(0)}(\omega)$ is rewritten as

$$\begin{aligned} \text{Im } \Gamma_t^{(0)}(\omega) &= \omega \Gamma_1^{(0)} + O(\omega^3), \\ \Gamma_1^{(0)} &= \frac{g^2 k_B T}{8\pi^2 M_0} \iint dq dP \text{ (principal part)} \\ &\quad \times \frac{|C_{q,p}|^2 (\Omega_q^2 + \Omega_p^2)}{\Omega_q^2 \Omega_p^2} \\ &\quad + \frac{2g^2 k_B T}{\pi M_0} \int \frac{|C_{q,q}|^2}{\Omega_q^2} dq. \end{aligned}$$

(3.A.5)

The numerical factor of $\Gamma_1^{(0)}$ is not calculated, because it has little effect of the results.

References

- 1) H. Takayama, Y.R. Lin-Liu, and K. Maki: Phys. Rev. B21 (1980) 2388.
- 2) Y. Ono, A. Terai and Y. Wada: J. Phys. Soc. Jpn. 55 (1986) 1656.
- 3) For a review see, R. Jackiw: Rev. Mod. Phys. 49 (1977) 681.
- 4) J.-L. Gervais and B. Sakita: Phys. Rev. D11 (1975) 2943.
- 5) E. Tomboulis: Phys. Rev. D12 (1975) 1678.
- 6) J.-L. Gervais and A. Jevicki: Nucl. Phys. B110 (1976) 93.
- 7) H. Mori: Prog. Theor. Phys. 33 (1965) 423.
- 8) H. Ito, A. Terai, Y. Ono, and Y. Wada: J. Phys. Soc. Jpn. 53 (1984) 3520.
- 9) J.C. Hicks and G.A. Blaisdell: Phys. Rev. B31 (1985) 919.
- 10) A. Terai, M. Ogata and Y. Wada: J. Phys. Soc. Jpn. 55 (1986) 2296.
- 11) Y. Ono and H. Ito: J. Phys. Soc. Jpn. 54 (1985) 4828.
- 12) C.Kittel: Quantum Theory of Solids (Wiley, New York, 1963) Chap.6, p.126.
- 13) J. Goldstone and R. Jackiw: Phys. Rev. D11 (1975) 1486. See also §1.2.
- 14) A. Terai, H. Ito, Y. Ono and Y. Wada: J. Phys. Soc. Jpn. 54 (1985) 2641.
- 15) M. Nakahara and K. Maki: Phys. Rev. B25 (1982) 7789.
- 16) M.J. Rice and E.J. Mele: Phys. Rev. Lett. 49 (1982) 1455.
- 17) K. Maki: Phys. Rev. B26 (1982) 2187.
- 18) Y. Leblanc, H. Matsumoto, H. Umezawa and F. Mancini: Phys. Rev. B30 (1984) 5958; J. Math. Phys. 26 (1985) 2940.

Chapter IV Peierls Potential for a Soliton in Su-Schrieffer-Heeger's Model

§4.1 Introduction

In the previous chapter, we have studied the soliton motion in the continuum model of trans-polyacetylene. It is, however, important to consider the lattice pinning effect on the soliton motion. In the present chapter, we investigate the lattice pinning energy (or Peierls potential barrier) in Su-Schrieffer-Heeger's (SSH)¹⁾ model, which was originally proposed for polyacetylene.

Generally speaking, the excitation energy of the soliton in discrete models varies according to the relative position, to the lattice sites. On the analogy of dislocations in solid, we can consider the variation of the energy as the Peierls potential barrier.

Numerical calculations for the (discrete) SSH model were carried out by several groups.²⁻⁹⁾ Ono, Ohfuti and Terai developed a method to obtain static solutions.⁸⁾ In their method, self-consistent equations for the lattice displacements and the electronic wave functions were directly solved by iteration. Namely, the electronic Hamiltonian was diagonalized for given lattice displacements and the obtained eigenfunctions were used to calculate the lattice displacements through the self-consistent equation derived so as to minimize the total energy. The new lattice displacements were then used to obtain new electronic wave functions.

In this chapter, we extend the above method in order to obtain the soliton solutions at arbitrary locations. We use a self-consistent equation which is derived from the condition of minimizing the total energy under the following two constraints: The first comes from the periodic boundary condition. If we use bond variables $y(n)=u_{n+1}-u_n$, with u_n being the displacement of the n -th (CH) unit, the periodic boundary condition requires $\sum y(n)=0$.⁹⁾ The second constraint is imposed so as to fix the soliton center at an arbitrary point. Explicitly this condition is written as $y(n_0+1)-y(n_0)=Q$, where n_0 is a fixed integer and Q is some constant. This means that the optical component [defined by $\psi(n)\equiv(-1)^n(-y(n)+y(n-1))/4$]¹⁰⁾ of the (n_0+1) -th site is fixed at the value, $Q(-1)^{n_0}/4$. By changing the value of Q , we can obtain the soliton solutions whose centers are located at various points, as will be discussed in §4.2.

Excitation energies of the obtained solitons are also calculated to estimate the Peierls potential barrier. We show that the Peierls potential is hardly observable and less than $10^{-10} E_s$ in polyacetylene, with E_s being the excitation energy of the soliton (about 0.4 eV). In order to check the result, we estimate the Peierls potentials for different values of the electron-phonon coupling constant. As expected, the barrier increases as the electron-phonon coupling becomes stronger and the soliton width becomes narrower.

In the following section, the formulation to obtain the soliton solutions is explained. The Peierls potential barriers are calculated in §4.3. Discussion is given in §4.4.

§4.2 Soliton Solutions

Su, Schrieffer and Heeger proposed the following Hamiltonian,¹⁾ (see also §1.3),

$$H = \frac{M}{2} \sum_n \dot{u}_n^2 + \frac{K}{2} \sum_n (u_{n+1} - u_n)^2 - \sum_{n,s} [t_0 - \alpha(u_{n+1} - u_n)] (C_{n+1,s}^\dagger C_{n,s} + C_{n,s}^\dagger C_{n+1,s}), \quad (4.2.1)$$

where u_n is the displacement of the n -th (CH) unit from its undimerized equilibrium position, $C_{n,s}^\dagger$ and $C_{n,s}$ the creation and annihilation operators of a π -electron with spin s at the n -th site, respectively, M the mass of the (CH) unit, K the spring constant mainly due to σ -bonds, t_0 the nearest-neighbor transfer integral of the π -electrons in the undimerized state, and α the coupling constant which comes from the modulation of the transfer integral due to the change of the nearest-neighbor distance. For polyacetylene, we take, according to SSH,¹⁾

$$\begin{aligned} \alpha &= 4.1 \text{ eV/\AA}^{\circ}, \\ t_0 &= 2.5 \text{ eV}, \\ K &= 21 \text{ eV/\AA}^{\circ 2}. \end{aligned} \quad (4.2.2)$$

Afterwards, when we calculate the Peierls potential energies for narrower solitons, we change the value of α from $4.0 \text{ eV/\AA}^{\circ}$ to $6.0 \text{ eV/\AA}^{\circ}$.

We employ the periodic boundary condition,

$$\begin{aligned} U_{N+1} &= U_1, \\ C_{N+1,s} &= C_{1,s}, \\ C_{N+1,s}^\dagger &= C_{1,s}^\dagger, \end{aligned} \quad (4.2.3)$$

where N is the total number of the lattice sites. When we consider the static solutions, we use the bond variable defined by

$$y(n) = U_{n+1} - U_n. \quad (4.2.4)$$

Eigenvectors $\{\phi_i(n)\}$, which diagonalize the last term on the right-hand side of eq. (4.2.1), can be obtained by the following eigenvalue problem,

$$\varepsilon_i \phi_i(n) = -[t_0 - \alpha y(n-1)] \phi_i(n-1) - [t_0 - \alpha y(n)] \phi_i(n). \quad (4.2.5)$$

Within the adiabatic approximation, the self-consistent equation for the bond variable $y(n)$ is derived by varying the average of H over the electronic ground state with respect to $y(n)$. In the above variation, we impose the following two constraints,

$$\sum_n y(n) = 0, \quad (4.2.6a)$$

$$y(n_0+1) - y(n_0) = 0, \quad (4.2.6b)$$

where the first constraint comes from the periodic boundary

condition, $u_{N+1}=u_1$. In order to understand the second one, it is useful to discuss the configuration of the soliton solution. In Fig. 4.1, a typical configuration is shown, which is calculated by Terai and Ono⁹⁾ under the first constraint, (4.2.6a). Here the alternating bond variable is $\tilde{y}(n)=(-1)^{n+1}y(n)$. The solution has, in general, optical and acoustic components defined by ¹⁰⁾

$$\begin{aligned}\psi(n) &= (-1)^n (-u_{n+1} + 2u_n - u_{n-1}) / 4 \\ &= (-1)^n (-y(n) + y(n-1)) / 4, \\ \varphi(n) &= (u_{n+1} + 2u_n + u_{n-1}) / 4,\end{aligned}\tag{4.2.7}$$

respectively. The two components are depicted in Figs. 4.1(b) and 4.1(c). Comparing eq. (4.2.6b) with (4.2.7), we see that the second constraint means that the optical component of the (n_0+1) -th site is fixed at the value, $Q(-1)^{n_0}/4$. Let us now return to the self-consistent equation. With the help of Lagrange's method of indeterminate coefficients, it is straightforward to derive the self-consistent equation by varying the Hamiltonian under the above constraints. We obtain,

$$y(n) = -\frac{2\alpha}{K} \sum'_{i,s} \phi_i(n) \phi_i(n+1) + \lambda + \mu (\delta_{n,n_0+1} - \delta_{n,n_0}),\tag{4.2.8}$$

where λ and μ are Lagrange multipliers and the sum over i and s is restricted to the occupied states. In eq. (4.2.8), we have used the fact that $\phi_i(n)$ can be taken real. By using

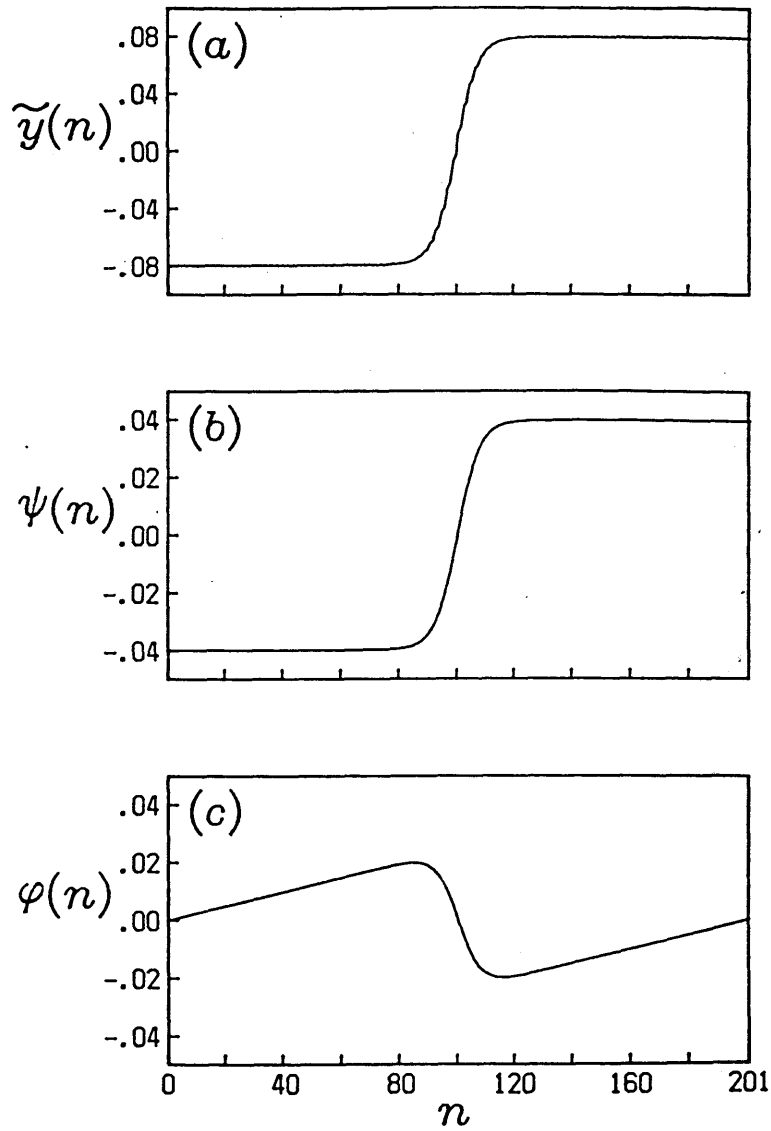


Fig. 4.1 Typical configuration of a soliton solution with $N=201$ and $N_e=201$; (a) the alternating bond variable $\tilde{y}(n)$, (b) the optical component $\psi(n)$ and (c) the acoustic component $\varphi(n)$. The definitions are shown in the text. The unit of the ordinate is \AA . (Cited from Ref. 9, A. Terai and Y. Ono: J. Phys. Soc. Jpn. 55 (1986) 213.)

eqs. (4.2.6), it is readily seen that λ and μ are expressed in terms of $\{\phi_i(n)\}$ as follows;

$$\begin{aligned}\lambda &= \frac{2\alpha}{KN} \sum_n \sum_{i,s}' \phi_i(n) \phi_s(n+1), \\ \mu &= \frac{\alpha}{K} \sum_{i,s}' [\phi_i(n_0+1) \phi_s(n_0+2) - \phi_i(n_0) \phi_s(n_0+1)] \\ &\quad + \frac{Q}{2}.\end{aligned}\tag{4.2.9}$$

The self-consistent equation is solved by iteration:^{8,9)} First, the eigenvalue problem, eq. (4.2.5) is solved numerically for an appropriately chosen set of $\{y(n)^{(1)}\}$, and next, the obtained eigenfunctions are substituted into the right-hand side of eq. (4.2.8) and eq. (4.2.9) to yield a new set, $\{y(n)^{(2)}\}$, which is again used as the initial values of $\{y(n)^{(1)}\}$. This iteration is continued until the change of $\{y(n)\}$ defined by

$$\gamma = \frac{\sum_n [y(n)^{(2)} - y(n)^{(1)}]^2}{\sum_n [y(n)^{(1)}]^2},\tag{4.2.10}$$

becomes negligibly small.

Typical configurations of the obtained soliton solutions are depicted in Fig. 4.2, where the total number of the lattice sites N and the electron number N_e are chosen to be $N=201$ and $N_e=201$. The fixed site number n_0 is 100 and the constant Q is changed from 0 to 0.01977. We can see that the center of the soliton varies as the constant Q increases.

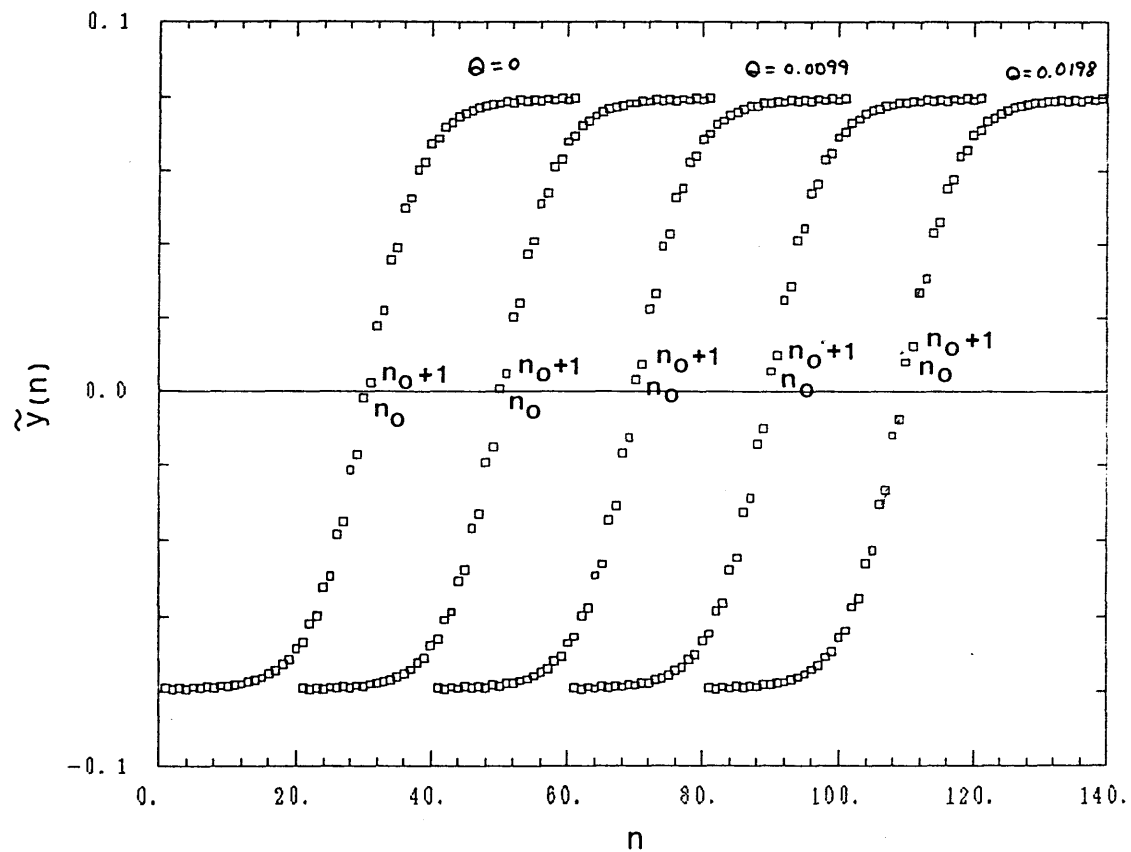


Fig. 4.2 Typical configurations of the obtained soliton solutions near the fixed site $n_0=100$ for various values of Q . The alternating bond variable $\tilde{y}(n)=(-1)^{n+1} y(n)$ is shown.

§4.3 Peierls Potential Barrier of Solitons

Excitation energies of the obtained solutions are estimated by the following formula,^{8,9)}

$$E_s = \frac{K}{2} \sum_n y(n)^2 + \sum_{i,s}' \varepsilon_{i,s} - \frac{N}{N_0} (E_e^{(0)} + E_L^{(0)}), \quad (4.3.1)$$

where $E_e^{(0)}$ and $E_L^{(0)}$ are the electronic and lattice energies of the perfectly dimerized state with total lattice number N_0 . In Fig. 4.3, the dependences of the excitation energies on γ are depicted for several values of Q . As an iteration is carried out, the magnitude of γ decreases by one step. In the limit of $\gamma \rightarrow 0$, the excitation energy for each Q approaches a universal value,

$$\begin{aligned} E_s &= 0.163172478 \quad t_0 \\ &= 0.627 \quad \Delta_0 \\ &= 0.408 \quad \text{eV} . \end{aligned} \quad (4.3.2)$$

In order to estimate the Peierls potential barrier precisely, we continue the iteration until the quantity γ , eq. (4.2.10), which represents the change of $\{y(n)\}$, becomes less than 10^{-14} . (In the final stage of the iteration, the estimation of the energy begins to fluctuate owing to errors of the computer.) Nevertheless we do not have any meaningful energy difference for various values of Q . We thus conclude that the Peierls potential barrier is negligible for the soliton in the SSH model, if we use the parameters in eq. (4.2.2) proposed for polyacetylene. The potential barrier is less than $10^{-10} E_s$, if any.

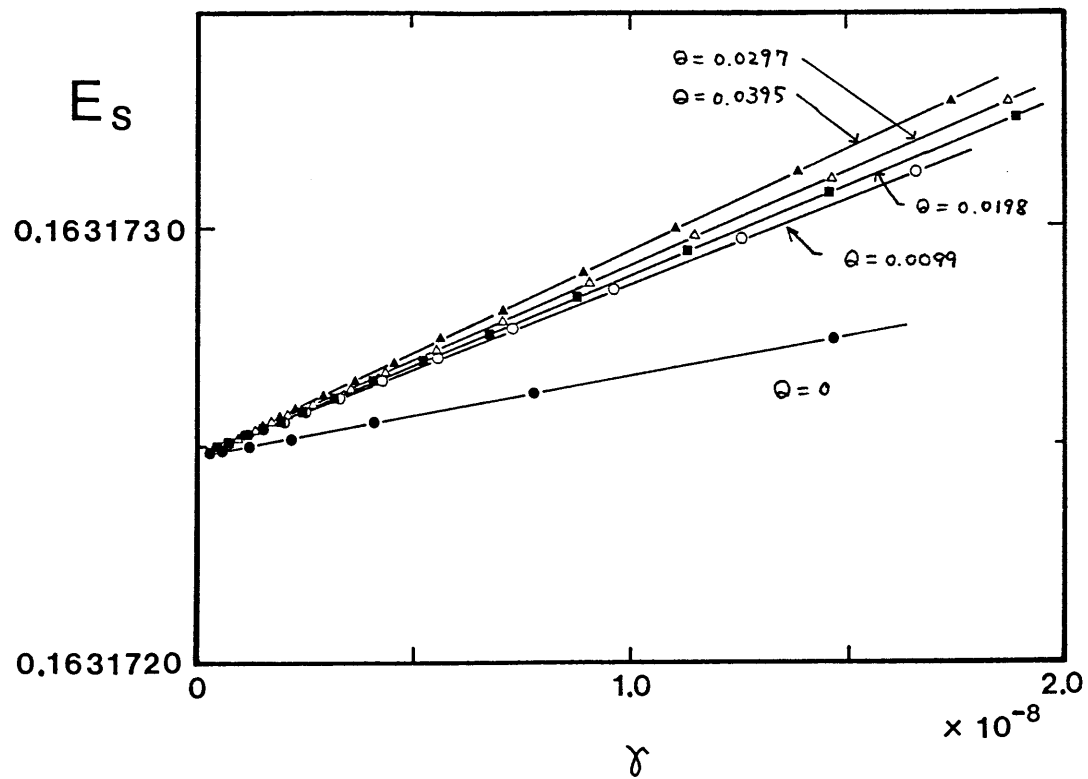


Fig. 4.3 Excitation energy of the soliton solutions as a function of the convergence parameter γ , for several values of Q . As an iteration is performed, the magnitude of γ decreases by one step. Solid lines are to guide the reader's eye. Note that the ordinate scale is magnified.

In order to check the calculation, we perform the similar estimation of E_s , using different values of the coupling constant α (in the present analysis $\alpha=4.0\sim 5.8\text{eV/\AA}$). Since stronger coupling constants lead to narrower solitons, we choose $N=101$, $N_e=101$ and $n_0=50$. In Fig. 4.4, the explicit configurations of the obtained solitons are shown, where $\alpha=5.2\text{eV/\AA}$ and Q is changed from 0 to 0.105. The γ -dependence the excitation energies is depicted in Fig. 4.5. It is apparent that the energies of different values of Q approach different values in the limit of $\gamma\rightarrow 0$.

We define the location of the center of the soliton by using the optical component $\{\psi(n)\}$ as follows:

$$X_{sol} = m - \psi(m) / [\psi(m) - \psi(m-1)] , \quad (4.3.3)$$

where m is the smallest integer satisfying the relations, $\psi(m)>0$ and $\psi(m-1)<0$. The dependence of E_s on X_{sol} is depicted in Fig. 4.6, where X_{sol} is calculated according to eq. (4.3.3) using the obtained soliton solutions for various Q 's.

The Peierls potential barrier E_p is calculated through the least square method by fitting the data in Fig. 4.6 to

$$E_s = E_{s0} + \frac{E_p}{2} \cos [2 (X_{sol} - (n_0+1)) \pi / d] . \quad (4.3.4)$$

The obtained values are

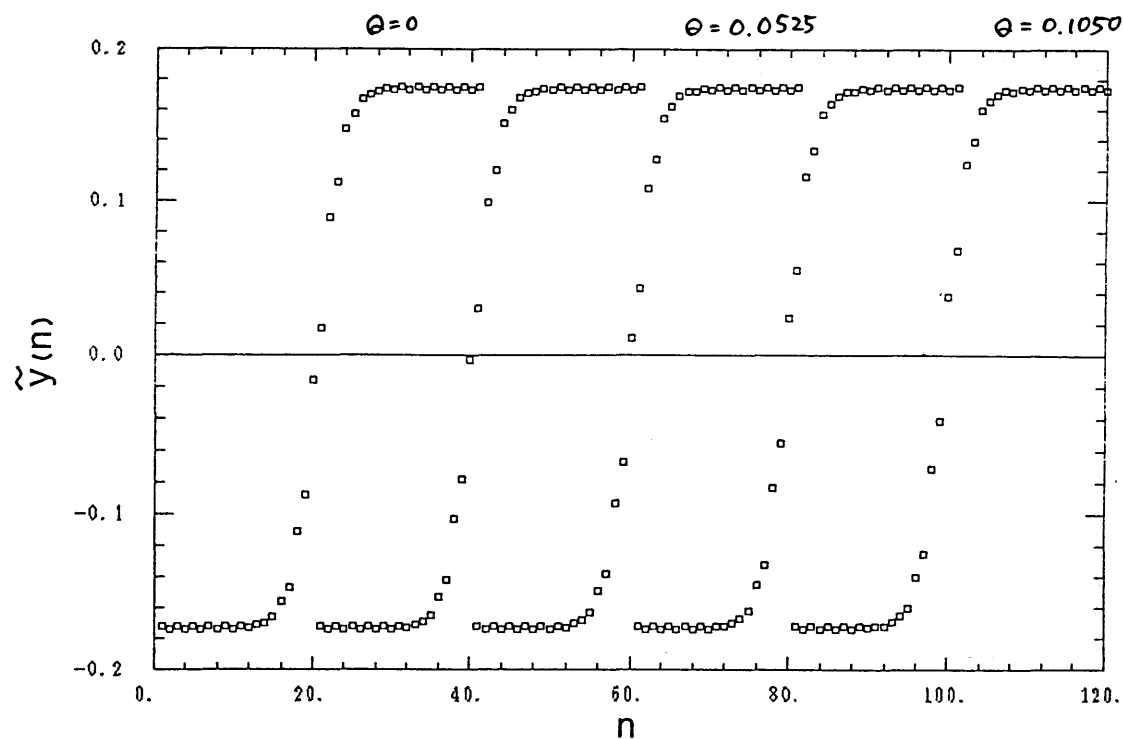


Fig. 4.4 Typical configurations of the obtained soliton solutions near the fixed site $n_0=50$. The coupling constant α is 5.2eV/Å which is stronger than that of trans-polyacetylene.

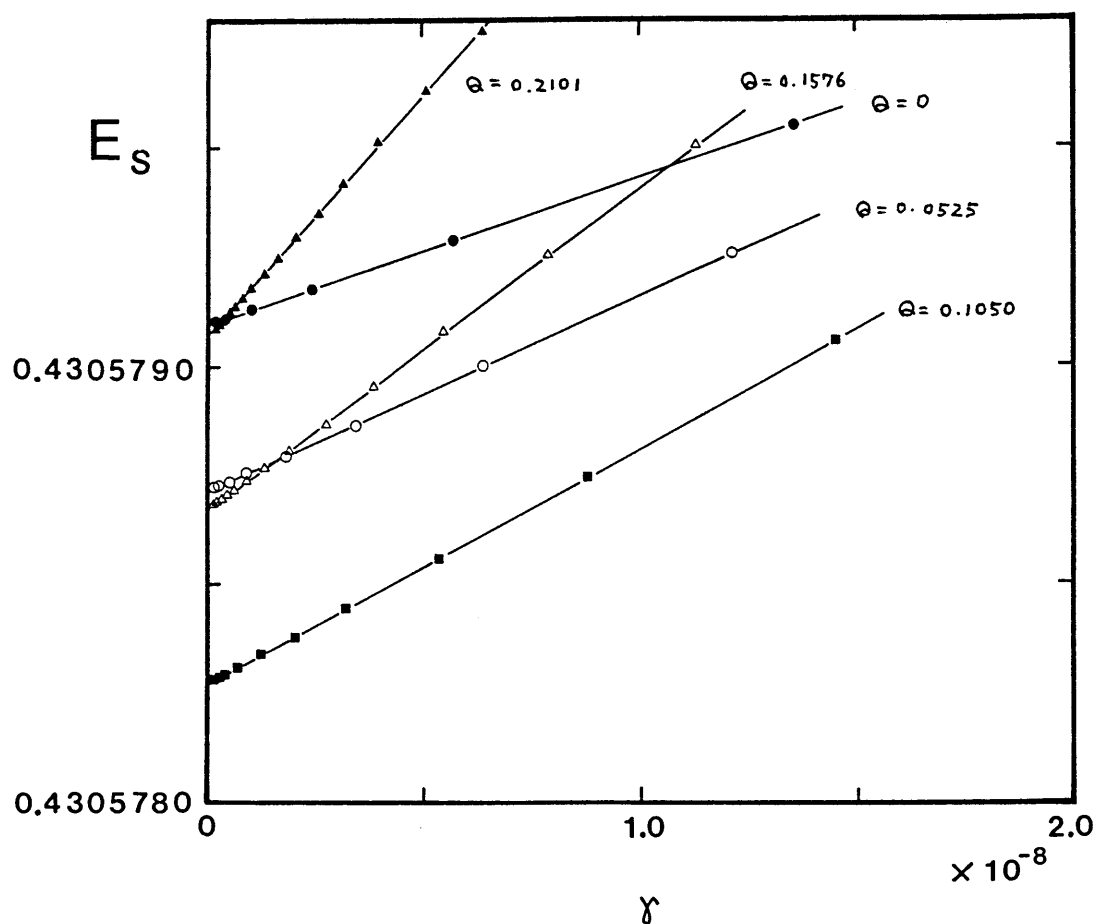


Fig. 4.5 Excitation energy of the soliton solutions as a function of the convergence parameter γ , for several values of Q and $\alpha=5.2\text{eV/\AA}$. Solid lines are to guide the reader's eye. The ordinate and the abscissa are the same as those in Fig. 4.3.

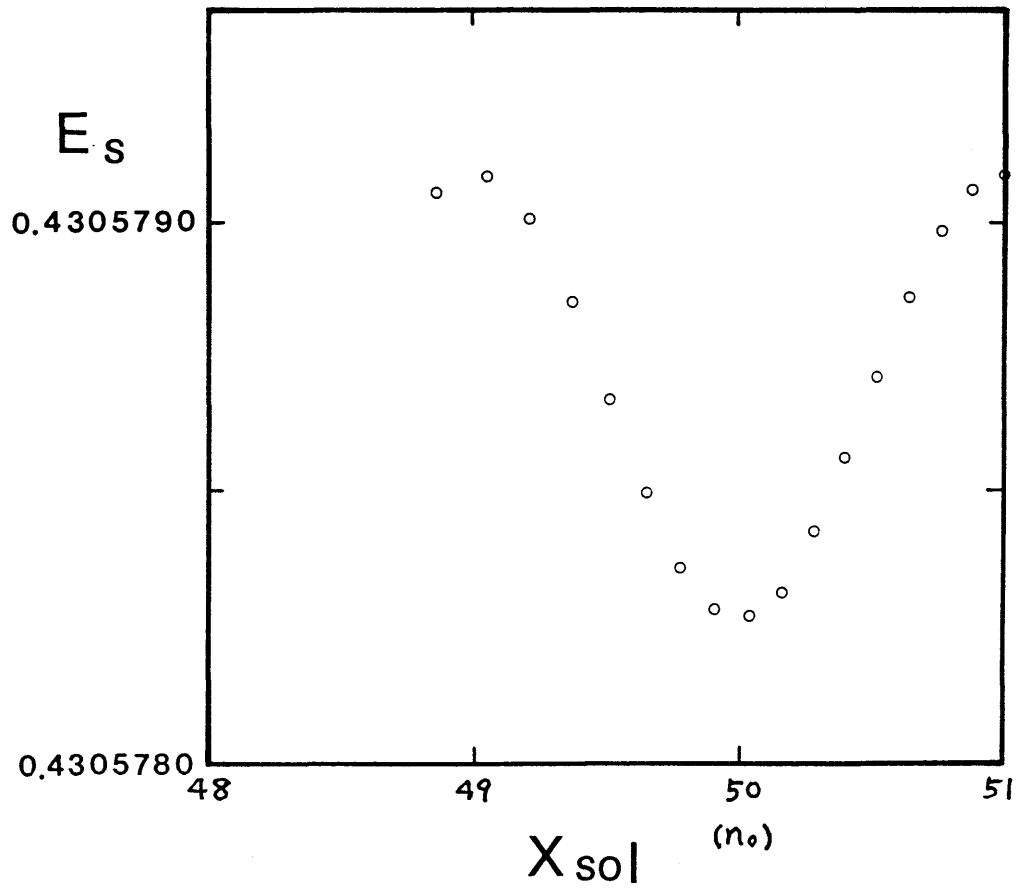


Fig. 4.6 The soliton excitation energy as a function of the location of the soliton center, X_{sol} . The solid line is a functional fitting of the data (see eq. (4.3.4)).

$$\begin{aligned}
E_{s0} &= 0.431 \quad t_0, \\
E_p &= 8.22 \times 10^{-7} \quad t_0, \\
d &= 2.00.
\end{aligned}$$

(4.3.5)

In the same way, the Peierls potential barrier is calculated for various coupling constant α . The ratio of E_p to the soliton excitation energy E_s as a function of α is depicted in Fig. 4.7, where we can see the exponential dependence on α . It is interesting to plot E_p/E_s as a function of the soliton width. We calculate the soliton width by the following formula,

$$\begin{aligned}
\xi &= v_F / \Delta_0 \\
&= 2at_0 / 4\alpha \bar{u},
\end{aligned}$$

(4.3.6)

where v_F is the Fermi velocity, Δ_0 the gap of the electronic band and \bar{u} is the absolute value of the lattice displacement in the perfectly dimerized state. In eq. (4.3.6), we use the expression of the soliton width in the TLM model.¹¹⁾ From Fig. 4.8, we can see that the quantity E_p/E_s depends on ξ/a in the following form

$$E_p/E_s = A \exp(-C\xi/a),$$

(4.3.7)

with $A=1.84$ and $C=4.97$.

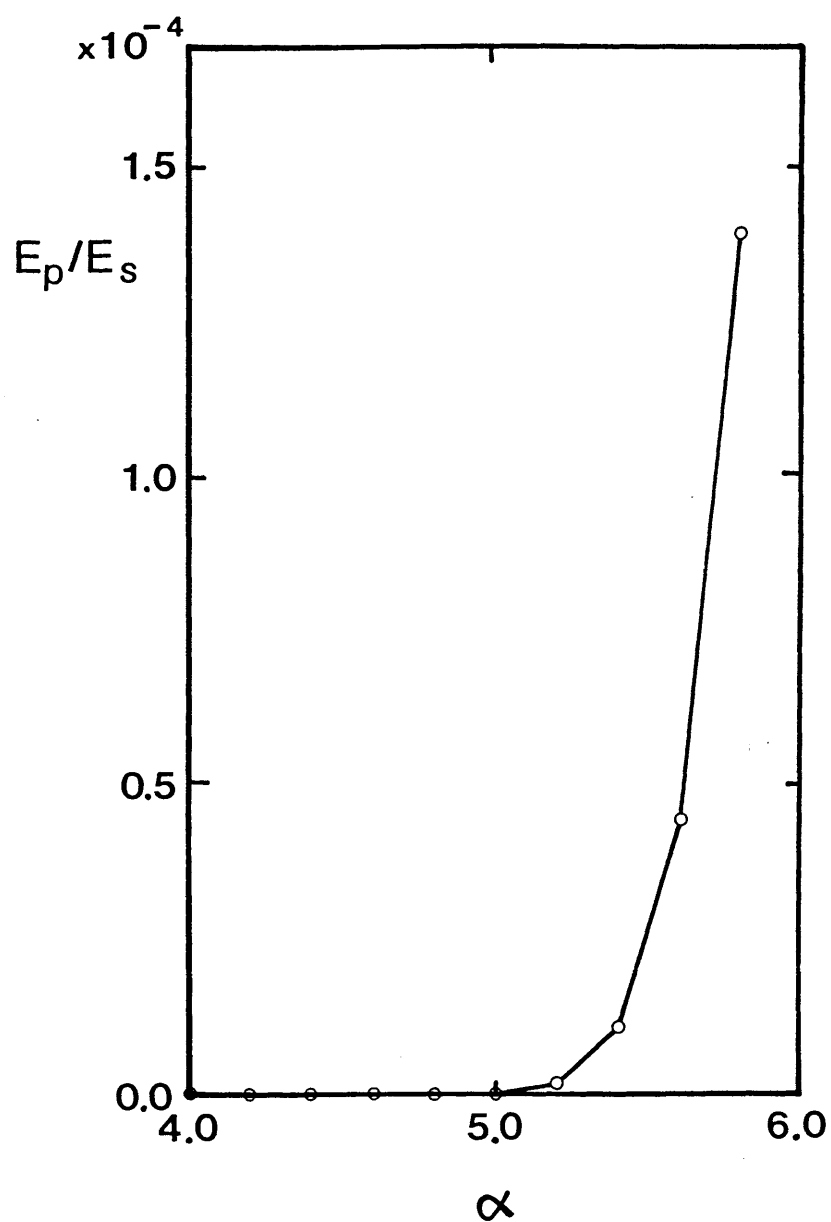


Fig. 4.7 The ratio of the Peierls potential barrier to the soliton excitation energy, as a function of the coupling constant α .

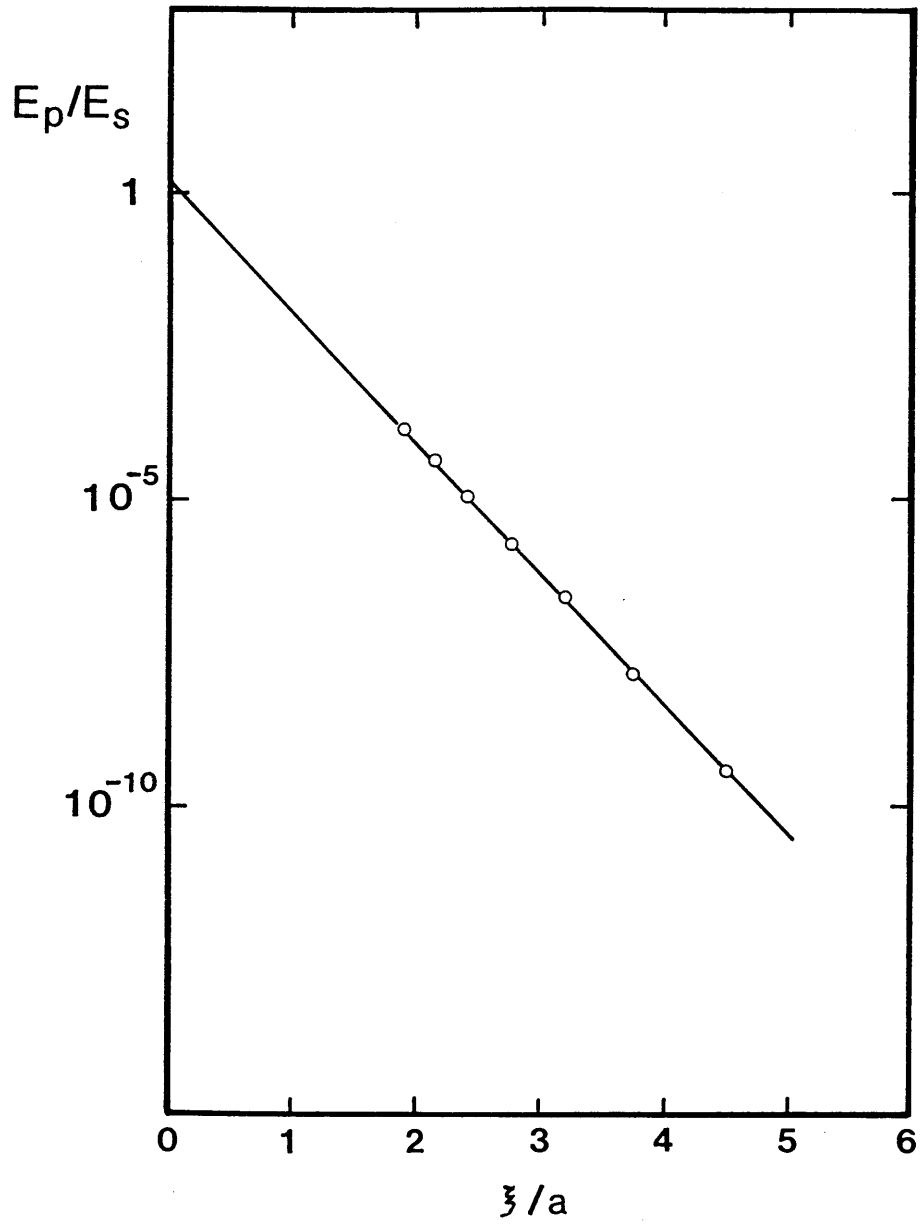


Fig. 4.8 Semilog plot of the ratio of the Peierls potential barrier to the soliton excitation energy, as a function of the soliton width defined in eq. (4.3.6). The solid line is a functional fitting in the form of eq. (4.3.7).

§4.4 Discussion

In Su-Schrieffer-Heeger's model, the Peierls potential barrier of a soliton has been estimated by obtaining the soliton solutions at arbitrary positions relative to the lattice sites. When the parameters are adjusted to polyacetylene, the Peierls potential is found to be less than $10^{-10} E_s$.

Su, Schrieffer, and Heeger¹⁾ suggested that the Peierls potential barrier is about $20K=10^{-4}E_s$. Although it is not clear how they estimated the potential barrier, the value is inconsistent with our result. On the other hand, Terai and Ono⁹⁾ studied linear modes around a soliton in the SSH model by solving numerically the eigenvalue problem for the linear mode. As one of the linear modes, they obtained the Goldstone mode corresponding to the translational motion of the soliton. The frequency of the Goldstone mode was found to be $0.00\omega_0$. This is consistent with our result that the Peierls potential barrier is negligible. Guinea⁵⁾ studied the soliton motion by integrating the equation of motion numerically within the adiabatic approximation. He found that the soliton moved at a constant velocity when it was slow enough. This is also consistent with our result.

We have obtained the soliton solution $u_s(n, X_{sol})$ which has a continuous variable, X_{sol} , and satisfies the relation,

$$u_s(n, X_{sol} + 2) = u_s(n+2, X_{sol}). \quad (4.4.1)$$

Therefore it will be possible to promote the soliton coordinate, X_{sol} , to a new dynamical variable by means of the collective

coordinate method.¹²⁾ It remains a future problem to investigate the soliton motion in the SSH model, where the interaction with acoustic phonons can be taken into account.

For various values of the electron-phonon coupling constant α , we have calculated the soliton solutions and the Peierls potential barriers. The ratio of the potential barrier to the soliton excitation energy depends on the soliton width exponentially. It is worth while noting that, in the discrete ϕ^4 model, the potential barrier has the following form,¹³⁾

$$E_p \propto E_k \left(\frac{d}{a} \right)^3 e^{-2\pi^2 d/a} \quad (4.4.2)$$

where E_k is the excitation energy of the kink and d is the kink width. For highly discrete models ($d/a < 1$), the potential barrier becomes,¹⁴⁾

$$E_p = E_0 e^{-8.48 d^2/a^2} \quad , \quad (4.4.3)$$

where E_0 is the energy difference between the maximum and the minimum of the ϕ^4 potential. The dependence of E_p on the soliton width in the SSH model remains to be explained in the future.

References

- 1) W.P. Su, J.R. Schrieffer and A.J. Heeger: Phys. Rev. Lett. **42** (1979) 1698; Phys. Rev. B22 (1980) 2099.
- 2) W.P. Su and J.R. Schrieffer: Phys. Rev. Lett. **46** (1981) 783; W.P. Su : Phys. Rev. B27 (1983) 370.
- 3) W.P. Su and J.R. Schrieffer; Proc. Natl. Acad. Sci. USA **77** (1980) 5626.
- 4) J.E. Hirsch: Phys. Rev. Lett. **51** (1983) 296.
- 5) F. Guinea: Phys. Rev. B30 (1984) 1884.
- 6) S. Stafstrom and K.A. Chao: Phys. Rev. B29 (1984) 7010; Phys. Rev. B30 (1984) 2098.
- 7) S. Stafstrom: Phys. Rev. B31 (1985) 6058.
- 8) Y. Ono, Y. Ohfuti and A. Terai: J. Phys. Soc. Jpn. **54** (1985) 2641.
- 9) A. Terai and Y. Ono: J. Phys. Soc. Jpn. **55** (1986) 213.
- 10) A.R. Bishop, D.K. Campbell, P.S. Lomdahl, B. Horovitz and S.R. Phillpot: Phys. Rev. Lett. **52** (1984) 671; Synth. Metals **9** (1984) 223.
- 11) H. Takayama, Y.R. Lin-Liu and K. Maki: Phys. Rev. B21 (1980) 2388.
- 12) For review see, R. Jackiw: Rev. Mod. Phys. **49** (1977) 681.
- 13) Y. Ishibashi: J. Phys. Soc. Japan **46** (1979) 1254.
- 14) J.A. Combs and S. Yip: Phys. Rev. B28 (1983) 6873.

Chapter V. Summary, Future Problems, and Discussion

In the present thesis, we have studied dynamics of kinks and solitons in three typical systems; the ϕ^4 system, the sine-Gordon system, and trans-polyacetylene. For trans- $(\text{CH})_x$, we have used a continuum model (TLM model) in the adiabatic approximation. By applying the collective coordinate method, the above three systems can be treated in a similar manner. As a result, we have shown that kink (or soliton) dynamics in the systems bears a striking resemblance to each other.

Two mechanisms are pointed out for Brownian-like motion of the kink: One is a random walk and the other is an ordinary Brownian motion. The relation between the two mechanisms is clarified with the help of the fluctuation-dissipation theorem.

In the static limit (or in the long time regime), the latter mechanism is dominant and the Einstein relation,

$$D = \frac{k_B T}{M \Gamma} , \quad (5.1.1)$$

holds, where M is mass of the kink and Γ is the friction caused by the momentum transfer between the kink and thermally excited phonons.

On the other hand, when the frequency is not zero, the two mechanisms coexist. Because the former mechanism (random walk induced by shifts of the kink) is not related to real dissipation, it makes a contribution to the dynamical component of the friction, not to the static component. As a result, this mechanism appears only when the frequency is not zero. In this

case, the real part of the dynamical diffusion constant becomes proportional to $(k_B T)^2$. As the temperature increases, however, there occurs a crossover to $k_B T / M \Gamma$.

The only difference between the above three systems is temperature dependence of the friction Γ : (i) In the ϕ^4 system $\Gamma \propto T^2$, (ii) in the sine-Gordon system, the soliton never changes its velocity and thus the friction is equal to zero, and (iii) in the TLM model, $\Gamma \propto T$. This difference is attributed to the following properties of the kink-phonon interaction; in the ϕ^4 system, the effective potential for the phonons is reflectionless, whereas in the TLM model, it is not.

For trans-(CH)_x, quantum effect on the friction is also studied. Since the number of the optical phonons is exponentially small in the region $k_B T < \hbar \omega_0$, ω_0 being the optical phonon frequency, the friction becomes exponentially small.

As the first step to investigate the soliton dynamics in the discrete Su, Schrieffer, and Heeger's model, the Peierls potential barrier is estimated. We have shown that it is negligible when we use the parameters proposed for polyacetylene.

There are some problems left to future. We list up them in the following.

1) Effect of the friction on the structure factor $S(k, \omega)$.

In the sine-Gordon case, $S(k, \omega)$ obtained in the molecular dynamics¹⁾ agreed rather well with the predictions by the ideal gas phenomenology. On the other hand, for the ϕ^4 case, the agreement was less quantitative. It may be

partly attributed to the violation of the ideal gas phenomenology due to the friction.

2) Quantum effect on the friction of the ϕ^4 kink.

In the low temperature region, Γ will be reduced because the number of thermal phonons is much less than that of the classical phonons. As shown in Appendix 2.C, cancellations among many diagrams take place in the classical calculation. It is of particular interest whether a similar cancellation will occur in the quantal case.

3) Relation to the damped nonlinear equations.

By considering a coupling to the heat bath, the time evolution can be studied with a Langevin equation or a damped nonlinear equation driven by a random force R ,²⁾

$$\frac{\partial^2 \phi}{\partial x^2} = \frac{\partial^2 \phi}{\partial x^2} - \frac{\partial U}{\partial \phi} - \gamma \frac{\partial \phi}{\partial x} + R(x, t), \quad (5.1.2)$$

where $U[\phi(x, t)]$ is the potential part of the Hamiltonian density, and γ is the damping constant. Recently Kaup et al. calculated the average velocity of the kink when a spatially independent external force F is added to eq. (5.1.2).³⁾ They obtained,

$$\langle v \rangle = - \frac{\pi F}{4\gamma} \left(1 + \frac{C k_B T}{E_k} + \dots \right), \quad (5.1.3)$$

where C is a positive constant in the order of unity. The second term in the parenthesis is a correction due to thermal fluctuations. It seems that the fluctuations effectively

reduce the damping constant γ . The relation between this result and ours is of great interest.

4) Kink dynamics in highly discrete systems.

When the temperature is low, the kinetic energy of the kink becomes less than the Peierls potential barrier. In this case, the kink can not move freely any longer and thus the diffusion constant will approach to zero.⁴⁾ Recently, some attempts to treat the kink dynamics in the discrete systems have been performed (see also §1.1).⁵⁾

5) Kink-antikink collisions and other phenomena.

As referred to in §1.1, the kink-antikink collision has been extensively studied numerically to find out highly nontrivial phenomena, such as two bounce structures, multi-bounce structure, and so on.⁶⁾ Molecular dynamics simulations have shown that various phenomena take place, as well as the kink-antikink collisions (see Figs. 1.1~1.3); for example, creation of a kink-antikink pair, and long-lived breather-like structures. It is important to investigate mechanisms of these phenomena.

6) Ergodicity of nonlinear systems.

Of course, there have been many attempts to explore this problem. An approach through the kink dynamics may throw new light on this problem. Precursory work has been carried out.⁷⁾

7) Interaction between the soliton and acoustic phonons in trans-polyacetylene.

Though the coupling of the soliton to acoustic phonons

is weaker than that to optical phonons,^{8,9)} the acoustic phonons may be playing an important role in the soliton diffusion, because they exist abundantly at low temperatures. Maki discussed the diffusion mechanism of the soliton, regarding the system of the solitons as a Boltzmann-type gas with mean free path limited by acoustic phonons linearly coupled to the solitons.¹⁰⁾ He obtained a diffusion constant proportional to $T^{1/2}$ in one-dimensional phonon model, and $T^{-1/2}$ in three-dimensional phonon model. However, he used undistorted plane waves, $\exp(ikx)$, as the acoustic phonons, and thus the shift of the soliton and the momentum transfer due to the soliton-phonon interaction were not taken into account.

The deviation from $\exp(ikx)$ of the acoustic phonon mode can be obtained numerically in the Su, Schrieffer, and Heeger's model.¹¹⁾ It would be interesting to analyze the soliton-phonon collision in the SSH model and to study the soliton dynamics.

8) Comparison with experimental results.

As summarized in §1.3, NMR and ESR experiments have indicated that the solitons become more mobile at higher temperatures. It has been suggested that the diffusion constant of the "mobile soliton" may be proportional to T^2 .

It has not been possible yet to explain this temperature dependence. As discussed above, nonlinear interactions with the acoustic phonons must be taken into account. Furthermore, in real systems, there may be various effects on the soliton dynamics; for example, discreteness effects,

effects of disorder, impurity pinning, and effects of the polymer chains (or finite chain length effects), Coulomb interactions between the solitons, and three-dimensional effects (for example, confinement of the soliton). We have shown in Chapter IV that the Peierls potential barrier is negligible in the SSH model. Thus the energy dissipation due to the lattice pinning will not be effective in polyacetylene. It is a future problem to study the other effects.

References

- 1) T. Schreider and E. Stoll: Phys. Rev. B23 (1981) 4631.
- 2) S.E. Trullinger, M.D. Miller, R.A. Guyer, A.R. Bishop,
F. Palmer and J.A. Krumhansl: Phys. Rev. Lett. 40 (1978)
206.
R.A. Guyer and M.D. Miller: Phys. Rev. A17 (1978) 1205, 1774.
M. Imada: J. Phys. Soc. Jpn. 47 (1979) 699, 49 (1980) 1247.
- 3) D.J. Kaup: Phys. Rev. B27 (1983) 6787.
D.J. Kaup and El-sayed Osman: Phys. Rev. B33 (1986) 1762.
- 4) J.A. Combs, and S. Yip: Phys. Rev. B28 (1983) 6873, B29
(1984) 438.
C. Kunz and J.A. Combs: Phys. Rev. B31 (1985) 527.
- 5) P. Stancioff, C. Willis, M. El-Batanouny, and S. Burdick:
Phys. Rev. B33 (1986) 1912.
C. Willis, M. El-Batanouny, and P. Stancioff: Phys. Rev. B33
(1986) 1904.
- 6) D.K. Campbell and M. Peyrard: Physica 18D (1986) 47.
D.K. Campbell, M. Peyrard and P. Sodano: Physica 19D (1986) 165.
D.K. Campbell, J.F. Schonfeld, and C.A. Wingate: Physica 9D
(1983) 1.
- 7) M. Imada: J. Phys. Soc. Jpn. 52 (1983) 1946.
- 8) Y. Leplanc, H. Matsumoto, H. Umezawa and F. Mancini: Phys.
Rev. B30 (1984) 5958; J. Math. Phys. 26 (1985) 2940.
- 9) J.T. Gammel: Phys. Rev. B33 (1986) 5974.
- 10) K. Maki: Phys. Rev. B26 (1982) 2181, 2187, 2192.
- 11) A. Terai and Y. Ono: J. Phys. Soc. Jpn. 55 (1986) 213.